

T 1980

PYROLYSIS OF RESIDUES OBTAINED FROM
CO-STEAM LIGNITE LIQUEFACTION

by

Mukesh K. Gupta

1977

ProQuest Number: 10782135

All rights reserved

INFORMATION TO ALL USERS

The quality of this reproduction is dependent upon the quality of the copy submitted.

In the unlikely event that the author did not send a complete manuscript and there are missing pages, these will be noted. Also, if material had to be removed, a note will indicate the deletion.



ProQuest 10782135

Published by ProQuest LLC (2018). Copyright of the Dissertation is held by the Author.

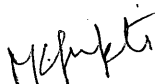
All rights reserved.

This work is protected against unauthorized copying under Title 17, United States Code
Microform Edition © ProQuest LLC.

ProQuest LLC.
789 East Eisenhower Parkway
P.O. Box 1346
Ann Arbor, MI 48106 – 1346

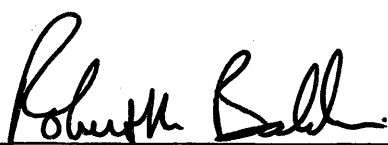
T 1980

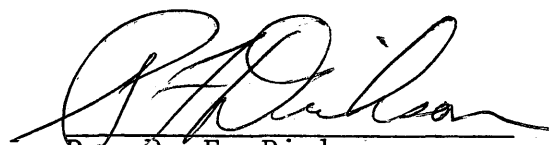
A Thesis submitted to the Faculty and the Board of Trustees of the Colorado School of Mines in partial fulfillment of the requirements for the degree of Master of Science in Chemical and Petroleum-Refining Engineering.

Signed: 
Mukesh K. Gupta

Golden, Colorado

Date: 12th Sept., 1977

Approved: 
Dr. R. M. Baldwin
Thesis Advisor


Dr. P. F. Dickson
Head of Department

Golden, Colorado

Date: 9-13, 1977

ABSTRACT

Pyrolysis of coal residues obtained from CO-Steam lignite liquefaction was studied at Grand Forks Energy Research Centre, Grand Forks, North Dakota. The purpose of the study was to investigate the quality of residue by pyrolysis and also to study residue and pyrolysis kinetics. ✓

Pyrolysis of the samples was accomplished using an Elemental Analyzer, a Controlled Atmosphere Pyrolysis System and a Solids Pyrolyzer. Residue samples for pyrolysis were obtained by tetrahydrofuran (THF) extraction of a product oil collected from a batch stirred autoclave at different times during a run. The pyrolysis products were analyzed with a gas chromatograph.

The results indicated that nearly 75% of the volatile matter and 55% of fixed carbon was converted into liquid or gaseous products during the first 60 minutes in the autoclave. Coking was observed in Run 23 due to the lack of hydrogen donor solvent (tetralin). The type of kinetic expression which successfully described the data taken in the study is given by an equation of the form:

$$\frac{dx}{dt} = k_n (a-x)^n$$

Exponent "n" is the order of the reaction, "x" is the observed fractional weight loss at time t, and "a" is the maximum possible reactive fraction at the temperature concerned. The

rate constants for the two lignite coals studied (reaction conditions held constant) were quite comparable indicating that a change of coal did not affect the kinetics appreciably.

TABLE OF CONTENTS

	Page
ABSTRACT	iii
LIST OF FIGURES.	vii
LIST OF TABLES	x
ACKNOWLEDGMENTS.	xi
INTRODUCTION	1
LITERATURE SURVEY.	6
Coal Liquefaction Processes	6
CO-Steam Liquefaction	11
Kinetic Modeling of Pyrolysis Reactions	14
EXPERIMENTAL DESIGN.	16
EQUIPMENT.	21
EXPERIMENTAL PROCEDURE	35
Autoclave Run	35
Sample Preparation.	35
Pyrolysis in Elemental Analyzer	37
Pyrolysis in Controlled Atmosphere Pyrolysis System.	39
ANALYSIS OF DATA	42
DISCUSSION OF RESULTS.	58
Results Obtained by Pyrolysis at 1400 ^o C	58
Removal of Residue, Volatile Matter, Light Gases (CO, CO ₂ , CH ₄ , H ₂ O), Fixed Carbon and Ash	58
Data Fitting.	62
Kinetic Modelling of the Data	65
Correlation of Results to Run Conditions.	79
Reproducibility	110
Results Obtained by Pyrolysis at 800 ^o C.	111

	Page
Amount of Volatile Matter, Heavy Liquids, Light Gases, Fixed Carbon and Ash Obtained During Pyrolysis	111
Correlation of Results to Run Conditions.	111
CONCLUSIONS.	117
RECOMMENDATIONS FOR FURTHER STUDY.	118
LITERATURE CITED	119
APPENDIX A - RAW DATA OF PYROLYSIS AT 1400°C	121
APPENDIX B - SAMPLE CALCULATION FOR RUN 28, VOLATILE MATTER (1400°C).	126
APPENDIX C - DATA FROM PYROLYSIS AT 800°C.	134

LIST OF FIGURES

Figure	Page
1. GFERC Coal Liquefaction Process	3
2. Elemental Analyzer.	22
3. Controlled Atmosphere Pyrolysis System.	29
4. Continuous Atmosphere Pyrolysis Chamber	32
5. Block Diagram of Elemental Analyzer	38
6. Block Diagram of Controlled Atmosphere Pyrolysis System (CAPS)	40
7. Calibration Curve of CO	44
8. Calibration Curve of CO ₂	45
9. Calibration Curve of H ₂ O.	46
10. Calibration Curve of CH ₄	47
11. Calibration Curve of C ₂ H ₄	48
12. Calibration Curve of C ₂ H ₆	49
13. Calibration Curve of C ₃ H ₈	50
14. Gas Chromatogram of Anthracene Oil from Unit CAPS	52
15. Gas Chromatogram of Anthracene Oil from GC-Mass Spectrometer.	54
16. Run 27, Weight Percent Conversion of Coal (Residue) to Liquid Coal.	66
17. Run 27, Weight Percent Removal of Volatile Matter from Coal.	67
18. Run 27, Weight Percent Removal of Fixed Carbon from Coal	68
19. Run 27, Weight Percent Removal of Carbon Dioxide from Coal	69
20. Run 27, Weight Percent Removal of Methane from Coal	70
21. Run 27, Weight Percent Removal of Water from Coal	71
22. Run 28, Weight Percent Conversion of Coal (Residue) to Liquid Coal.	72
23. Run 28, Weight Percent Removal of Fixed Carbon from Coal.	73
24. Run 28, Weight Percent Removal of Volatile Matter from Coal.	74

Figure	Page
25. Run 28, Weight Percent Removal of Carbon Monoxide from Coal	75
26. Run 28, Weight Percent Removal of Carbon Dioxide from Coal	76
27. Run 28, Weight Percent Removal of Methane from Coal	77
28. Run 28, Weight Percent Removal of Water from Coal	78
29. Run 27, Comparison of Experimental Weight Percent Conversion of Coal (Residue) to Liquid Coal with 1st and 2nd Order Kinetic Models	80
30. Run 27, Comparison of Experimental Weight Percent Removal of Volatile Matter with 1st and 2nd Order Kinetic Models	81
31. Run 27, Comparison of Experimental Weight Percent Removal of Fixed Carbon from Coal with 1st and 2nd Order Kinetic Models	82
32. Run 27, Comparison of Experimental Weight Percent Removal of Methane from Coal with 1st and 2nd Order Kinetic Models	83
33. Run 27, Comparison of Experimental Weight Percent Removal of Carbon Dioxide from Coal with 1st and 2nd Order Kinetic Models	84
34. Run 27, Comparison of Experimental Weight Percent Removal of Water from Coal with 1st and 2nd Order Kinetic Models	85
35. Run 28, Comparison of Experimental Weight Percent Conversion of Coal (Residue) to Liquid Coal with 1st and 2nd Order Kinetic Models	86
36. Run 28, Comparison of Experimental Weight Percent Removal of Volatile Matter from Coal with 1st and 2nd Order Kinetic Models	87
37. Run 28, Comparison of Experimental Weight Percent Removal of Fixed Carbon from Coal with 1st and 2nd Order Kinetic Models	88
38. Run 28, Comparison of Experimental Weight Percent Removal of Methane from Coal with 1st and 2nd Order Kinetic Models	89
39. Run 28, Comparison of Experimental Weight Percent Removal of Carbon Monoxide from Coal with 1st and 2nd Order Kinetic Models	90

Figure	Page
40. Run 28, Comparison of Experimental Weight Percent Removal of Carbon Dioxide from Coal with 1st and 2nd Order Kinetic Models	91
41. Run 28, Comparison of Experimental Weight Percent Removal of Water from Coal with 1st and 2nd Order Kinetic Models.	92
42. Run 27, Residue, Plot of 1st Order Kinetic Equation.	93
43. Run 28, Residue, Plot of 1st Order Kinetic Equation.	94
44. Run 27, Residue, Plot of 2nd Order Kinetic Equation.	95
45. Run 28, Residue, Plot of 2nd Order Kinetic Equation.	96
46. Run 27, 1st Order Plot of Residue with 95% Confidence Interval	97
47. Run 27, 2nd Order Plot of Residue with 95% Confidence Interval	98
48. Run 27, 1st Order Plot of Volatile Matter with 95% Confidence Interval.	99
49. Run 27, 2nd Order Plot of Volatile Matter with 95% Confidence Interval.	100
50. Run 28, 1st Order Plot of Residue with 95% Confidence Interval	101
51. Run 28, 2nd Order Plot of Residue with 95% Confidence Interval	102
52. Run 28, 1st Order Plot of Volatile Matter with 95% Confidence Interval	103
53. Run 28, 2nd Order Plot of Volatile Matter with 95% Confidence Interval	104
54. Comparison of Weight Percent Conversion of Coal (Residue).	106
55. Comparison of Weight Percent Removal of Fixed Carbon from Coal.	108
56. Comparison of Weight Percent Removal of Volatile Matter from Coal	109

LIST OF TABLES

Table	Page
1. Explanation of Symbols of Figure 1.	4
2. Lignite Analysis.	17
3. Explanation of Symbols of Figure 2.	23
4. Explanation of Symbols of Figure 3.	30
5. Run Conditions.	36
6. Analysis of Gas Mixture	43
7. Conversion Factors.	43
8. Constituents of Anthracene Oil Found by the Unit CAPS	53
9. Constituents of Anthracene Oil Found by GC-MS . .	55
10. Weight Percent of the Constituents Present in Anthracene Oil	56
11. Products of Pyrolysis at 1400 ^o C for Runs 27, 28 .	59
12. Products of Pyrolysis at 1400 ^o C for Runs 31, 30 .	60
13. Products of Pyrolysis at 1400 ^o C for Run 23. . . .	61
14. Values of Constants a and b	64
15. Values of Rate Constants and 'a'.	105
16. Reproducibility Results, Run 27, Sample 1	110
17. Product of Pyrolysis at 800 ^o C Based on Residue. .	112
18. Products of Pyrolysis at 800 ^o C Based on Liquid Product	113

ACKNOWLEDGMENTS

I would like to express my sincere gratitude to Dr. Robert M. Baldwin and Dr. R. L. Bain for their counsel and guidance. I would like to express my appreciation to Dr. Everett Sondreal and Dr. Curtis L. Knudson for allowing me to work at Grand Forks Energy Research Center, Grand Forks, North Dakota. I also wish to thank Dr. Knudson for his help and guidance in my work. Financial support from the Office of Research Services, Colorado School of Mines, and Energy Research and Development Administration, University Programs, is also gratefully acknowledged.

INTRODUCTION

Energy shortages, pollution controls and reliance on foreign oil sources have renewed interest in using coal liquefaction to produce a clean fuel oil from coal. Many power plants burn petroleum-derived fuel oil and natural gas in order to meet environmental pollution regulations. If a coal-derived oil were used to replace petroleum-derived oil now being used as power plant fuel, precious petroleum oils and gas now consumed by power plants would be relieved for use in home heating, industry and transportation, thus easing the shortage of petroleum-derived fuels.

Grand Forks Energy Research Center (GFERC) Process

Converting coal to a liquid generally requires the addition of hydrogen. Hydrogen is a very expensive raw material, therefore, liquefaction of coal using hydrogen directly is a costly process. A way around this problem is to produce the hydrogen needed for the liquefaction of coal from less expensive raw materials. This can be done using the water-gas shift reaction. In this reaction, water and carbon monoxide react to form hydrogen and carbon dioxide. Both starting materials, water and carbon monoxide, are relatively inexpensive and readily available (i.e., using CO generated from gasification of coal).

Grand Forks Energy Research Center (GFERC), Grand Forks, North Dakota, is using the CO-Steam process to hydrogenate

lignite to make light oils. The process under development at GFERC is being studied in a batch stirred autoclave reactor by charging coal slurry to a pre-heated reactor in order to minimize the effects of heat-up time. A flow diagram of the process is given in Figure 1 and the symbols in the figure are explained in Table 1. During experimental runs, a 3-4 gram liquid sample was collected from the autoclave at different time intervals. The organic product was extracted from this sample with tetrahydrofuran (THF) using millipore filtration. The insoluble product obtained from THF extraction was then pyrolyzed in an inert atmosphere of helium to study the quality of reaction residue as a function of time. Two pyrolyzing temperatures (800°C and 1400°C) were selected. At 1400°C , the products were mostly light gases (CO , CO_2 , CH_4 , H_2O , C_2H_6) and were analyzed by a gas chromatograph. At 800°C , the products were light gases and also heavier materials resembling anthracene oil. The analysis at 1400°C was done to determine the amount of maximum volatile matter present in the residue, while analysis at 800°C gave an indication of the presence of heavier organic materials.

This thesis deals with examination of autoclave residues (THF insolubles) from the GFERC process for several different lignite coals and processing conditions. Time-dependent samples were obtained to allow for kinetic interpretation of the residue data. For the kinetic study, every sample was pyrolyzed at 1400°C for 24 seconds. A model developed by Wisner¹ was found to fit the data reasonably well, and rate

Figure 1. GFERC Coal Liquefaction Process

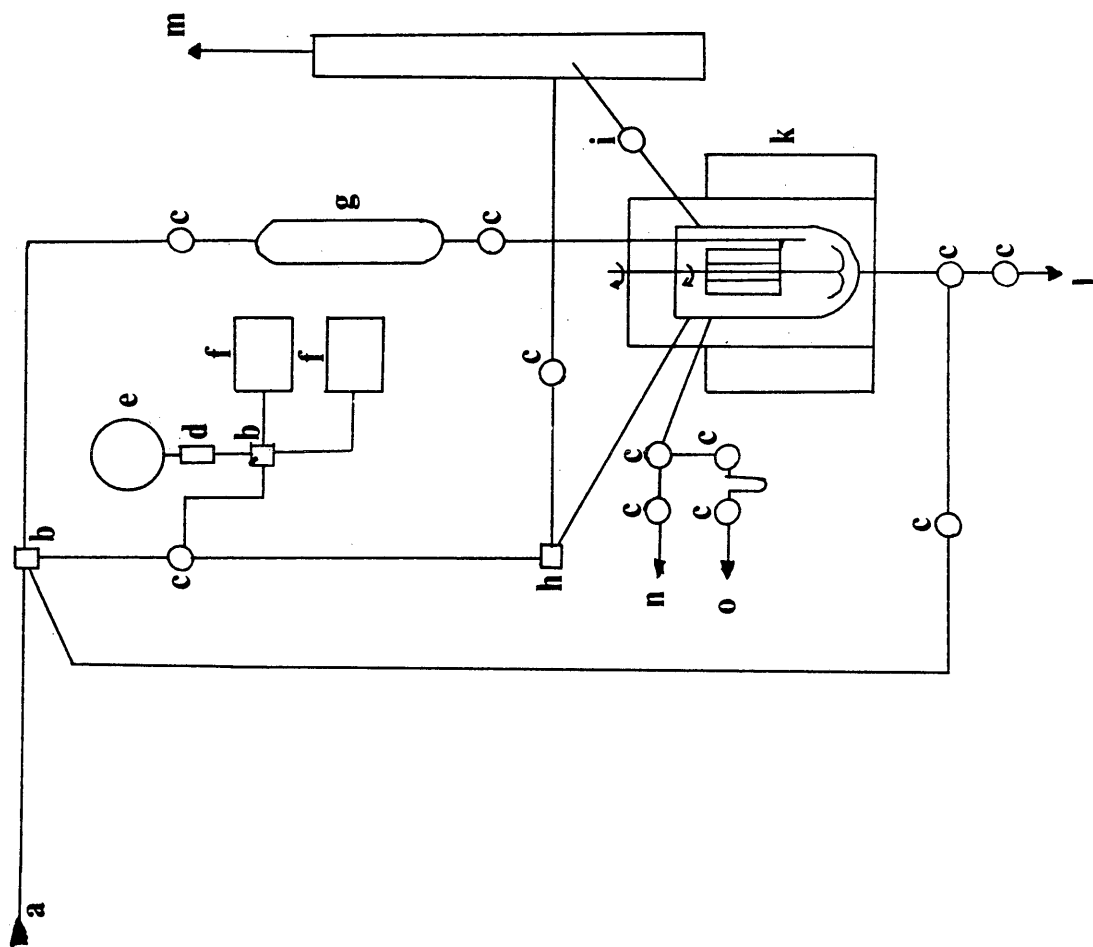


Table 1

A	= Inlet for CO-H ₂ mixture
B	= Cross Coupling
C	= Valve
D	= Surge Check Valve
E	= 0 - 8000 psi Gage
F	= 0 - 6000 psi Pressure Transducer
G	= 300 C.C. Charger
H	= Tee Coupling
I	= Rupture Disc Assembly
J	= Vent Stack
K	= 1 Litre Autoclave
L	= Liquid Sample Collector Outlet
M	= Vent
N	= Outlet for Gas Sampling
O	= Vent for Purging Oven

constants were also evaluated, as shown later. The amount of volatile liquids and light gases evolved by pyrolyzing at 800°C gave an idea about the suitability of the liquefaction residues for further use, i.e., whether they can be used for gasification or carbonization. The amount of volatile liquids obtained from different samples in a run can be compared to the original reactant slurry to give an idea about the changes produced in the coal molecule; i.e., how far the large structures present in the coal have been broken to yield smaller, more volatile molecules. Fixed carbon and ash were the other two parameters studied to determine the quality of residue. These two parameters were determined after pyrolysis. The criteria used for evaluating a run was a minimum amount of residue and a residue which contained maximum volatile liquids but small amounts of fixed carbon.

LITERATURE SURVEY

Coal Liquefaction Processes

Coal can be converted into liquid fuel by several processes.² One such process is pyrolysis, or destructive distillation. A typical pyrolysis process involves heating coal at 1800-2500^oF in the absence of air. The amount of gas, coke, and other materials obtained varies with the type of coal used, but usually the yields per ton of coal obtained are 10,000-12,000 cu ft of gas having a heating value of 450-550 Btu/cu ft, 1400-1500 lb of coke and 1-10 gal of tar and light oils.

In the COED process,² pulverized coal is heated successively to higher temperatures in a series of fluidized bed reactors (600^oF, 850^oF, 1000^oF and 1500^oF) at a pressure of 6-10 psig. Yields per ton of coal are 8,000-10,000 scf of gas with a heating value of 550-650 Btu/scf after scrubbing, 1-1.5 bbl of syncrude obtained after hydrotreating and char. TOSCO II process² uses an oil shale retorting process for coal. At a pyrolyzing temperature of 800-970^oF yields per ton of coal are .3-.5 bbl of oil, and .5 ton of char having 80% of the original heating value. The Garrett flash pyrolysis process² pyrolyzes dry pulverized coal in an entrained bed reactor by heating with recycled hot char at 1100^oF. The wt % yields obtained are 57% char, 35% tar, and 7% pyrolysis gas with a heating value of 700 Btu/scf and H₂S free.

Nelyubin, et al.³ studied the thermal decomposition of 'Kusbas' coal at a programmed temperature rise of 5°C/min with a final temperature of 900°C in an inert atmosphere. In the sequence: telinite, micrinite, fusinite, the weight loss during thermal decomposition decreases from 25.7% to 18.8% and the total yield of hydrogen, methane and other hydrocarbon gases also decreased. Telinite is a variety of pure coal composed of plant cell-wall material. Micrinite is an opaque granular variety of carbon-rich maceral. Fusinite is mineral charcoal consisting of carbonized woody tissues.

Van-Heck, et al.⁴ studied the coking of bituminous coals at various heating rates ranging from 10⁻²°C/min to 10⁵°C/min and at final temperature up to 1200°C. In the C-H system above 2700°K, no saturated hydrocarbons are stable, while C₂H₂ and its polymers are stable and concentrations of these compounds should reach a maximum at about 3400°K. At still higher temperatures only atomic species of carbon and hydrogen are present. Therefore, Van-Heck, et al. were able to predict that the production of C₂H₂ directly from coal via high temperature pyrolysis should be technically feasible.

Girling⁵ obtained products in the range C₄ to C₁₀ from a series of coals by heating them in stages from ambient temperature up to 700°C. Aliphatic and aromatic compounds were evolved even below 100°C. The amounts of hydrocarbons evolved varied considerably from coal-to-coal. Only for the middle rank coals was a substantial portion of the total evolution

obtained below 300°C. Excluding anthracite, the amounts of paraffins evolved above 300°C did not vary greatly with the rank, but emission below 300°C was greatest in the case of the middle rank coals (i.e., of 82.5 and 87.5% carbon). The amounts of aromatics emitted above 300°C increased with rank up to 89% carbon, but the evolution below 300°C increased with rank only up to 87.5% carbon and then decreased steeply. There was little variation in the amounts of olefins emitted above 300°C from the coals studied. The amounts evolved below 300°C decreased steadily with increasing coal rank.

Berkowitz⁶ suggests three sequential reaction steps for pyrolysis of which two are characterized by predominantly peripheral molecular changes and one by extensive skeletal breakdown and reorganization. The temperature ranges for the three phases are <350-400°C, 400-650°C and 650->1000°C. The dominant chemical changes below 350°C can be identified with molecular stripping, i.e., with decarboxylation, elimination of -OCH₃ group, partial loss of carbon bound - CH₃ groups and partial dehydroxylation. In the second phase hydrogen is progressively eliminated from the coal as temperature rises beyond 400°C and much of the original oxygen content survives, apparently intact. Some investigators,⁷ however, believe that oxygen in - OH groups is eliminated in this phase. In Phase III, Berkowitz predicts a rapid molecular growth and ordering or in other words a progressive growth of aromatic structures. Hydrogen is the major product while methane, carbon monoxide

and water are the minor products of pyrolysis in this phase.

A second process, direct hydrogenation, involves partial hydrogenation of coal usually in the presence of a catalyst. In this process the carbon-carbon bonds in the coal molecules are only partially broken to yield liquid hydrocarbons, while in the production of SNG, they are completely broken to give methane. In the Synthoil² process, dry pulverized coal feed in recycle oil is subjected to reaction with hydrogen in rapid, turbulent-flow fixed bed reactors packed with pelletized cobalt molybdate catalyst at about 840^oF and 2,000-4,000 psi. The primary product obtained is 3 bbl of low sulfur oil per ton of coal with a concurrent hydrogen consumption of 3000 scf per bbl of product oil. In the H-coal process,² dried, pulverized coal is slurried with coal-derived oil and preheated with hydrogen. This mixture is then fed to an ebulliating bed reactor containing a cobalt-moly catalyst at about 850^oF and 2700 psig. Liquid yields in excess of 4 bbl per ton of coal are reported with a hydrogen consumption of 14,000-20,000 scf per ton of coal processed. In a process patented by UOP,² pulverized coal is mixed with solvent and then hydrogenated. After ash separation, the hydrocarbon stream is catalytically hydrotreated. Yields of over 4 bbls of low sulfur syncrude per ton of coal have been reported.

A third process, indirect hydrogenation,² involves reacting coal and steam to yield synthesis gas, which is a mixture of carbon monoxide and hydrogen. In 1933, Fischer and Tropsch showed that, in the presence of certain types of

catalysts, carbon monoxide may be hydrogenated to afford a complex mixture of aliphatic hydrocarbons similar to a high paraffin crude. In the ARGE system,² one volume of purified synthesis gas ($\sim H_2/CO$ ratio 2) obtained from coal and steam reaction is blended with about 2 volumes of recycle gas and reacted at 430-490^oF and 360 psig in a fixed bed tubular reactor containing pelletized precipitated iron catalyst. Yields obtained are mainly paraffinic-olefinic low and middle distillate oils. In the Synthol process, one volume of purified synthesis gas is blended with 2 volumes of recycle gas and reacted at 600-645^oF and 310 psig in a circulating bed reactor using a promoted iron catalyst. The liquid products obtained contain more low boiling aromatic hydrocarbons than ARGE products, but only about 35% light oil (120-520^oF boiling point).

Solvent extraction is another process by which coal can be converted to liquid fuels. This process represents a modification of direct hydrogenation for production of liquids. A high boiling hydrogen donor or non-donor solvent, usually derived from the coal, and a small quantity of hydrogen (if the solvent does not act efficiently as a hydrogen donor) are used to dissolve coal at elevated temperatures and pressures. In the solvent refined coal (SRC) process,² dry pulverized coal is mixed with recycle coal-derived solvent and hydrogen and reacted at 815^oF and 1000 psi to form a solution. The solution is then filtered to remove undissolved residues and the filtrate flashed to yield a low sulfur, ash

free solvent refined coal as the residue and recover process solvent (the distillate). In the Consol Synthetic Fuel (CSF) process,² dry pulverized coal is preheated to 450°F and then slurried with a coal-derived solvent. Temperature and pressure are next raised to 765°F and 150 psig respectively and coal extracted by the solvent to obtain an overhead product and a bottom slurry product of insolubles and extract. The slurry of coal extract and insolubles is then separated by hydroclones to isolate the insolubles from the organic extract. Insolubles are carbonized to recover additional light oils and these oils are mixed with the extract. The resulting liquid is then catalytically hydrotreated to recover a hydrogen donor solvent (for recycle), distillate light fuels (naphtha) and low sulfur fuel oil.

Carbon Monoxide-Steam Liquefaction

Early CO-Steam Work

In 1921 Fisher⁸ reported using carbon monoxide and water in hydrogenating coal. He reported higher yields of ether-soluble material using carbon monoxide and water than with hydrogen at similar conditions. Low conversion along with several other problems caused the carbon monoxide plus water approach to coal hydrogenation to be ignored after 1925.

Cellulose Liquefaction

The Bureau of Mines⁹ has experimentally converted cellulose, the primary constituent of organic solid waste, to a

low sulfur oil. All types of cellulosic wastes have been converted to oil by reaction with carbon monoxide and water at temperatures of 350°C to 400°C and pressures near 4000 psig in the presence of various catalysts and solvents. Cellulose conversions of 90 percent and better were obtained.

Lignite and Other Coals Liquefaction

Batch tests were conducted by Appell, et al.^{10,11,12,13} using a 500 ml rocking autoclave filled with 2 moles of carbon monoxide, lignite coal, water and solvent. The objective of the work was to convert lignite to low sulfur fuel oil. It was believed that hydrogenation of coal using carbon monoxide and water proceeded via nascent hydrogen formed by the water-gas shift reaction. Now it appears that carbon monoxide and water react with lignite in a more complex manner and a number of factors are involved. Carbon monoxide and steam gave higher conversion levels and reaction rates than those obtained using hydrogen under similar conditions. Results also indicated that both carbon monoxide and water must be present if good conversions are to be obtained, and that increasing the carbon monoxide pressure has a greater effect on conversion than increasing the steam pressure. These effects are dependent on the ratio of carbon monoxide to water. Conversion of lignite increased with increasing amounts of carbon monoxide and steam. An optimum temperature was found, with decreased conversions resulting after the temperature was increased past 400°C.

Appell, et al.¹⁴ also did work using different solvent types and catalysts on CO-Steam coal liquefaction. Several lignite tars and pitches were used as solvents and all gave good results for lignite liquefaction. The type of solvent was found to be more important than the amount. In the presence of a good solvent, it was possible to reduce the operating pressure and still maintain acceptable conversions (85-90%). Heterocyclic amines were found to have a catalytic effect when used with carbon monoxide and water. The effectiveness of the heterocyclic amines was related to the increased boiling point of the solvent.

Yavorsky, et al.¹⁵ found that the conversion of bituminous coal increases with temperature in the range of 375-425°C but does not exceed 75 percent. The effect of solvent on conversion is more pronounced on bituminous coal than on lignite. Conversion of bituminous coal and lignite increased sharply with pressures up to 1000 psig initial pressure, but above 1000 psig, the increase in conversion with increase in pressure was smaller.¹³ Handwerk¹⁶ proposed that conversion of coal to liquid and coal desulfurization increased with an increase in reaction temperature over the range studied, Handwerk also suggested that changes in carbon monoxide pressures did not have any definite effect on coal conversion in the pressure range examined.

Kinetic Modelling of Pyrolysis Reactions

Chermin, et al.¹⁷ have postulated a mathematical model for coal pyrolysis kinetics based on consecutive reaction theory. Based on this model they could satisfactorily explain the degasification and the plastic behavior of coking coals. They found the activation energy of pyrolysis of coking coal to be about 50 kcal/mole.

According to Berkowitz⁶ most, if not indeed all, coal devolatilization reactions follow pseudo first-order kinetics. Calculations proceeding from such kinetics show that initial isothermal weight loss rates are frequently far too great to allow interpretation of the weight loss versus time curves in terms of a single first order chemical reaction. Therefore, he suggested that the relatively slow disengagement of volatile matter, which follows after the initial fast discharge and extends the weight loss versus time curve to many hours, may reflect diffusion control over evolution of pyrolytic material. The evolution of hydrogen, water, carbon monoxide and methane follow pseudo first order kinetics and the activation energies based on diffusion as a rate-controlling step, are generally smaller than 15 kcal/mole.

Wiser¹ proposed that the initial coal pyrolysis reactions are second order and the process then gradually deteriorates to a first order reaction. The temperature range studied by Wiser was from 409°C to 497°C. The general form of the rate equation used to fit the first part of the curve was

$$dx/dt = k_n (a-x)^n$$

where $n \neq 1$ and denotes the order of the reaction, x is the observed weight loss at the time t , as a fraction of the initial sample weight, a is the maximum weight loss obtainable at the temperature concerned, and k_n is the n th order rate constant. Wiser used this model to explain the data for the first 60 minutes with $n = 2$.

After 60 minutes, a first order expression was used to fit the data,

$$\frac{dx}{dt} = k_1 (a-x)$$

Wiser obtained an enthalpy of activation of 35.6 kcal/mole for the second order reaction and 4.1 kcal/mole for the first order reaction.

EXPERIMENTAL DESIGN

The main objective of the study was to determine the quality of unreacted residue obtained from the CO-Steam coal liquefaction process by pyrolysis of these residues. A secondary goal was to obtain some information about residue kinetics as CO-Steam liquefaction proceeds. Residue will be defined as the THF insoluble portion of the whole product produced by CO-Steam liquefaction of lignite.

Two different lignites were used for examination. These lignites were obtained from the Beulah mine, North Dakota, one from Beulah Standard No. II mine, and the other sample from the mine site location Orange Pit no. 43. Proximate and ultimate analyses are given in Table 2. These two coals were selected because of their wide differences in oxygen and carbon content. Sulfur and nitrogen in North Dakota lignites have usually the same relative concentrations, and are low in relation to higher-rank coals.

A 3-4 gram liquid sample was collected from the autoclave at different time intervals during a run. The organic product was extracted from this sample with tetrahydrofuran (THF) using millipore filtration. The insoluble product obtained from THF extraction was used for pyrolysis.

The two maximum temperatures chosen for pyrolysis of the residue were attained by temperature programming the pyrolysis unit at a rate of $100^{\circ}\text{C}/\text{sec}$ until final temperatures of 800°C and 1400°C were reached. The rate of $100^{\circ}\text{C}/\text{sec}$ was selected since that was the slowest rate available

Table 2. - Lignite Analysis*

	<u>Beulah Std. #2</u>	<u>Orange Pit #43</u>
Proximate Analysis:		
Moisture (as received)	28.39%	36.96%
Volatile matter (MF)*	42.25%	40.96%
Fixed carbon (MF)	47.73%	49.36%
Ash (MF)	10.02%	9.95%
Inorganic Content (ppm MF Lignite):		
SiO ₄	8590	31300
Al	17933	6106
Fe	10694	5564
Ti	119	119
P	87	217
Ca	7150	17714
Mg	1628	4500
Na	1706	3027
K	83	165
S	5080	7880
Ultimate Analysis:		
Hydrogen	4.31%	2.62%
Carbon	64.57%	79.19%
Nitrogen	.92%	1.22%
Oxygen	19.08%	5.81%
Sulfur	1.10%	1.21%
Ash	10.02%	9.95%

*(MF) = moisture free

*Lignite analysis was supplied by GFERC, Grand Forks, North Dakota and should not be reproduced without their permission.

and heating the sample slowly was desirable in order to avoid any reaction during pyrolysis. The sample was maintained isothermally at the final temperature so as to affect complete changes in the sample at that temperature.

The temperature of 800°C was found to be optimum to give the maximum amount of volatile liquids from the residue. At temperatures lower than 800°C, light gases and a small amount of volatile liquids were evolved from the pyrolysis unit, while at temperatures higher than 800°C, mostly light gases and very small amounts of volatile liquids were evolved. Data obtained from pyrolysis of the THF residue to a maximum temperature of 800°C was used to give a qualitative idea of the use of CO-Steam residue for further processing. Products of this pyrolysis were predominantly light gases (CO, CO₂, CH₄, H₂O) and heavy oils which indicated the nature of the liquids remaining with the autoclave residue. Fixed carbon and ash were also determined after the sample was pyrolyzed. The amount of fixed carbon determined by pyrolysis at a maximum temperature of 800°C was inaccurate since some volatile matter was left after pyrolysis at 800°C. The relative amounts and types of volatile liquids (i.e., the constituents present in the anthracene oil solvent), fixed carbon and ash obtained by pyrolysis from different autoclave samples when compared to the raw coal pyrolysis products were used to give an idea about the quality of residue as a function of reaction time and also to identify an optimum reaction time with respect to residue quality. Different run

conditions can also be compared and a condition can be selected which gives a minimum amount of residue and maximum amount of volatile liquids. Hence this analysis was used to give the major constituents present in the autoclave residues and allow generalizations to be made as to the suitability of further processing of the autoclave residues, i.e., whether they can be used for carbonization or gasification.

The temperature of 1400°C was selected to determine the maximum amount of volatile matter present in the autoclave residues. At a temperature of 1400°C, the volatile matter was completely converted to light gases (CO, CH₄, CO₂, C₂H₄, C₂H₆, H₂O). Fixed carbon and ash were determined by heating the sample in air after pyrolysis. This analysis gave an idea about the quantity of volatile matter, fixed carbon and ash present in the autoclave residues. The relative amounts of volatile matter, fixed carbon, and ash obtained by pyrolysis from different autoclave samples when compared to the raw coal's products were used to give an idea about the reaction kinetics for autoclave residues and light gases as a function of run conditions in the coal liquefaction reactor. Residue kinetics can be used to indicate the actual changes in lignite structure during reaction in the autoclave (i.e., the amount of volatile matter and fixed carbon present in the reacting coal at different times during a run).

Three complete units were used for this study of the pyrolysis of autoclave residues, a Controlled Atmosphere Pyrolysis System (CAPS), an Elemental Analyzer (EA), and a

Solid Pyrolyzer. The units used for examining the autoclave residues were manufactured by the Chemical Data System Company, Oxford, Pennsylvania. A controlled Atmosphere Pyrolysis System (CDS-model 820D) was used for the study at 800°C. In this unit, the residue was pyrolyzed in an inert atmosphere of helium (a reactive atmosphere can also be used) by means of a Solid Pyrolyzer. The Solid Pyrolyzer consisted of a Pyroprobe and a temperature programmer. The Pyroprobe consisted of a platinum coil which could be temperature programmed. The major units of the CAPS system were a pyrolysis chamber, G.C. column, thermal conductivity bridge and a recorder. The volatile liquids and light gases liberated by the pyrolysis of autoclave residues were sent through the G.C. column (consisting of a SE-30 column) where all the volatile liquids were trapped. The light gases were then sent to a second system, an Elemental Analyzer (CDS-model 1200). The G.C. column in the CAPS was temperature programmed at 20°C/min until a final temperature of 300°C was reached. The liberated volatile liquids were then sent to a T.C. detector and their relative concentrations recorded. The elemental analyzer consisted essentially of a pyrolysis chamber, reactors, G.C. column, T.C. bridge and recorder. The light gases in the EA were passed through a G.C. column (consisting of a Porapak Q column) and analyzed. The EA was also used for examining the light gases liberated by pyrolysis at 1400°C.

EQUIPMENT

The equipment used in the study was manufactured by the Chemical Data Systems Company of Oxford, Pennsylvania. An Elemental Analyzer (CDS Model-1200) was used to study the light gases. A controlled atmosphere pyrolysis system (CDS Model-820 DEB/GC-FID) was used to study the volatile liquids. A Solids Pyrolyzer (CDS Model-100-371) was used to pyrolyze the samples.

A schematic flow diagram of the Elemental Analyzer (EA) is given in Figure 2 and the symbols are defined in Table 3. The whole unit is assembled in an oven, which can be temperature programmed from ambient to 300°C. The Elemental Analyzer has four eight-port (L,M,N,U)*, two six-port (Z,Z)* and two four-port (I,X)* valves rated to 300°C, and equipped with 1/16" swagelok fittings. The oxidation reactor (Q)* is made of 8" x 3/8" O.D. stainless steel tubing with 2" of copper oxide (CuO) wire packed in the center, held in place by quartz wool plugs. The reduction reactor is made of a 8" x 3/8" O.D. stainless steel tube with 2" of reduced copper wire packed in the center, held in place by quartz wool plugs. The reactor for determination of oxygen (R)* consists of platinized carbon packed in the center with the help of quartz wool plugs in an 8" x 3/8" O.D. stainless steel tube. The reactor for determination of sulfur or halogen (S)* consists

*The letters in parentheses are the ones on the figure.

Figure 2 Elemental Analyzer

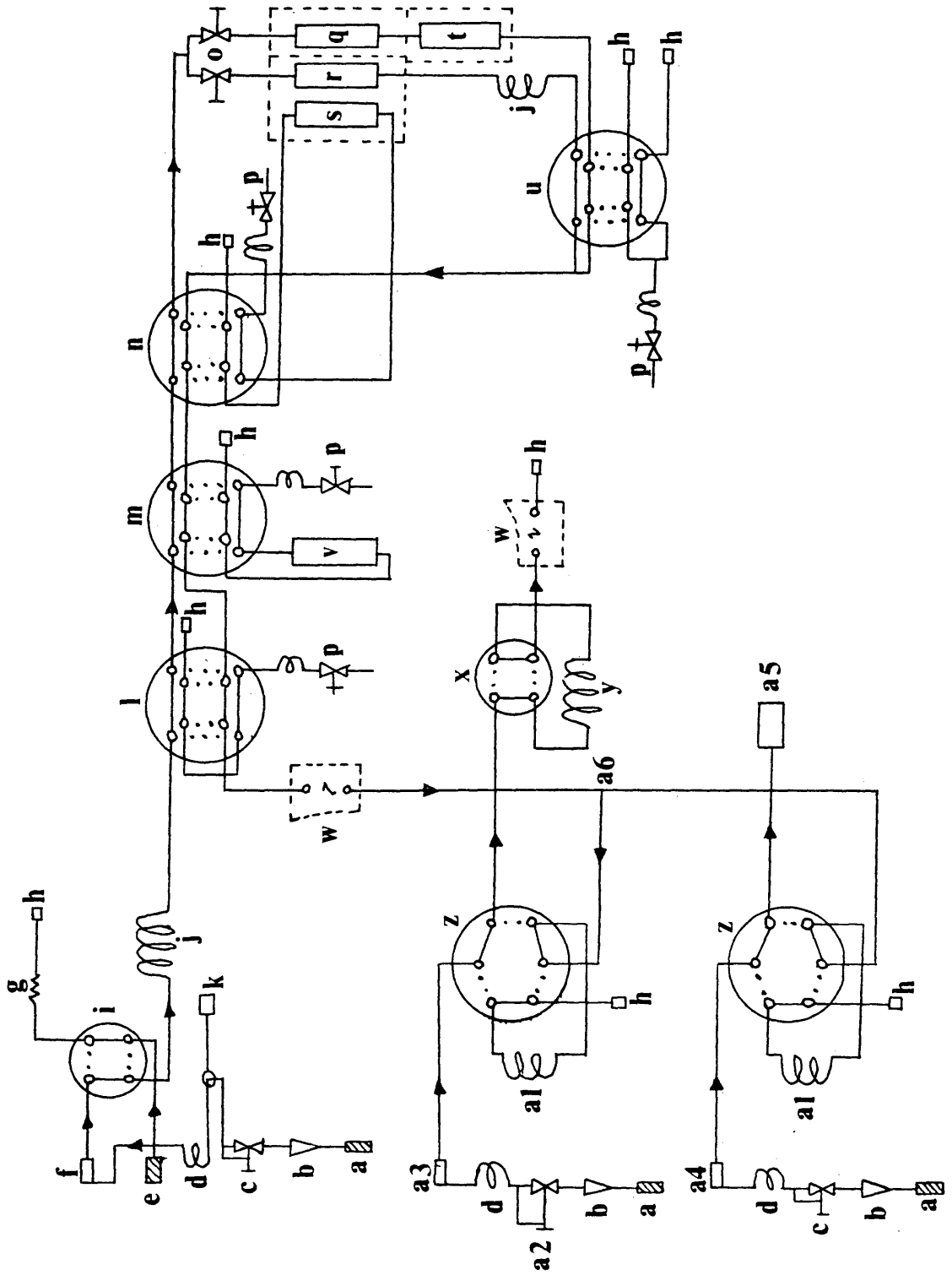


Table 3

A	= Carrier Gas Inlet
B	= Rotameter
C	= Flow Control
D	= Preheat Coil
E	= Inlet for the Gases from the Controlled Atmosphere/ Pyrolysis System (CAPS) CDS-820 DEB/GC-FID
F	= Reactor Injection Port
G	= Restriction
H	= Vent
I	= Sample Select Valve
J	= Delay Coil
K	= Interface Inlet
L	= Reactor or Bypass Selection Valve
M	= Catalytic or Thermal Reactor Selection Valve
N	= CHN-O or S/X(halogens) Reactor Selection Valve
O	= Micro Metering Valves
P	= Purge Valve
Q	= Oxidation Reactor (CHN Determination)
R	= Oxygen Determination Reactor
S	= Sulfur or Halogen Determination Reactor
T	= Reduction Reactor (for CHN Determination)
U	= Vent/Reactor Select Valve
V	= Thermal Reactor
W	= 1/2 of Thermal Conductivity Detector
X	= Column (G.C.) or Backflush Valve
Y	= Functional Group Analysis (G.C.) Column
Z	= Valve to Transfer Gases to G.C. Column or Vent
A1	= F.G.A. Transfer Coil
A2	= Pressure Regulator
A3	= F.G.A. Injection Port
A4	= Injection Port for G.C.
A5	= Gas Chromatograph
A6	= Splitting Tee

of platinum packed in the middle with quartz wool plugs around the ends of a 8" x 3/8" O.D. stainless steel tube.

The reactor temperature can be set to any desired temperature between ambient and maximum incrementally in 1°C steps with the Digidial Control. The maximum temperatures for Thermal Reactor (V)*, CHN-Oxidation Reactor (Q)*, CHN-Reduction Reactor (T)* Oxygen or SX Determination Reactor (R,S)* are 750°C, 800°C, 700°C and 975°C respectively.

Functional Group Analysis Column (Y)* is packed with Porapak Q for analysis of light gases. The maximum temperature which this column can withstand is 300°C, but for analyzing light gases column temperature was maintained at 110°C. The thermal conductivity (T.C.) bridge (Y)* has two positions on its polarity switch, by which the polarity of T.C. bridge output to the recorder can be reversed. The bridge current control can be set from about 60 milliamps (ma) to the normal operating region of between 150 and 200 ma with a maximum of 200 ma. The maximum temperature for T.C. detector is 350°C while the normal operating temperature is between 200-250°C. The injection ports have a maximum temperature of 300°C while their normal operating temperature is 200-250°C. The transfer lines have a maximum temperature of 300°C while their normal operating temperature is 200-250°C. The temperatures at various points in the instrument are sensed by platinum resistance thermometers and are controlled by zero crossing, fully proportional temperature controllers. A pulsating lamp is provided for each temperature

control point which will pulsate until the set temperature is reached and will then glow intermittently. The recorder used for recording the concentrations of light gases was made by Honeywell (Model-Electronic-196).

A sample was introduced into the unit by direct injection by means of a pyroprobe into the Reactor Injection Port (F)* or from the Controlled Atmosphere Pyrolysis System (E)* by means of the sample select valve (I)*. Sample then proceeds through a delay coil (J)* into the reactor bypass valve (L)* which is in parallel with the various reactors. When the reactor bypass valve is in the bypass position (dotted lines on L), sample flows directly from delay coil to the first half of the thermal conductivity cell (W)*, FGA (Z)*, and SD (Z)* transfer valves. This enables the reactor to be eliminated from the flow system for system checking or to transfer a sample to the internal or external G.C. When the reactor bypass valve is in the reactor position (solid lines on L), sample flows into the reactor select catalytic/thermal valve (M)*. With this valve in the catalytic position the flow then enters the reactor select CHN-O/S-X valve (N)*. With this valve in the CHN-O position sample will pass through the catalytic reactor, split flow adjust valves (O)* and then to the CHN and O reactors. If one of the catalytic reactor split flow adjust valves is turned off then the entire flow will pass through the other reactor. The O reactor (R)* consists of a single stage whereas the CHN reactor consists of an oxidation reactor (Q)* followed by a reduction reactor (T)*.

From the reactor the sample flows into the vent select valve (U)* which in the CHN-0 position, recombines the two flows which then pass back through the reactor select CHN-0/S-X valve (N)*, the reactor select catalytic/thermal valve (M)* and the reactor bypass valve (L)*.

With the reactor select catalytic/thermal (C/T) valve in the thermal position, sample flows through the thermal reactor and then back through the reactor select C/T valve to the reactor bypass valve (L)*. After the reactor bypass valve (L)*, the sample flows to the first half of thermal conductivity cell and then it is split at the splitting tee (A6)* into two portions, one of which enters the structure determination transfer valve (Z)*. When the structure determination transfer valve is in the fill position the sample enters the structure determination transfer coil. This transfer coil has a volume of 66 ml so it will hold a peak of more than 2 minutes duration at a flow rate of 25 ml/min in this coil. The completion of the sample entering the transfer coil is indicated by the peak from the first half of the thermal conductivity detector returning to baseline plus a delay period. The duration of this period depends on the reactor flow rate and the flow path - either bypass (small) thermal or catalytic S-X or catalytic CHN-0 (large).

When the structure determination transfer valve is switched to the run position the structure determination coil is backflushed by a separate helium flow into the analytical gas chromatograph (A5)*. This arrangement allows the helium

flow in the elemental analyzer to be independent of those required for analysis. Standards may be conveniently injected into the analytical gas chromatograph (A5)* through the structure determination injection part (A4)*.

The other half of the flow after the splitting tee enters the functional group analysis transfer valve (Z)*. When the functional group analysis transfer valve is in the fill position the sample enters the functional group analysis coil (A1)*. This transfer coil has a volume of 66 ml so it will hold a peak of more than 2 minutes duration at a flow rate of 25 ml/min in the coil. The completion of the sample entering the transfer coil is about 1 minute (depending on the reactor flow rate) after the peak generated by the first half of the thermal conductivity detector returns to the baseline as described above. When the functional group analysis transfer valve is switched to the run position the functional group analysis coil is backflushed by a separate helium flow into the internal gas chromatograph column (Y)*. This arrangement allows the helium flow in the reactor path of the elemental analyzer unit to be independent of the internal gas chromatograph flow. The internal gas chromatograph column is operated so that it will separate CO, CH₄, CO₂, C₂H₄, C₂H₆, H₂S, NH₃ and H₂O for functional group analysis or N₂, CO, CO₂, H₂S and H₂O for elemental analysis.

As larger molecules could enter the internal gas chromatograph column a backflush valve (X)* is provided so that the larger molecules can be conveniently removed after the analysis

is complete. After the components elute from the column they are detected by the second half of the thermal conductivity detector (W)* and finally flow to the thermal conductivity vent. Standards may be conveniently injected into the internal G.C. through the functional group analysis injection port (A3)*.

A schematic flow diagram of controlled Atmosphere Pyrolysis System (CAPS) is given in the fig. 3 and the symbols are defined in Table 4. The entire unit is enclosed in an oven. The oven temperature can be varied from ambient to 300°C, but usually is not operated below 200°C. The CAPS system has two eight-port (E,F)*, one six-port (G)*, and one four-port (D)* valves. Trap (J)* is pulse heated by means of heating block (I)* and it consists of a U tube packed with Poropak Q. The maximum temperature which this column can withstand is 250°C. The sample (K)* and reference (L)* columns are packed with SE-30 and can be temperature programmed from ambient to 300°C. The thermal conductivity (T.C.) cell has two positions on its polarity switch and the output to the recorder can be reversed by switching the position on the polarity switch. The bridge current control can be set from 60 ma to the normal operating region of between 150 and 200 ma with a maximum of 200 ma. The maximum temperature for T.C. cell is 350°C while the normal operating temperature is between 200-250°C. A flame ionization detector (FID) (O)* can also be used to identify the pyrolysis products. The recorder used for recording the relative concentrations of

Figure 3 Controlled Atmosphere Pyrolysis System

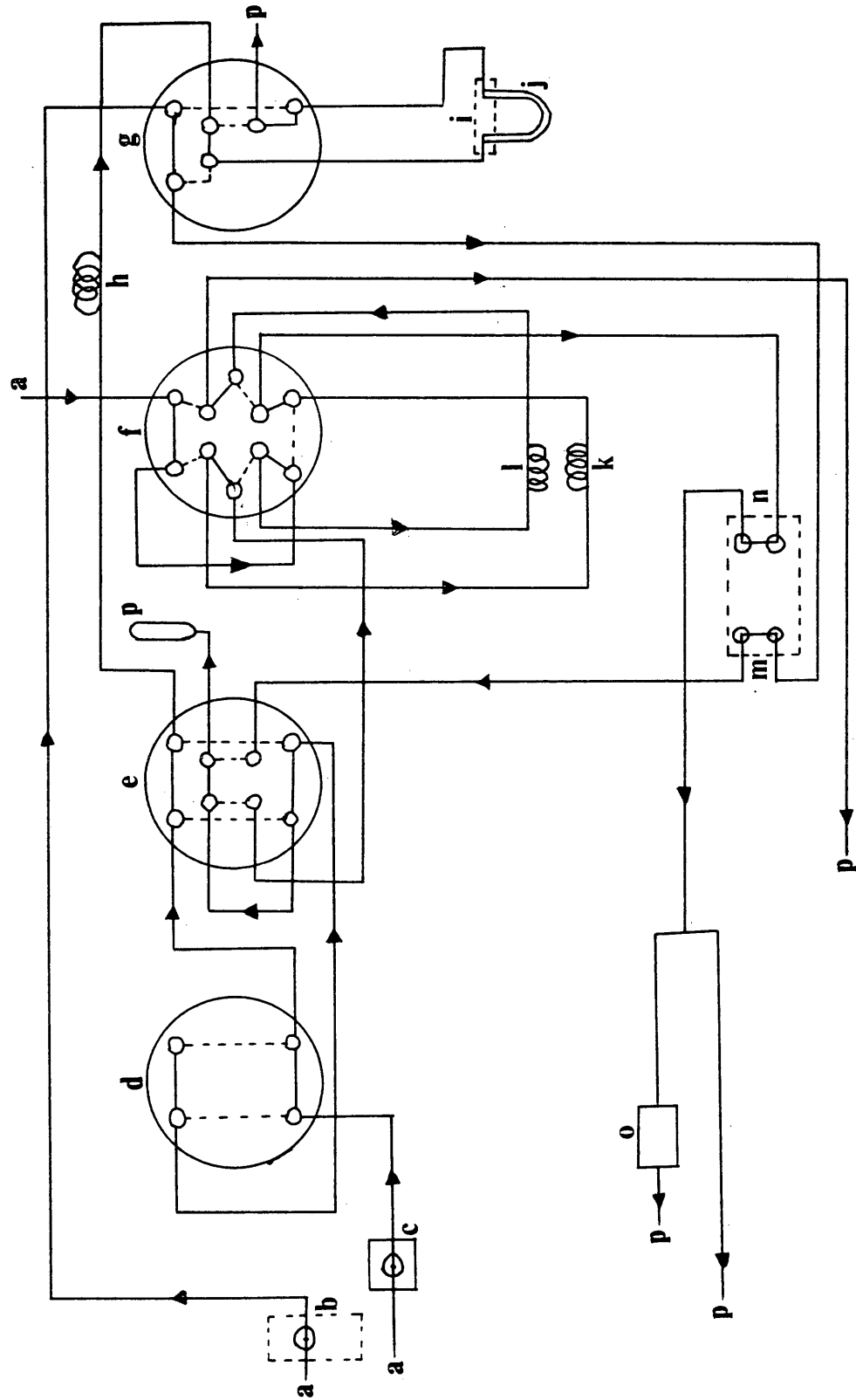


Table 4

- A = Carrier gas inlet
- B = Inlet for injecting the sample in the G.C. column
- C = Inlet for injecting the sample either to G.C. or to the trap
- D = Reactor or G.C. selection valve
- E = Trap or bypass selection valve
- F = Stop or flow valve
- G = Trap or transfer valve
- H = Delay coil
- I = Heating block
- J = U shaped trap
- K = Sample column in the G.C.
- L = Reference column in the G.C.
- M = 1/2 thermal conductivity detector
- N = 1/2 thermal conductivity detector
- O = Flame ionization detector
- P = Vent

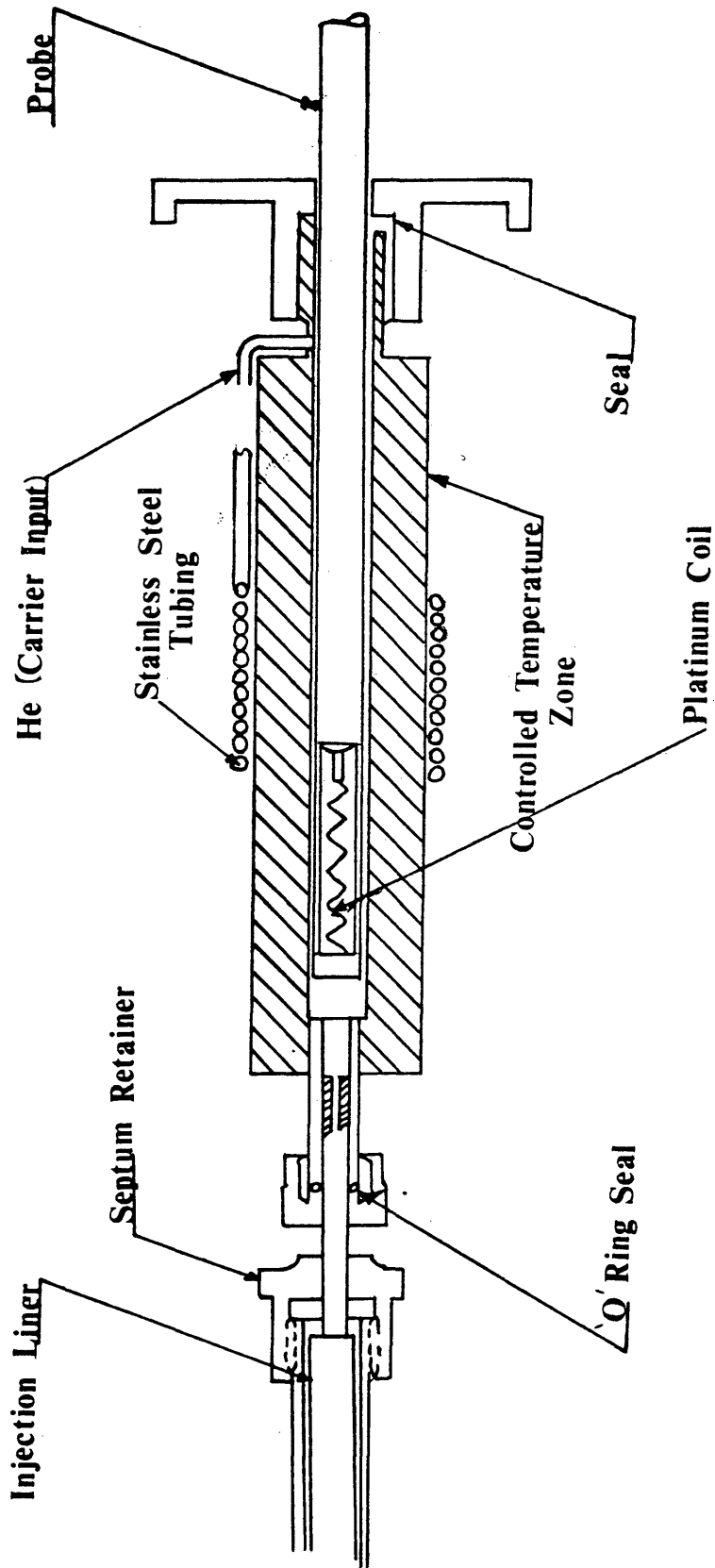
pyrolysis products was manufactured by Honeywell (Model Electronik-196). Controlled Atmosphere Pyrolysis Chamber (CDS-Model 100-372) shown in fig. 4 is used for pyrolyzing the samples and is situated in fig. 3 at position B and C. The probe used for pyrolysis is also shown in fig. 4. This chamber is made of stainless steel, and has a temperature range from ambient to 500°C. The temperatures at various points in the unit are sensed by platinum resistance thermometers and are controlled by zero crossing fully proportional temperature controllers. The transfer lines have a maximum temperature of 300°C while their normal operating temperature is 200-250°C.

Procedure for Operation

In the CAPS unit, either reactant gases or helium can be used for the atmosphere in the pyrolysis chamber. The gases after flowing through the flow controller are blended in a heated stainless steel mixer. After mixing (in the case of reactant gases), the gases are delivered to the inlet line of the controlled Atmosphere Pyrolysis Chamber (fig. 4).

The mixed gases or helium pass through a helix of 1/16" O.D. stainless steel tubing wound around the controlled temperature controlled atmosphere chamber (CTCAC) (fig. 4). The mixed gases reach CTCAC temperature before entering at the head of chamber and sweeping the gas-solid phase reaction zone. Reaction occurs upon actuating the ribbon or coil probe by pressing the run button on the temperature programmer

Figure 4 Continuous Atmosphere Pyrolysis Chamber



of the solid pyrolyzer system (CDS-model 100-371).

The reaction products pass through the reactor/G.C. selection valve (D)* if the sample is pyrolyzed in the injection port situated in fig. 3 at position C. When the reactor/G.C. valve (D)* is in the reactor position (solid lines of D) the reaction products enter trap or bypass valve (E)*. With this valve in trap position, the flow then passes through a 1/8" stainless steel delay coil to the inlet port of the trap or transfer valve (G)*. When the trap/transfer valve (G)* is in the trap position, the flow enters a U tube packed with Porapak Q (J)* and then through an exit vent (P)*. The vent (P)* can be used for monitoring the total mixed reactant gas flow.

The trapping efficiency of the Porapak Q U tube depends upon the temperature that it is maintained at. If the tube is inserted in liquid nitrogen, it will trap all materials liquefied at -190°C . To recover materials from the trap, the trap/transfer valve is switched to transfer position and the trap heated to the desired upper temperature. The reaction products then pass through the first half of the T.C. cell (M)* and then to the trap/bypass valve (E)*. With this valve in trap position, the flow then enters the stop/flow valve (F)*. With this valve in stop position, the flow enters the G.C. column (K)*, which can be temperature programmed. After the G.C. column, the flow enters the other half of T.C. cell after passing through the stop/flow valve. The signals from T.C. cell were recorded on a recorder

manufactured by Honeywell (model-Electronik-196). The flow then passes through a splitting tee where 1/20 of it goes to a flame ionization detector (O)* and the rest to the elemental analyzer or vent. The flow after FID is vented through vent (P)*.

A sample if pyrolyzed in the injection port shown in fig. 3 at B follows the same path as above except that it does not enter the trap if the trap/transfer valve is in the trap position.

The Solid Pyrolyzer consists of a probe shown in fig. 4 and a temperature programmer.

EXPERIMENTAL PROCEDURE

Autoclave Run

Coal slurry was charged to a pre-heated batch autoclave reactor containing solvent and an equimolar mixture of hydrogen and carbon monoxide gas. Hot charging of reactants was used to minimize the effects of heat-up time. During experimental runs, a 3-4 gram liquid sample was collected from the autoclave at different time intervals. The organic product was extracted from this sample with tetrahydrofuran (THF) using millipore filtration. The insoluble product obtained from THF extraction was used for pyrolysis. Table 5 shows the run numbers, corresponding reaction conditions, type of coal and solvent used and the feed composition for the autoclave runs from which residues were obtained. Ultimate analysis for the coals used were shown previously in Table 2.

Sample Preparation

Autoclave residues were first extracted with tetrahydrofuran (THF), to dissolve all the liquid products and the solvent. The resulting slurry was filtered through a 50 micron millipore filter to separate the THF-insoluble residue. The coal residue so obtained was dried in an oven at 60-80°C. A quartz tube filled with quartz wool at one end was weighed on a CAHN electronic balance, and the tube was then filled with 3-8 milligrams of coal residue and weighed again. The other end of the quartz tube was then filled with quartz

Table 5. Run Conditions.

Run No.	Temperature	Pressure	Coal	Solvent	Coal to Solvent Ratio
23 ³	438°C	1850 psi	Beulah Std. #2	Anthracene Oil	1:4
26 ³	437°C	3600 psi	Orange Pit #43	Anthracene Oil	1:4
27 ³	437°C	3900 psi	Beulah Std. #2	Anthracene Oil + Tetralin (6.4%)	1:4
28 ³	435°C	3950 psi	Orange Pit #43	Anthracene Oil + Tetralin (6.4%)	1:4
30 ¹	475°C	4300 psi	Beulah Std. #2	Anthracene Oil + Tetralin (6.4%)	1:4
31 ²	440°C	4100 psi	Beulah Std. #2	Anthracene Oil + Tetralin (6.4%)	1:4

¹Slow heat up

²Fresh gas charged during run

³Batch run, reactants charged into pre-heated reactor at reaction temperature and pressure

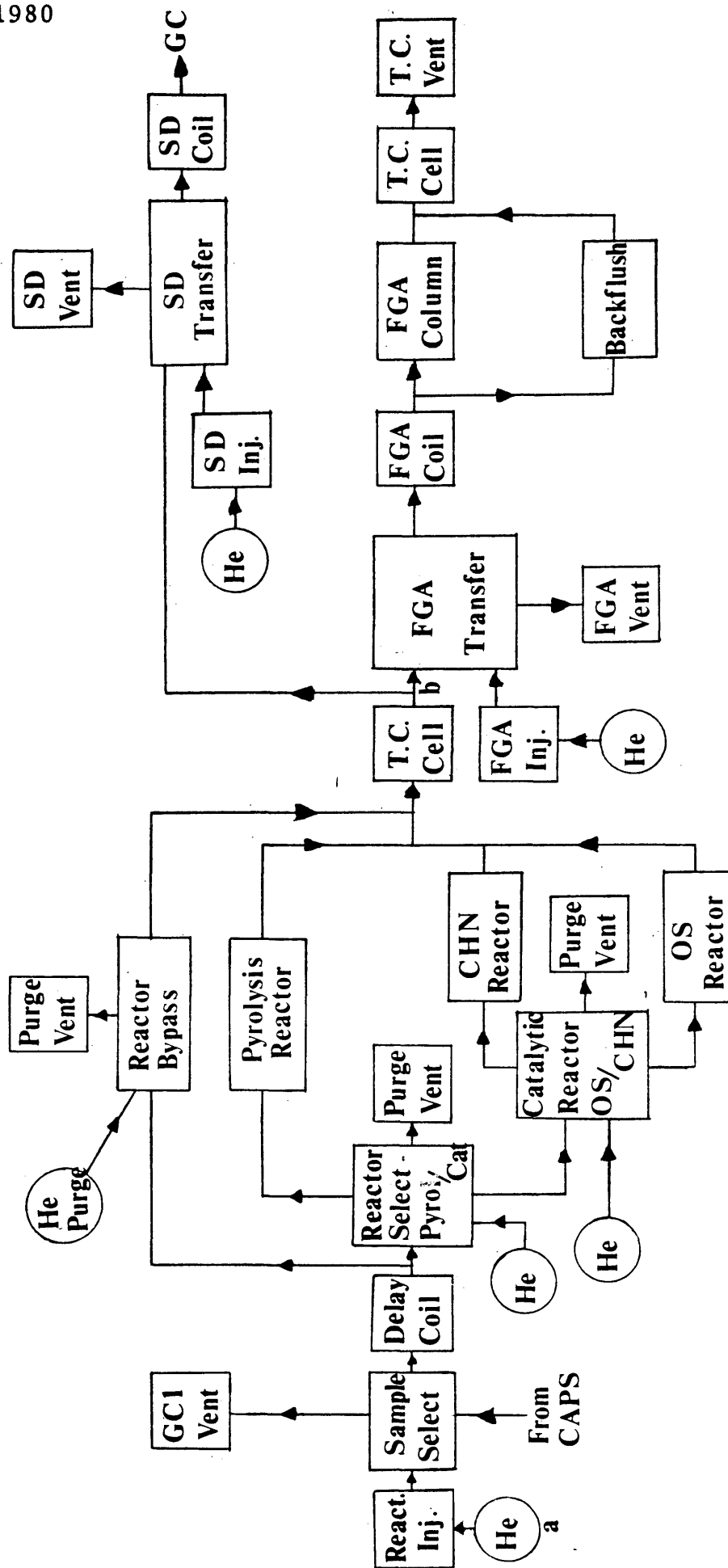
wool and the tube weighed again. The reason for filling the quartz tube with quartz wool at both ends was to prevent loss of solid sample due to rapid heating and handling.

Pyrolysis in Elemental Analyzer

A block diagram of the Elemental Analyzer (EA) is shown in fig. 5. The temperature of the oven enclosing the EA was maintained at 250°C. The flow rate of helium carrier gas to EA was kept constant by setting the flow every day with a soap bubble meter, and the pressure of helium gas at the inlet (A) of EA was maintained at 80 psig. Flow rates to Functional Group Analysis (FGA) column and thermal conductivity (TC) cell were kept at 0.316 ml/sec and 0.543 ml/sec, respectively. The T.C. detector was kept at a temperature of 225°C and the current flowing through it was regulated at 175 ma. The Porapak Q column in FGA was kept at 110°C.

To start a pyrolysis run, the quartz tube containing the sample was placed in a coil probe and the coil probe inserted into Reactor Injection Port. The recorder was then stabilized at the lowest attenuation. Sample was then pyrolyzed at a rate of 100°C/sec until a final temperature of 1400°C was reached. Sample was maintained isothermally at 1400°C for 10 secs after the final temperature of 1400°C was reached. The liberated products from the Reactor Injection Port passed through a reactor bypass to the first half of the T.C. bridge. The polarity of the T.C. bridge was switched after a combined peak of products appeared on the recorder. The

Figure 5 Block Diagram Of Elemental Analyzer

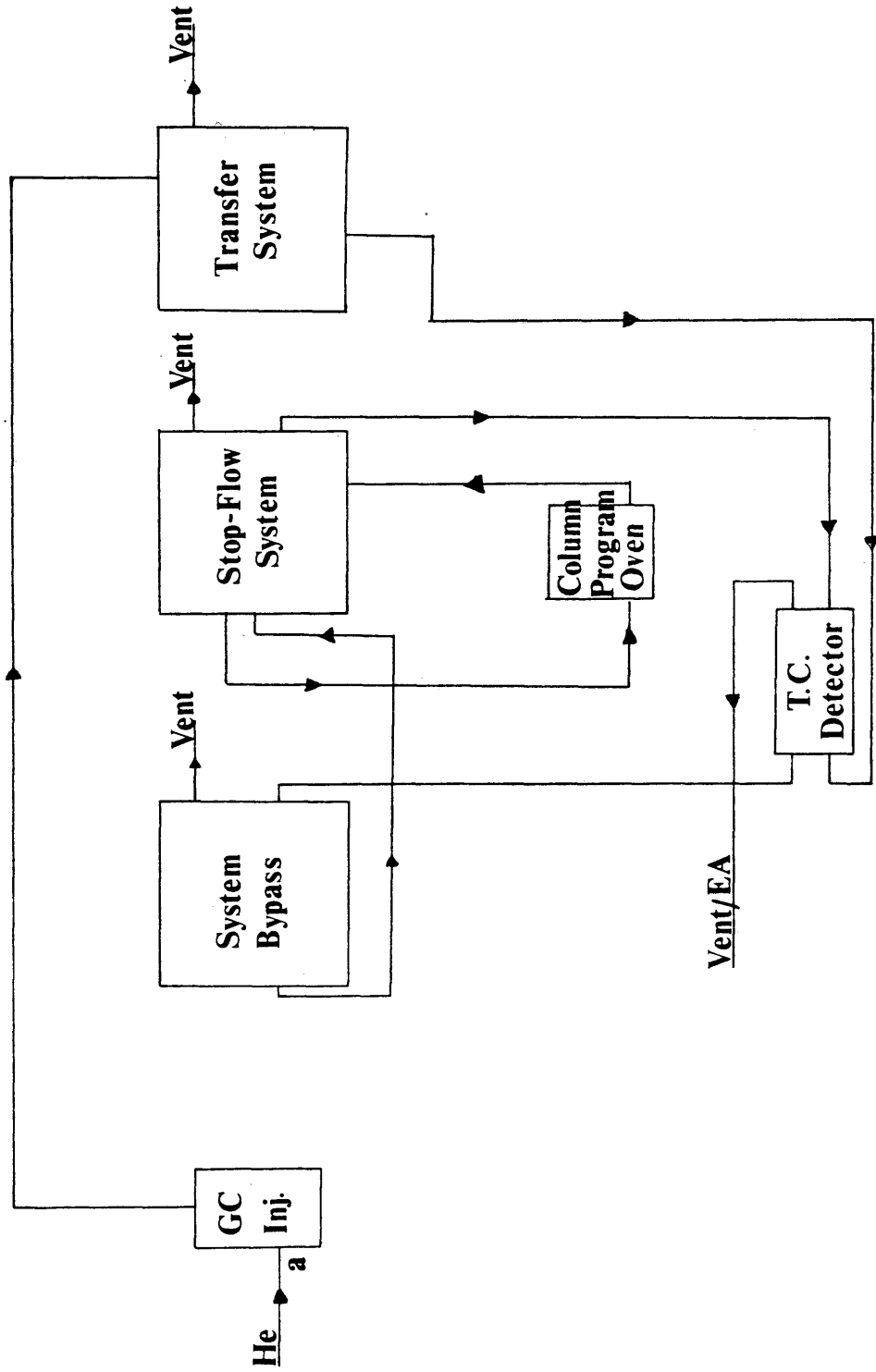


products were split in half at point B (fig. 5), and half of the product sent to FGA transfer system while the other half was sent to the structural determination (SD) transfer system. Volume of the FGA coil was 66 ml, therefore at a flow rate of 0.316 ml/sec, it held the sample for 3.48 min. The products were allowed to collect in the FGA coil for 2.5 min, after a combined peak of products appeared on the recorder, to make sure that all the products were trapped in the FGA coil and then the products were passed through the FGA column. It took 10 minutes to elute all the products from the FGA column, with water the last peak to appear on the recorder. After the water peak, the recorder was stopped and the FGA column backflushed for 10 minutes to purge the column. The peaks so obtained were then analyzed.

Pyrolysis in Controlled Atmosphere Pyrolysis System (CAPS)

A block diagram of the CAPS is shown in fig. 6. The oven enclosing the CAPS was kept at a temperature of 250°C. The flow rate of helium carrier gas to CAPS was kept constant by setting the flow every day with a soap bubble meter. The pressure of helium gas at the inlet (A) of CAPS was maintained at 80 psig while the flow rate to system bypass and stop flow systems were kept at 1 ml/sec. The temperature of the G.C. Injection port was maintained at 225°C. The T.C. detector was kept at a temperature of 225°C and the current flowing through it was regulated at 175 ma. Sample and reference SE-30 columns of the G.C. were kept at 60°C initially.

Figure 6 Block Diagram Of Controlled Atmosphere Pyrolysis System



The quartz tube containing the sample was placed in a coil probe and the coil probe inserted into the G.C. Injection port. The recorder was then stabilized at the lowest attenuation. Sample was then pyrolyzed at a rate of $100^{\circ}\text{C}/\text{sec}$ until a final temperature of 800°C was reached. Sample was kept isothermally at 800°C for 16 secs after the final temperature of 800°C was reached in 8 secs. The liberated products from the G.C. Injection port passed through a transfer system to the first half of the T.C. bridge. The polarity of T.C. bridge was switched after a combined peak of products was observed on the recorder. The products then passed through system bypass to the stop-flow system. The products were then sent through the G.C. column (in the column program oven), where all the heavier liquid products were trapped. Light gases passed on to the second half of the T.C. bridge and then to the EA. The light gases in the EA were analyzed as described above. The G.C. column was then heated at a rate of $20^{\circ}\text{C}/\text{min}$ until a final temperature of 300°C was reached to elute the lighter liquid components from the column. The G.C. column was kept isothermally at 300°C for 15 min after the final temperature of 300°C was reached. Liquid components eluted were sent directly to the TC detector. An integrator was used for peak area calculation.

ANALYSIS OF DATA

The light gases evolved during pyrolysis were analyzed quantitatively by using calibration curves obtained from injecting pure CO, CO₂ and a gas mixture into the elemental analyzer. The composition of the calibration gas mixture is given in Table 6. Benzene was used for obtaining the calibration curve for water. The analysis of calibration gases (except benzene) was done in the same fashion as product gases. For benzene, the catalytic reactor of the elemental analyzer was used to convert the liquid into CO₂ and H₂O. The calibration curves for light gases and water are presented in figs. 7 through 13. In the calibration curves, peak height is plotted against ml of sample injected for all light gases except water, in which case peak height is plotted against micro-litres of benzene injected. Factors for converting from ml (or μ l in the case of benzene) to grams of light gas are given in Table 7. The method used to analyze the gas was to read the peak heights of individual gases (identified from calibration gas retention times) and then use the calibration curves to obtain the amount of sample that would produce a peak of the same height. From the amount of sample, the weight of the gas was obtained by multiplying by the appropriate conversion factor.

Since the heavier liquid products obtained during pyrolysis resembled the components present in anthracene oil,

Table 6. - Analysis of Gas Mixture

<u>Constituent</u>	<u>Mole %</u>
CH ₄	90.70
C ₂ H ₆	3.48
C ₃ H ₈	.96
CO ₂	.67
N ₂	3.70
isobutane	0.19
n-butane	<u>.19</u>
Total	99.90

Table 7. - Conversion Factors

	From ml of Sample Injected to mgm Multiply by	
CO	1.1316	
CO ₂	1.7750	
CH ₄	.6432	
C ₂ H ₆	.0246	
C ₂ H ₄	1.1316	
C ₃ H ₈	.0068	
H ₂ O	.0676	(from μ L of sample to mgm)

Figure 7. - Calibration Curve of CO.

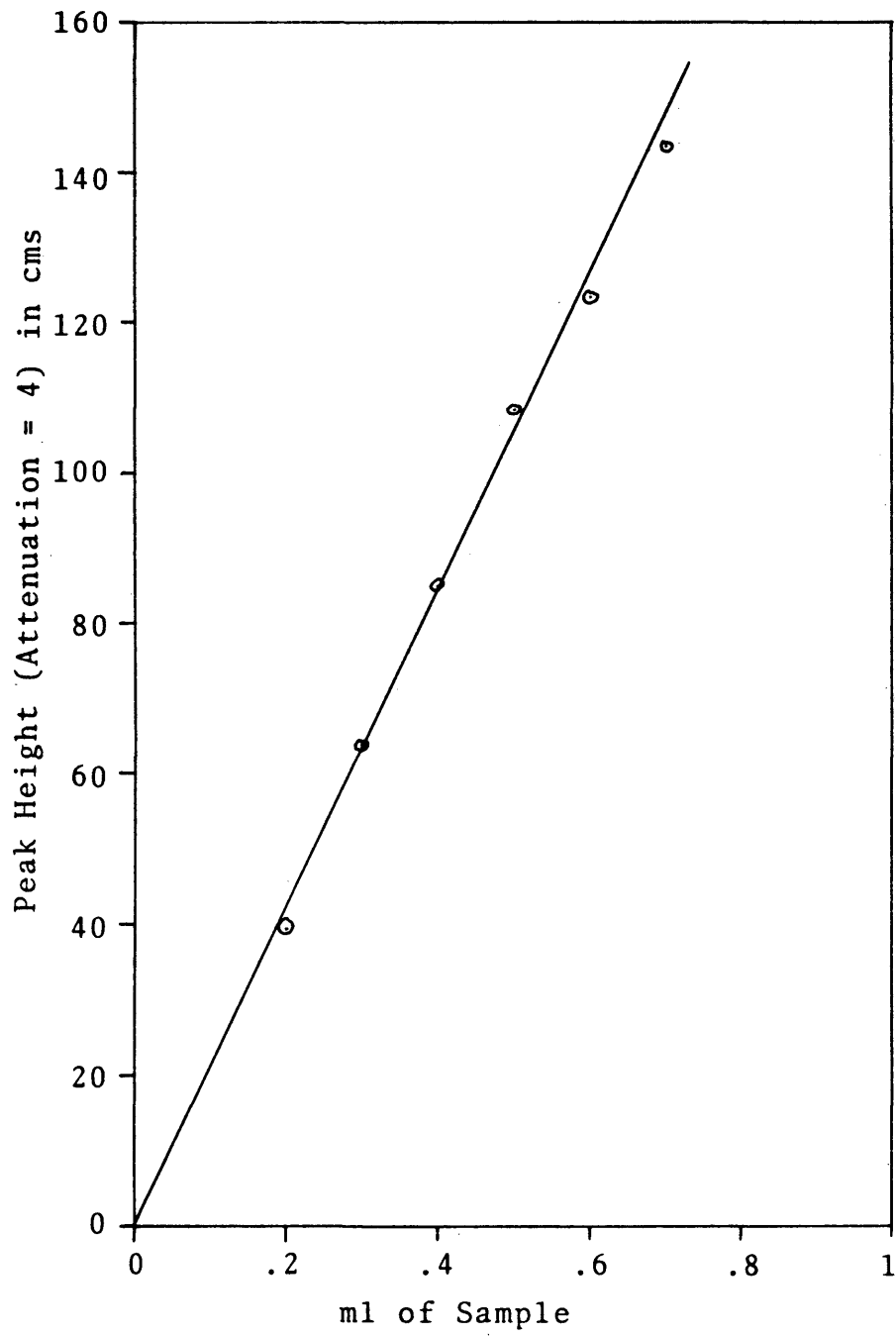


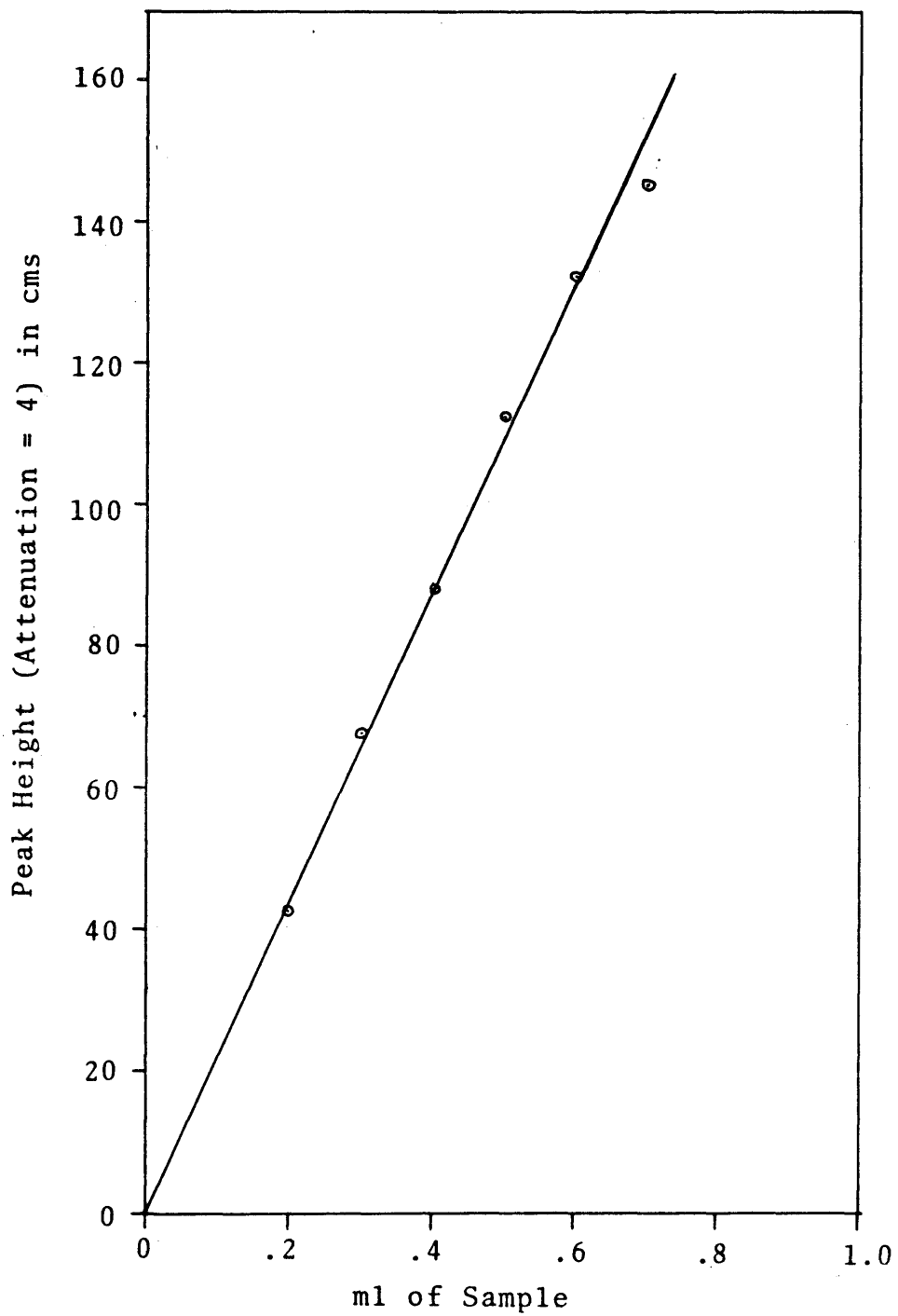
Figure 8. - Calibration Curve of CO₂

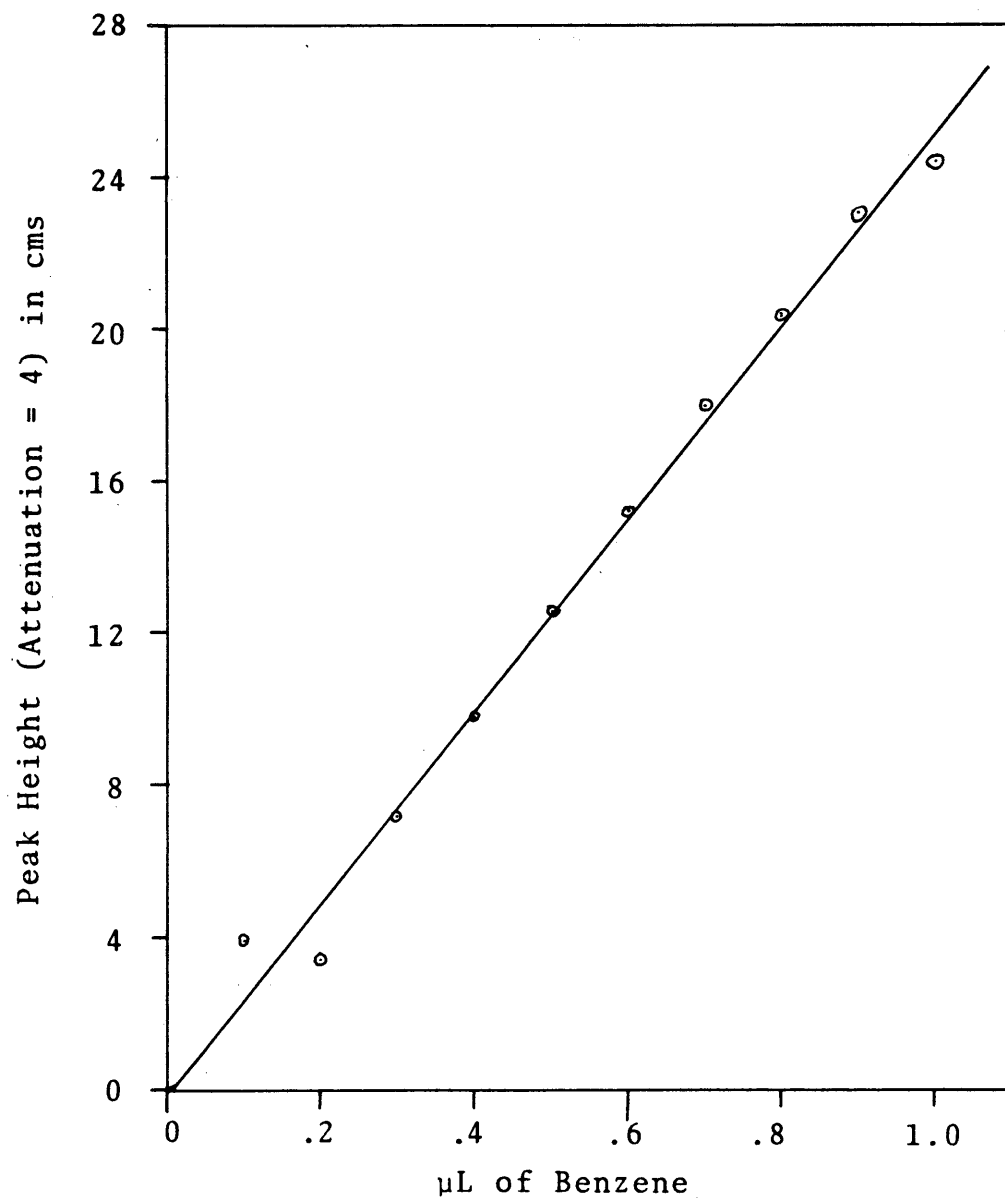
Figure 9. - Calibration Curve of H₂O

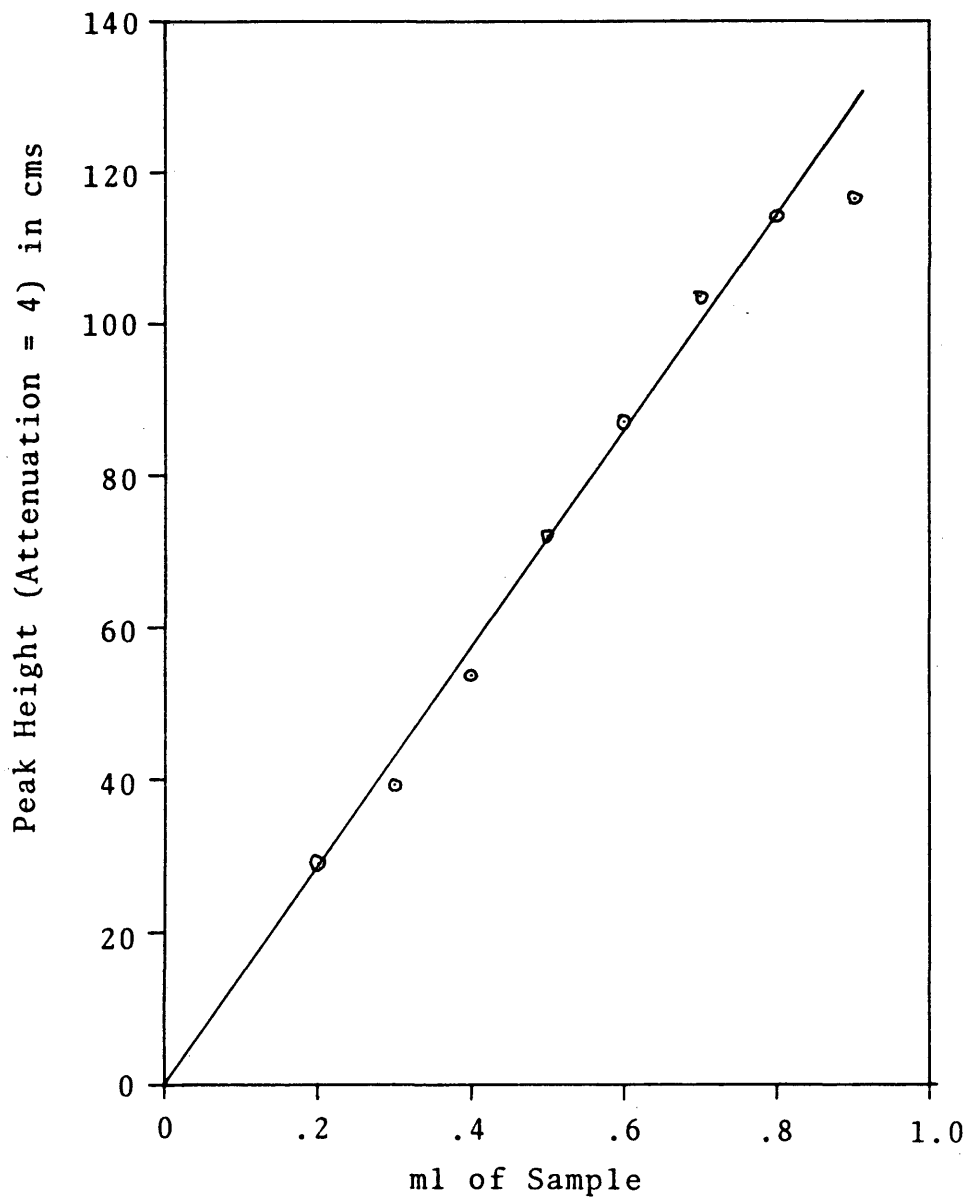
Figure 10. - Calibration Curve of CH₄

Figure 11. - Calibration Curve of C₂H₄

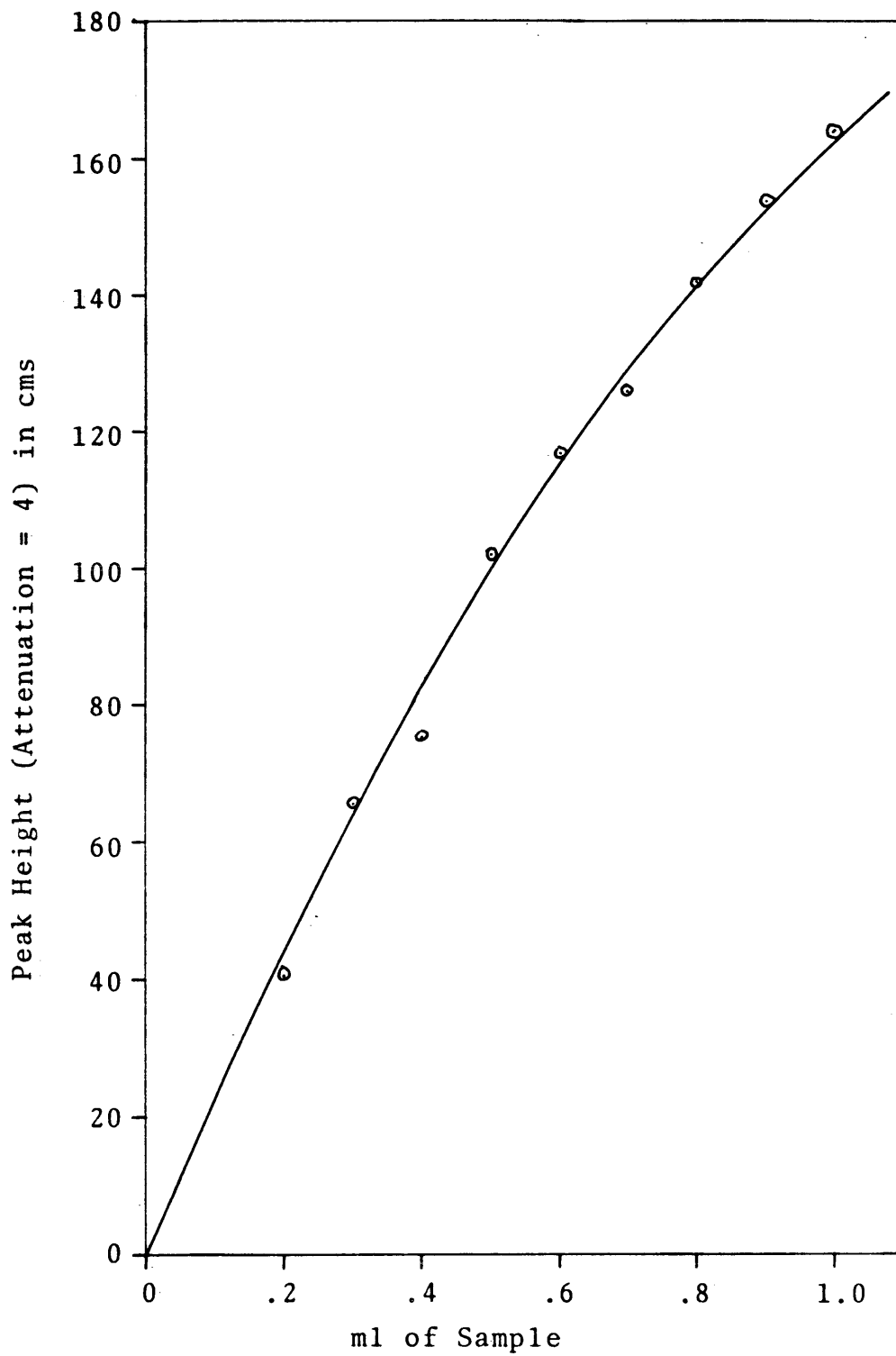


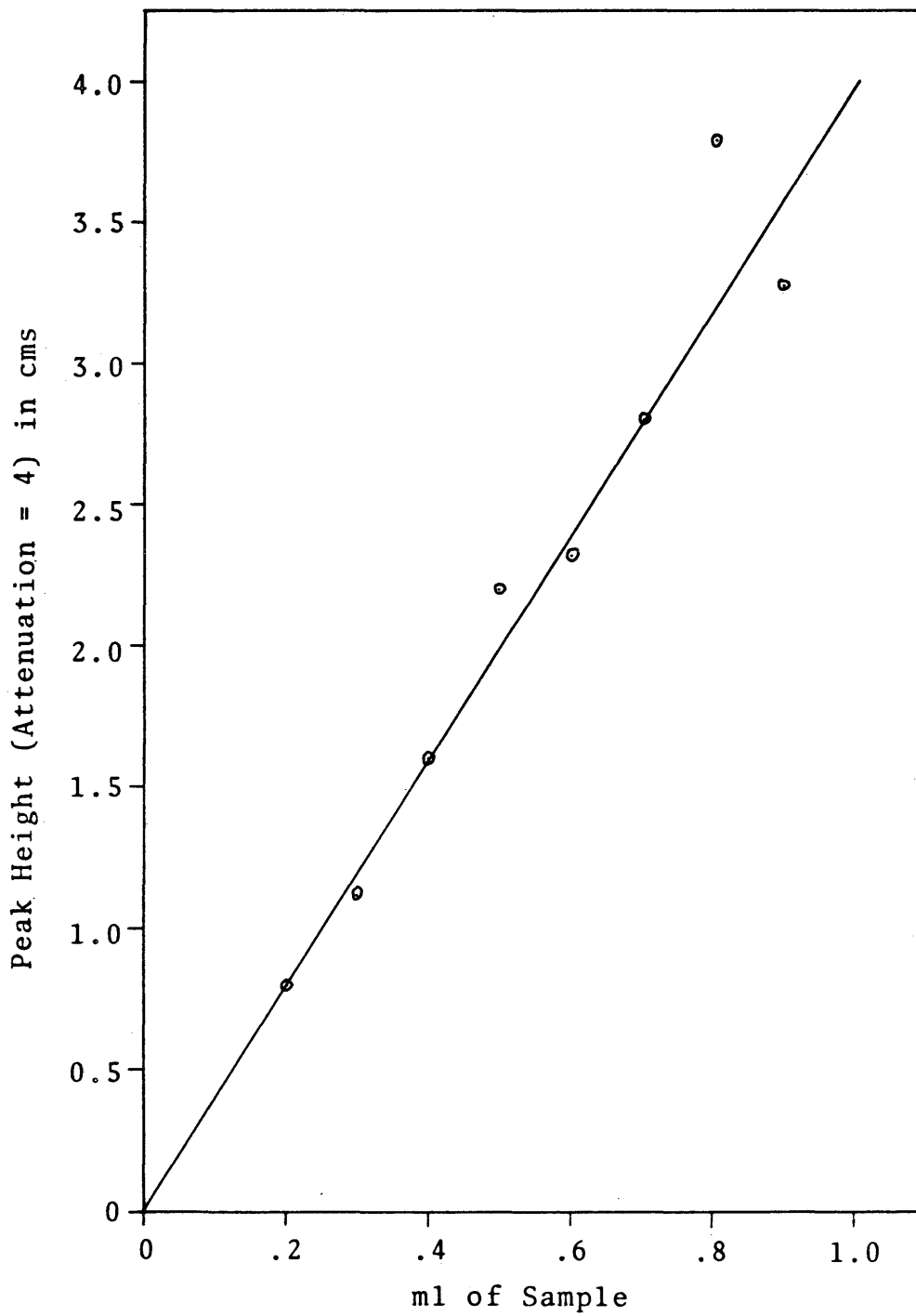
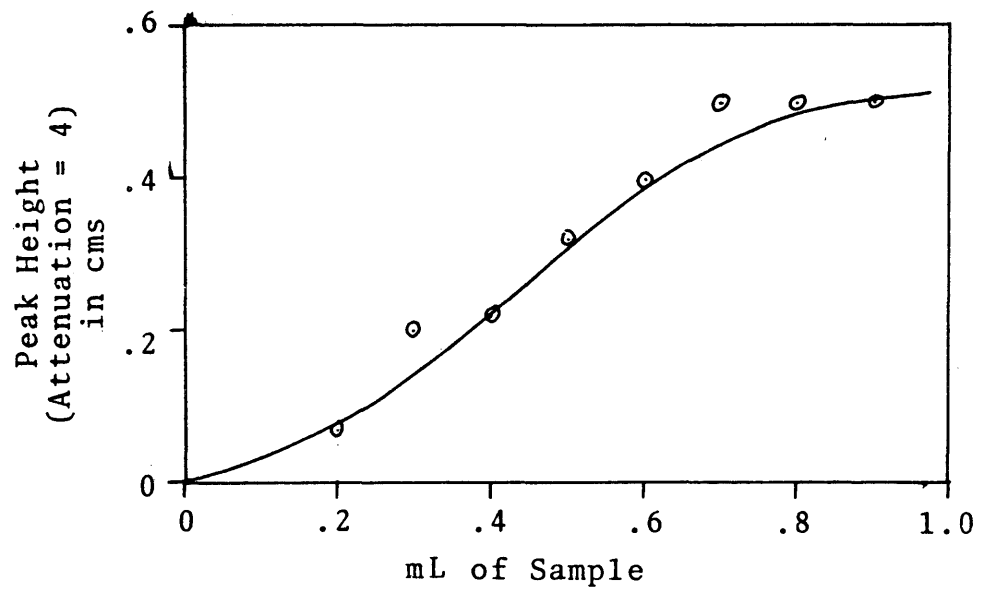
Figure 12. - Calibration Curve of C_2H_6 

Figure 13. - Calibration Curve of C_3H_8 

this oil was used for a calibration standard. Retention times of the liquid products were compared with the products of anthracene oil pyrolysis. A sample of anthracene oil was run twice a day, once at the start of the runs, and once at the end in the CAPS unit to obtain retention times and peak heights of the components present in the anthracene oil. One such run is shown in fig. 14 and the peaks are identified in Table 8. The change in the base line was due to the fact that the G.C. column was temperature programmed causing the baseline shift. A correction for the changing base line was obtained by temperature programming the G.C. column without a sample at the beginning of the runs each day. The reason for using the peak height instead of peak area (which is more accurate), was that the peak heights of the standard anthracene oil components during different runs were quite close as compared to peak areas which were quite erratic due to incomplete resolution and the shift in the base line. The peaks and their order was further confirmed by running a sample of anthracene oil on a GC-mass spectrometer. This analysis is shown in fig. 15, with the identification of the peaks given in Table 9 and the weight percent of each component in the anthracene oil given in Table 10. For obtaining the response factors, naphthalene was chosen as a standard. This also was the standard used for calculating the weight percentages of the different components in the anthracene oil. Since the same amount of anthracene oil was analyzed in CAPS as well as in the GC-mass spectrometer, the

Figure 14. - Gas Chromatogram of Anthracene Oil from Unit CAPS

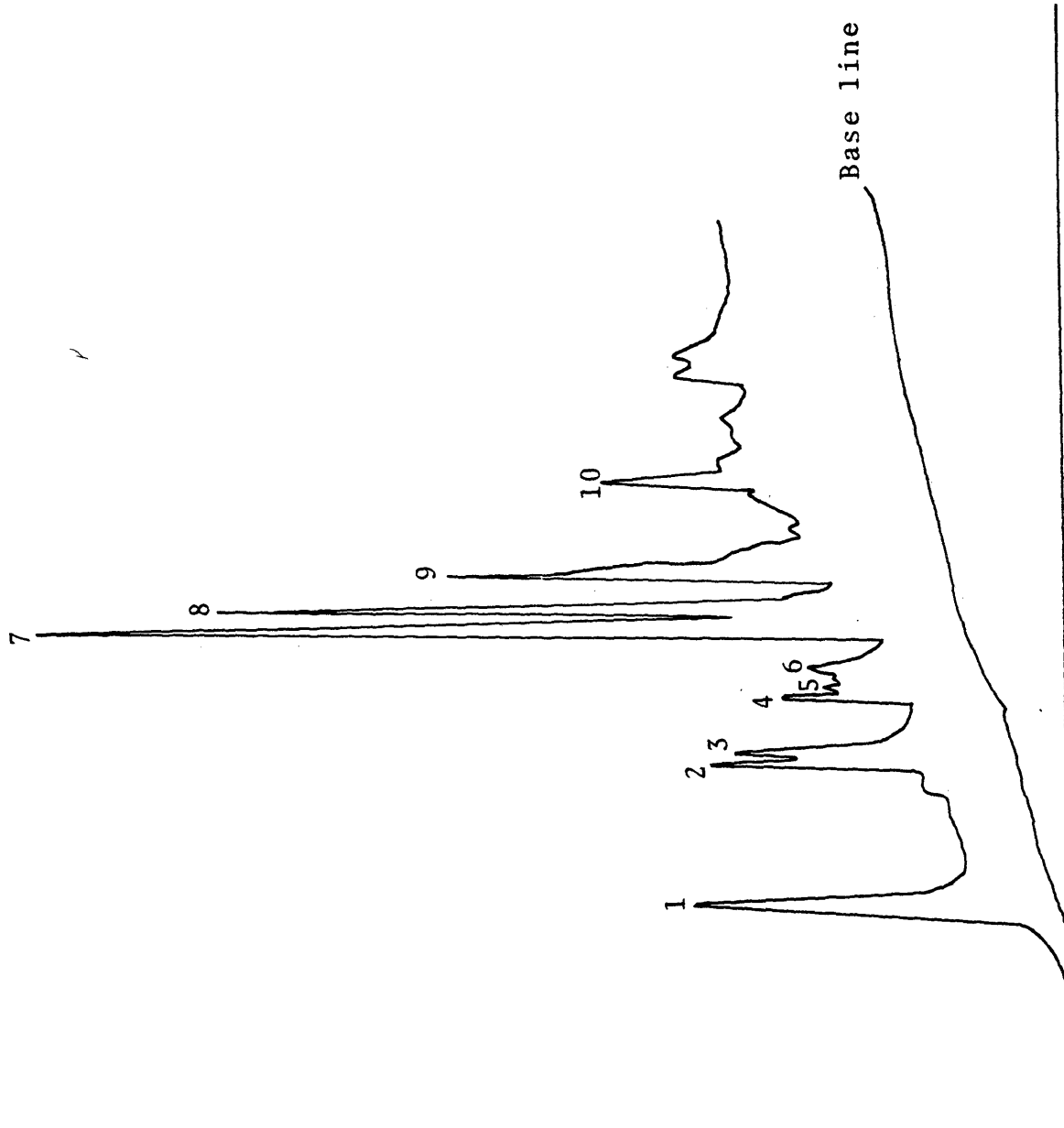


Table 8. - Constituents of Anthracene Oil Found by the Unit CAPS.

Constituent	Retention Time (secs)	Peak Height (Att. 5)
1. Naphthalene	83	5.15
2. β -Me-naphthalene	178	4.30
3. α -Me-naphthalene	186	4.05
4. Biphenyl	223	3.06
5. Dimethylnaphthalene	230	2.45
6. Dimethylnaphthalene	245	2.48
7. Acenaphthene	274	13.25
8. Dibenzofuran	286	10.60
9. Fluorene	310	7.17
10. Phenanthrene	373	4.70

Figure 15. - Gas Chromatogram of Anthracene Oil from GC-Mass Spectrometer

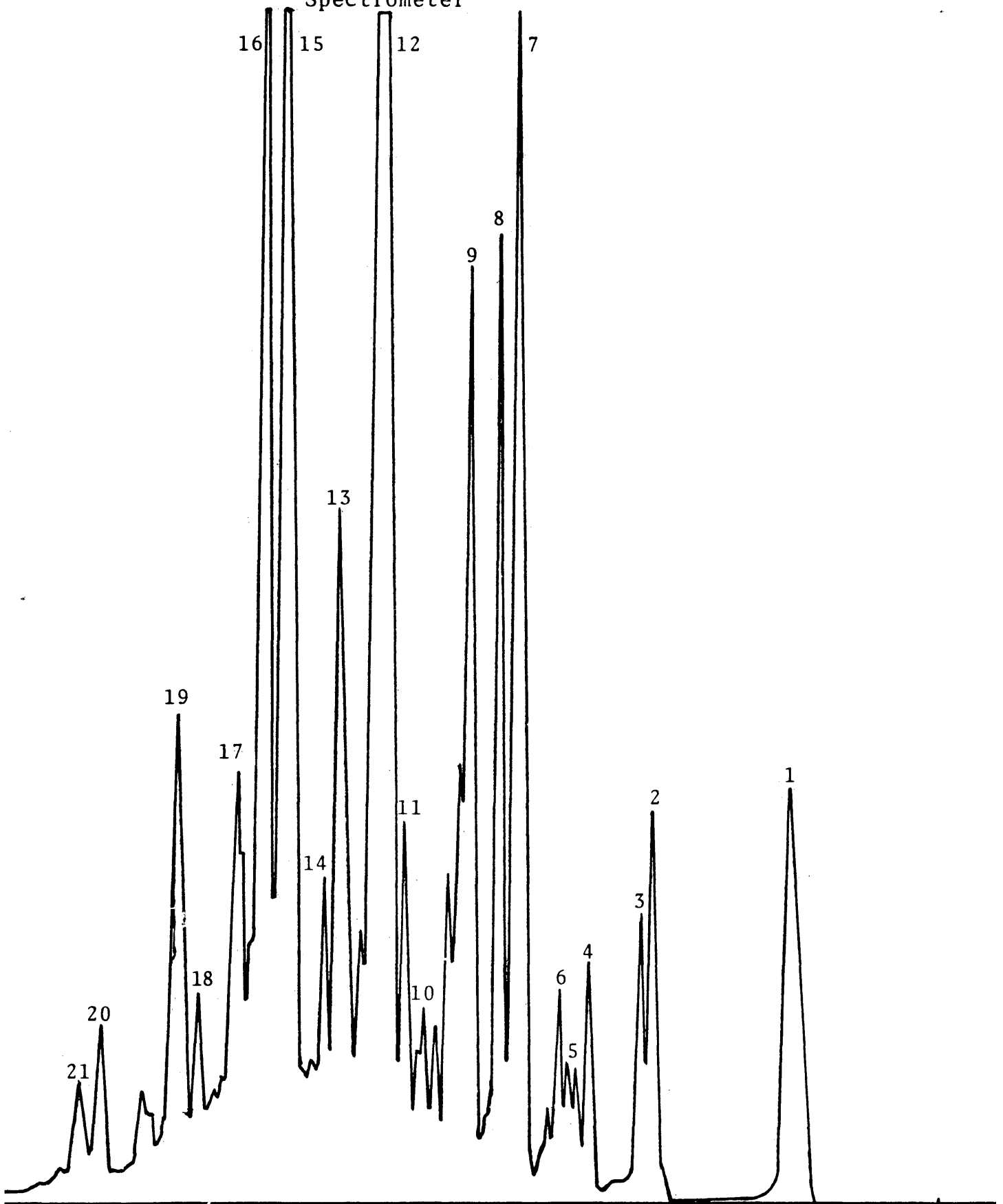


Table 9. - Constituents of Anthracene Oil Found by GC-MS.*

1. Naphthalene
2. β Methyl naphthalene
3. α Methyl naphthalene
4. Biphenyl
5. Dimethylnaphthalene
6. Dimethylnaphthalene
7. Acenaphthene
8. Dibenzofuran
9. Fluorene
10. Trimethylnaphthalene
11. Dibenzothiophene (?)
12. Phenanthrene
13. Methyl phenanthrene
14. Dihdropyrene
15. Fluoranthene
16. Pyrene
17. Methyl pyrene
18. Dimethyl pyrene
19. Chrysene
20. Benzofluoranthene
21. Benzopyrene

*The constituents of anthracene oil (figure 12) and analyses shown in Tables 9 and 10 were supplied by GFERC, Grand Forks, North Dakota and should not be reproduced without their permission.

Table 10. - Weight Percent of the Constituents Present in Anthracene Oil.

Item	Component	A Area % or wt %	B Response Factor	A x B	wt % (after normalizing)
1&2	Napthalene	3.99	1.00	3.99	3.72
3	β Methyl- napthalene	2.03	1.01	2.05	1.89
4	α Methyl- napthalene	1.36	1.04	1.41	1.26
5	Biphenyl	1.05	.96	1.02	.98
6	Dimethyl- napthalene	1.94	1.04	2.04	1.81
7					
8	Acenapthene	7.43	1.03	7.71	6.92
9	Dibenzofuran	4.85	1.00	4.85	4.51
10	Fluorene	4.62	1.01	4.69	4.30
11	Tri-methyl- napthalene	1.07	1.00	1.07	1.00
12	Dibenzothio- phene (1.78)				
13&14	Phenan- threne	16.58	.92	15.40	15.43
15	Me-phenan- threne	4.92	1.00	4.92	4.58
16	Dihydropy- rene	1.46	1.00	1.47	1.37
17	Fluoran- thene	10.32	.70	7.26	9.61
18	Pyrene	9.68	.80	7.79	9.01
19	Me-pyrene	3.45	1.00	3.46	3.22
20	Dimethyl pyrene	1.26	1.00	1.27	1.18
21	Chrysene	3.66	1.00	3.66	3.41
22	Benzofluor- anthene	1.94	1.00	1.94	1.81
		<u>81.68</u>		<u>76.01</u>	

weight percentages obtained by GC-mass spectrometer analysis corresponded directly to the peak heights obtained by analyzing the sample in the CAPS unit. Therefore, the peak heights obtained by the pyrolysis of the sample were analyzed by correlating them to the peak heights in Table 8 and then obtaining the weight percentages from Table 10.

DISCUSSION OF RESULTS

The following section contains the results of this investigation and a discussion of the significance of the results. The subjects contained in this section are listed below.

1. Results obtained by pyrolysis at 1400°C
 - a) Percent removal of residue, volatile matter, light gases (CO, CO₂, CH₄, H₂O), fixed carbon and ash
 - b) Data fitting
 - c) Kinetic modelling of the data
 - d) Correlation of results to run conditions
 - e) Reproducibility
2. Results obtained by pyrolysis at 800°C
 - a) Amounts of heavy liquids, light gases, fixed carbon and ash obtained during the pyrolysis
 - b) Correlation of results to run conditions

Removal of Residue, Volatile Matter, Light Gases (CO, CO₂, CH₄, H₂O), Fixed Carbon and Ash

The percent removal of the above constituents during reaction are given in Tables 11-13. These percentages are obtained by assuming raw coal as basis and also assuming that coal residue obtained from THF extraction of the auto-clave sample is representative of the raw coal. The raw data from which these percentages are obtained is given in

Table 11 - Products of Pyrolysis at 1400°C for Run 27, 28

Time (min) of Residue	% Removal* of Volatile Matter	% Removal of Fixed Carbon	% Removal of Ash	% Removal of CO	% Removal of CO ₂	% Removal of CH ₄	% Removal of H ₂ O	
8.0	31.04	63.96	40.93	-463.53	-32.20	54.22	45.70	65.91
29.0	49.29	78.84	49.69	-311.25	-54.0	40.35	55.96	51.2
86.0	56.38	79.81	50.41	-169.64	30.45	70.98	72.71	81.96
113.0	79.56	89.06	84.01	-77.5	62.77	82.45	90.03	90.61
146.0	86.51	92.84	86.76	7.85	83.98	93.22	94.88	95.41
Run 28								
7.0	26.13	55.69	26.62	-234.72	33.42	65.95	15.72	59.3
15.0	12.17	46.06	16.98	-292.36	-15.56	40.67	10.11	51.75
54.0	62.08	79.51	61.92	-75.0	41.48	64.05	39.74	57.47
84.0	69.32	80.91	69.47	-23.61	75.41	83.91	70.37	85.14
122.0	73.99	86.87	70.80	-4.861	71.72	82.57	66.17	76.68

*The residue data were supplied by GFERC, Grand Forks, North Dakota, and should not be reproduced without their permission.

Table 12 - Products of Pyrolysis at 1400°C for Run 31,30

Time (min) of Residue	% Removal* of Volatile Matter	% Removal of Fixed Carbon	Run 31				Run 30			
			% Removal of Ash	% Removal of CO	% Removal of CO ₂	% Removal of CH ₄	% Removal of H ₂ O			
53.0	33.25	50.97	-571.22	-77.54	.93	61.23	41.35			
209.0	45.05	39.28	-381.95	67.66	84.09	92.75	91.55			
229.0	40.55	39.79	-449.27	-7.34	35.48	75.59	64.34			
251.0	53.96	70.46	-345.85	-31.03	.13	76.29	53.15			
269.0	66.84	90.36	-297.07	-5.16	8.81	89.82	76.41			
94.0	55.27	75.32	-416.99	15.86	64.39	82.68	71.31			
99.0	76.74	87.02	-120.38	43.47	71.39	83.46	78.88			
154.0	64.58	86.82	-338.93	-58.1	-1.91	85.30	73.33			
212.0	68.32	88.59	-281.08	-36.57	17.45	90.42	79.63			

*The residue data were supplied by GFERC, Grand Forks, North Dakota, and should not be reproduced without their permission.

Table 13 - Products of Pyrolysis at 1400°C for Run 23

Time (min) of Residue	% Removal* of Volatile Matter	% Removal of Fixed Carbon	% Removal of Ash	% Removal of CO	% Removal of CO ₂	% Removal of CH ₄	% Removal of H ₂ O	
20.0	15.21	43.51	25.69	-204.40	-30.10	-28.34	-14.91	-47.22
78.0	-8.27	44.68	-24.70	-189.19	31.58	18.89	-2.19	-1.99
138.0	-7.03	50.88	-17.56	-253.24	22.90	1.77	20.83	9.13

*The residue data were supplied by GFERC, Grand Forks, North Dakota, and should not be reproduced without their permission.

Appendix A, and a sample calculation is also shown in Appendix B. The numbers with a negative sign in the tables indicate an increase in that substance instead of a decrease. For Run 26, only one sample was obtained at the end of the run and it was not analyzed, therefore the percent removal is given in Appendix A.

Data Fitting

Attempts to fit the data with second and higher order polynomials proved unsuccessful due to the initial steepness of the curve. Therefore, an equation of the form $y = at^b$ was investigated and found to satisfactorily represent the observed data points. Here y is the percent removal of a given compound, t is the time in minutes, and a and b are constants. Writing this equation in logarithmic form:

$$\ln y = \ln a + b \ln t.$$

The two constants were then evaluated as follows: let

$$\ln y = Y, \ln a = A, b = B, \text{ and } \ln t = T.$$

Therefore, a new linear equation is generated:

$$Y = A + BT$$

$$\text{and } S_{tt} = n (\Sigma T^2) - (\Sigma T)^2$$

$$S_{yy} = n (\Sigma Y^2) - (\Sigma Y)^2$$

$$S_{ty} = n (\Sigma TY) - (\Sigma T)(\Sigma Y)$$

where

$$S_{tt} = [\text{sum of } T \text{ squared}] \text{ minus } [\text{sum of } T] \text{ squared}$$

$$S_{yy} = [\text{sum of } Y \text{ squared}] \text{ minus } [\text{sum of } Y] \text{ squared}$$

$$S_{ty} = \text{sum of the product of } T \text{ and } Y \text{ minus the product of sum of } T \text{ and sum of } Y$$

n = number of observations.

Values for B and A may then be found from:

$$B = \frac{S_{ty}}{S_{tt}} \quad A = \bar{Y} - B\bar{T}$$

where \bar{Y} = average value of Y

\bar{T} = average value of X.

Constants a and b for the different constituents of Runs 27 and 28 by the above analysis are given in Table 14, and a sample calculation is given in Appendix B.

Ash in every run exhibited an abnormal behavior, increasing in the beginning and then decreasing slowly yielding in the end an ash content in the sample higher than the parent coal. Therefore, ash data points could not be fitted according to this equation and they were not further analyzed. The data points of Run 23 were also not fitted because coking was observed during the autoclave run and residue, fixed carbon and light gases increased instead of decreasing. Run 30 was a slow heat up run, and since kinetic analysis requires a precise knowledge of reaction time, no equation could be developed to fit these data points. In Run 31, only one sample was collected during the run after which time the reactor was cooled to 300°C, a fresh charge of gas added and the reactor reheated to the original temperature. Since no kinetic analysis is possible in this run due to varying reaction conditions, no equation was developed to fit the data points found from pyrolysis of Run 31. The above runs

Table 14. Values of constants a and b.

	a	b
Residue	.1544	.3311
Fixed Carbon	.2329	.2393
Volatile Matter	.5110	.1151
CO ₂	.2848	.2118
CH ₄	.2570	.2526
H ₂ O	.4055	.1570

	a	b
Residue	.0582	.5385
Fixed Carbon	.0777	.4747
Volatile Matter	.3290	.2022
CO	.1854	.2736
CO ₂	.3784	.1527
CH ₄	.0299	.6554
H ₂ O	.4141	.1256

were used for qualitative analysis by comparing results with Run 27 and 28, as discussed later. CO in Run 27 exhibited an abnormal behavior of first increasing, then decreasing and then again increasing. This might be due to the error in analysis and therefore no equation was developed to fit these data points. The graphs for the constituents of Runs 27 and 28 are presented in figures 16-28, in which the experimental data is presented and the calculated fit shown.

Kinetic Modelling of the Data

Attempts to kinetically model the data using pure first order, pure second order, and first, then second order models all proved unsuccessful. A model proposed by Wisler (1) was then tested and found to adequately fit the observed kinetics of this experimental investigation. The rate expression was of the form:

$$\frac{dx}{dt} = k_n (a-x)^n \quad (1)$$

where n denotes the order of the reaction. X is the observed weight loss at time t as a fraction of the initial sample weight, and a is the maximum possible reactive fraction at the temperature concerned. Integrated first and second order rate expressions of the form:

$$\ln \frac{a}{a-x} = k_1 t$$

$$\frac{1}{a-x} - \frac{1}{a} = k_2 t$$

where k_1 = first order rate constant and k_2 = second order rate constant were both investigated.

Figure 16. Run 27, Weight Percent Conversion of Coal (Residue) to Liquid Coal.

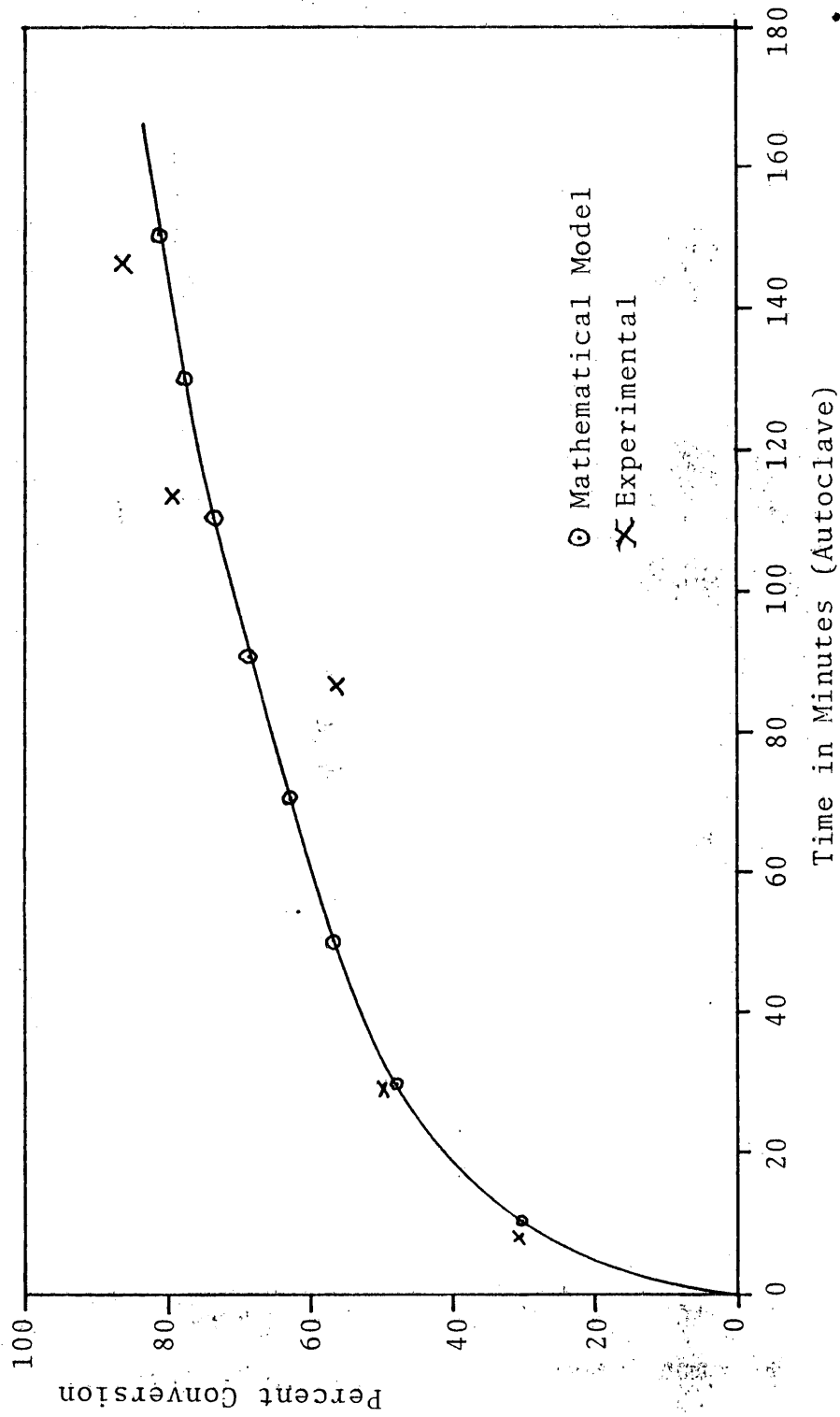
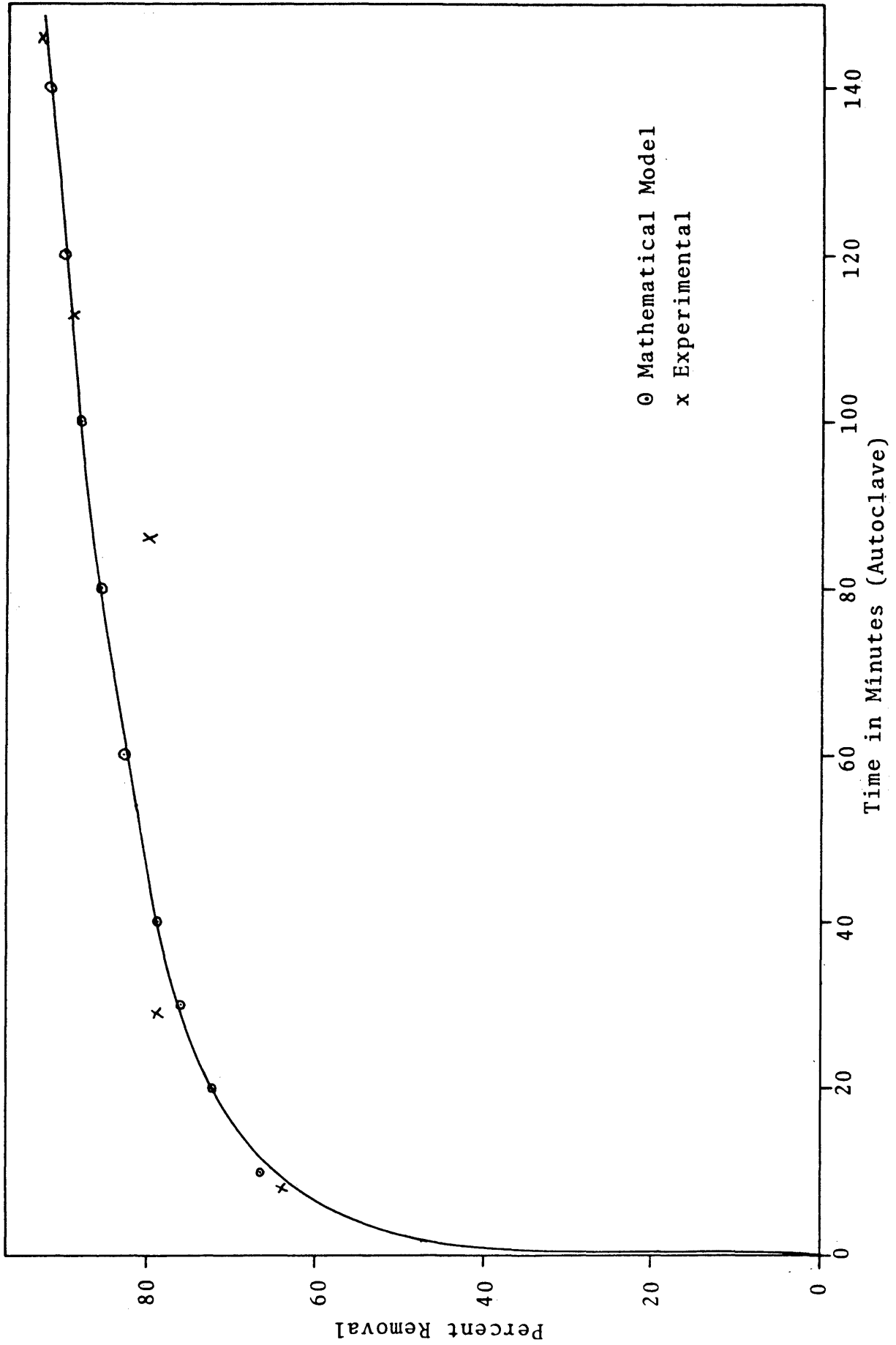


Figure 17. Run 27, Weight Percent Removal of Volatile Matter from Coal.



o Mathematical Model
x Experimental

Figure 18. Run 27, Weight Percent Removal of Fixed Carbon from Coal.

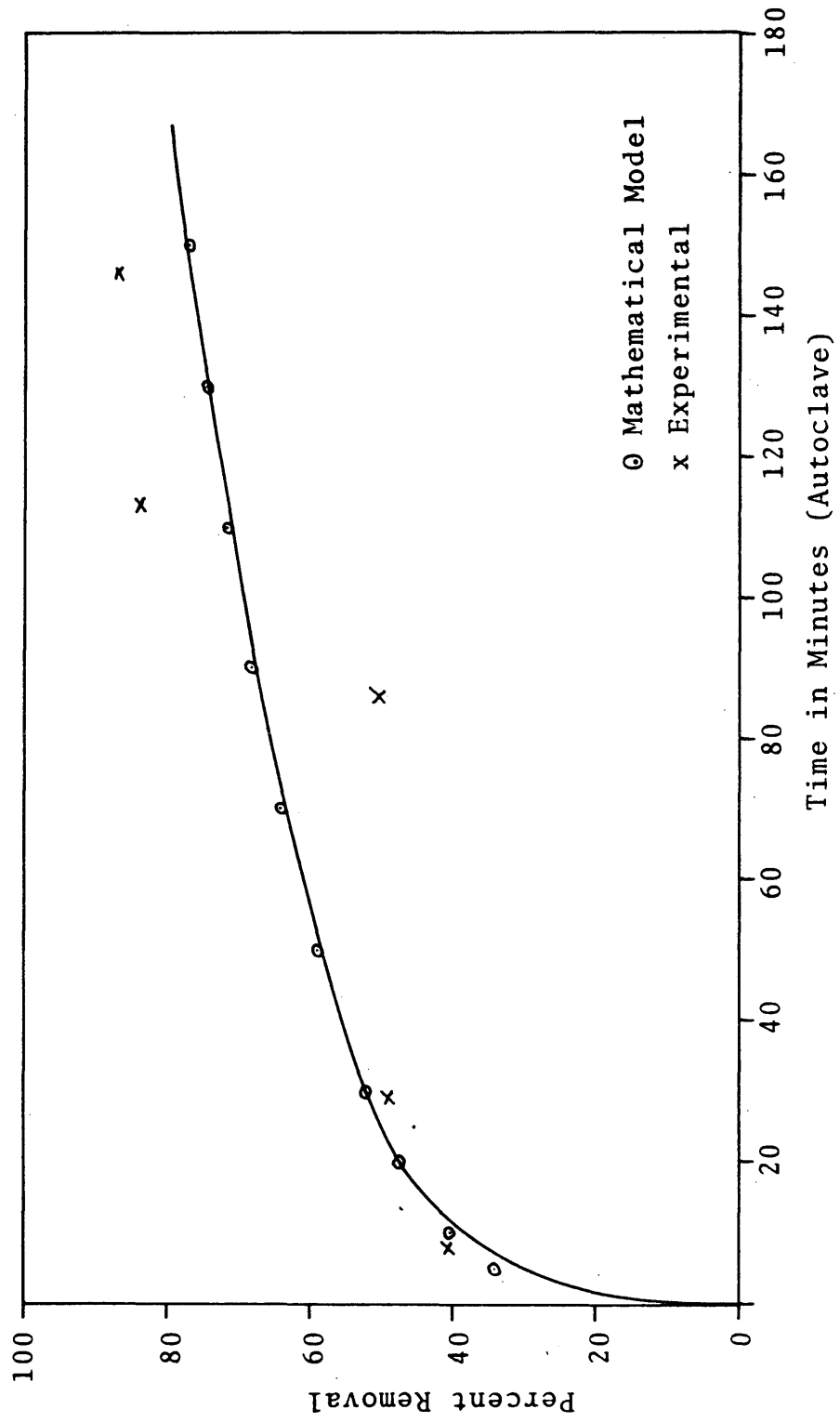


Figure 19. Run 27, Weight Percent Removal of Carbon Dioxide from Coal.

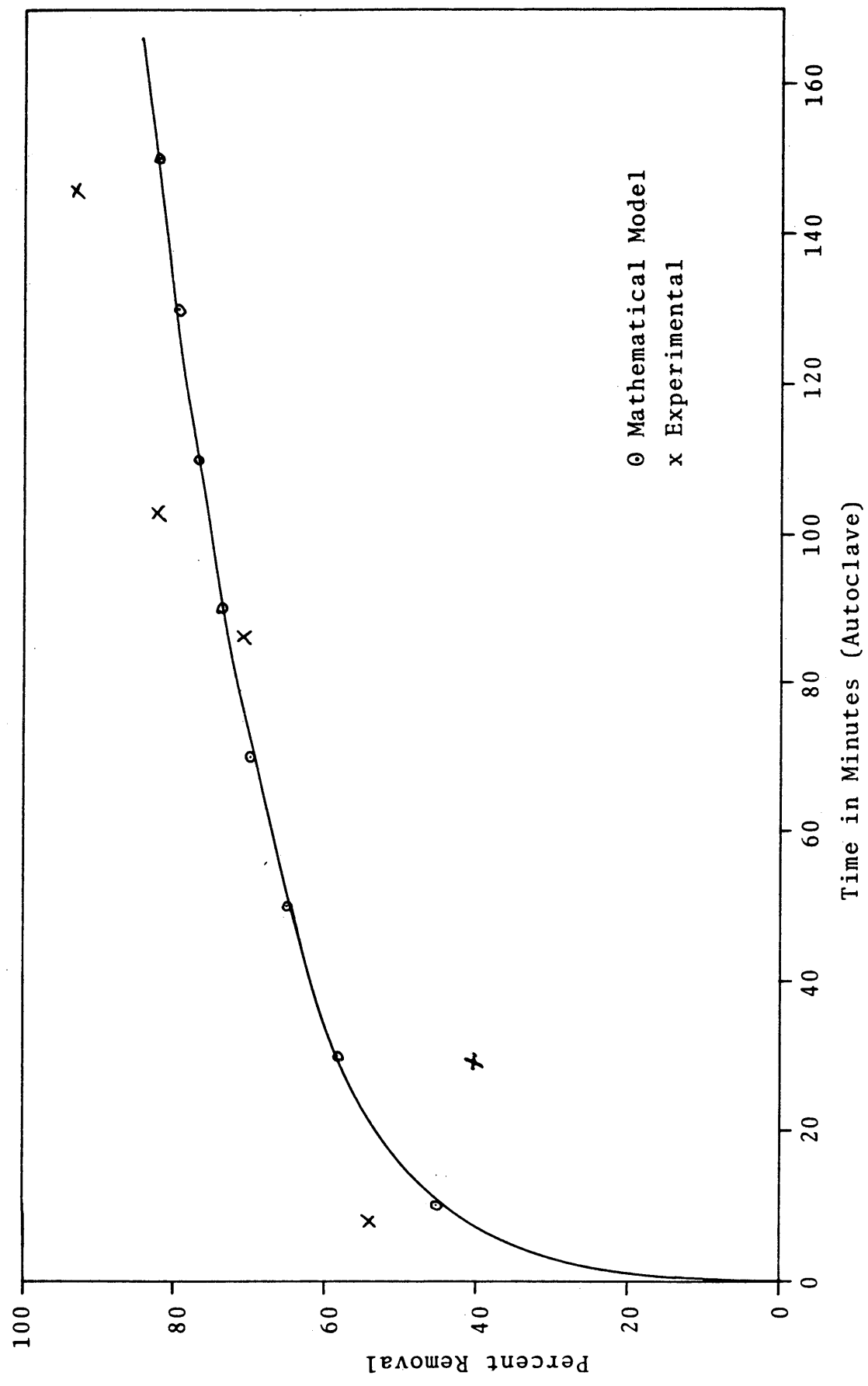


Figure 20. Run 27, Weight Percent Removal of Methane from Coal.

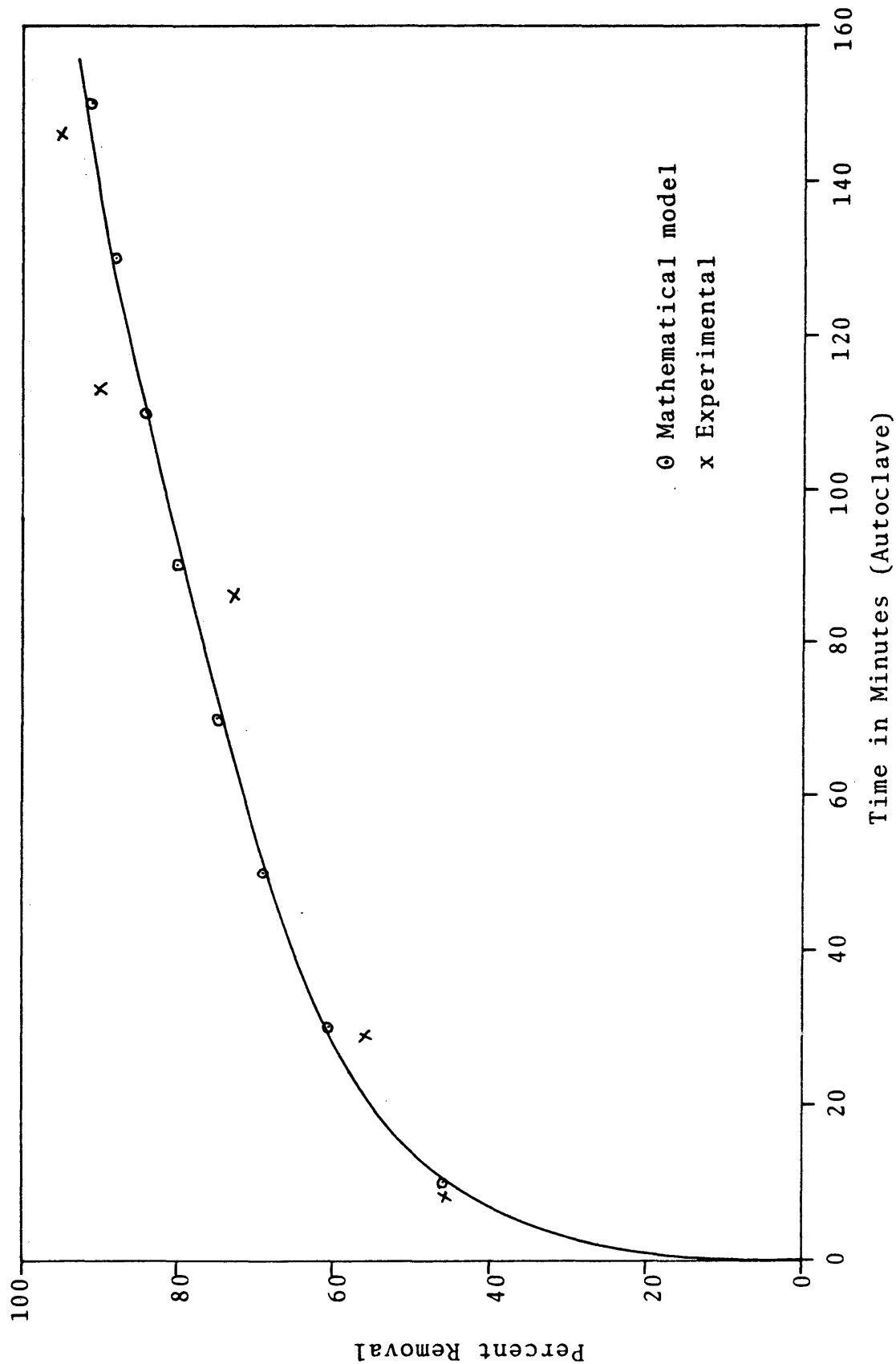


Figure 21. Run 27, Weight Percent Removal of Water from Coal.

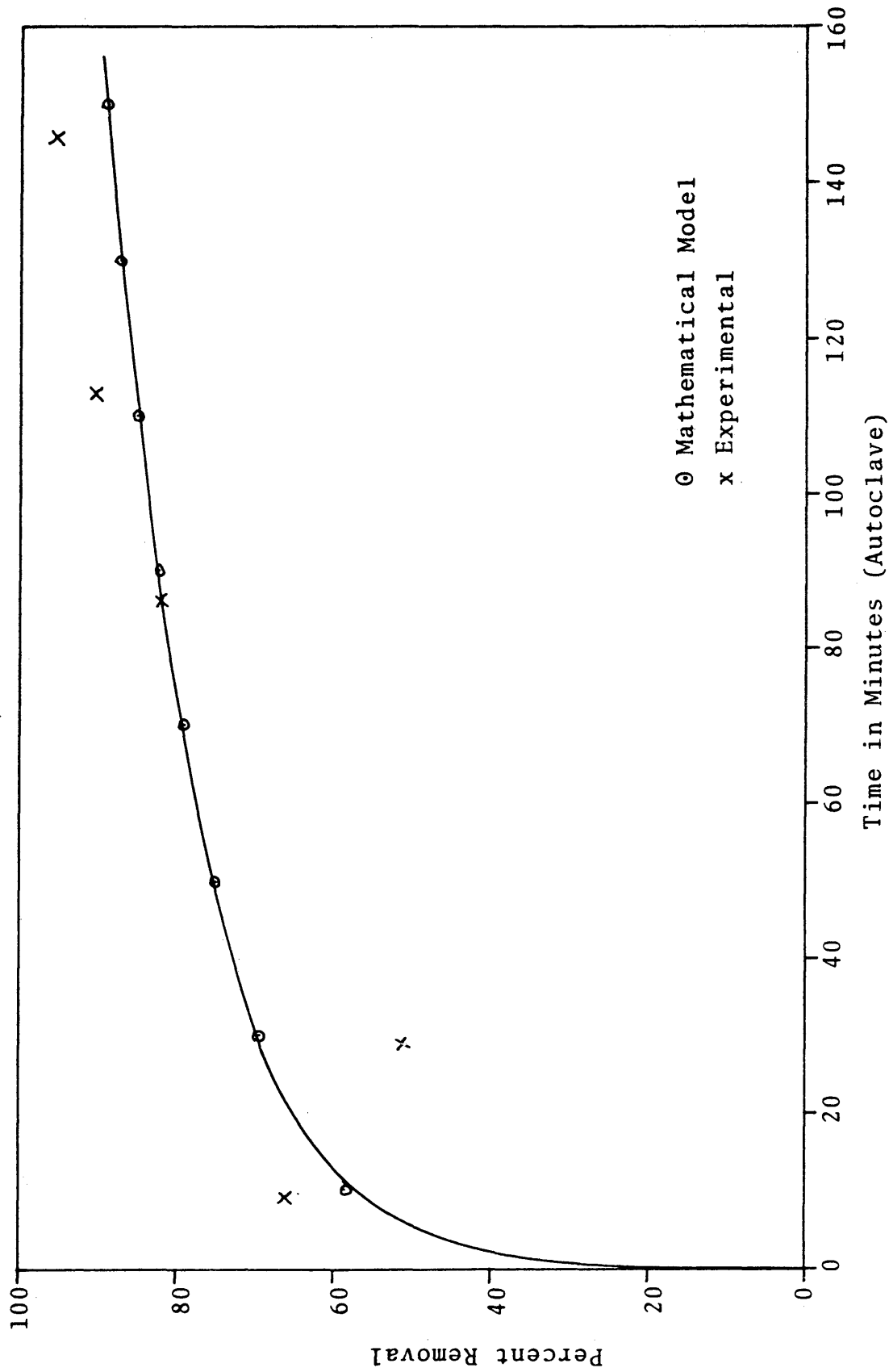


Figure 22. Run 28, Weight Percent Conversion of Coal (Residue) to Liquid Coal.

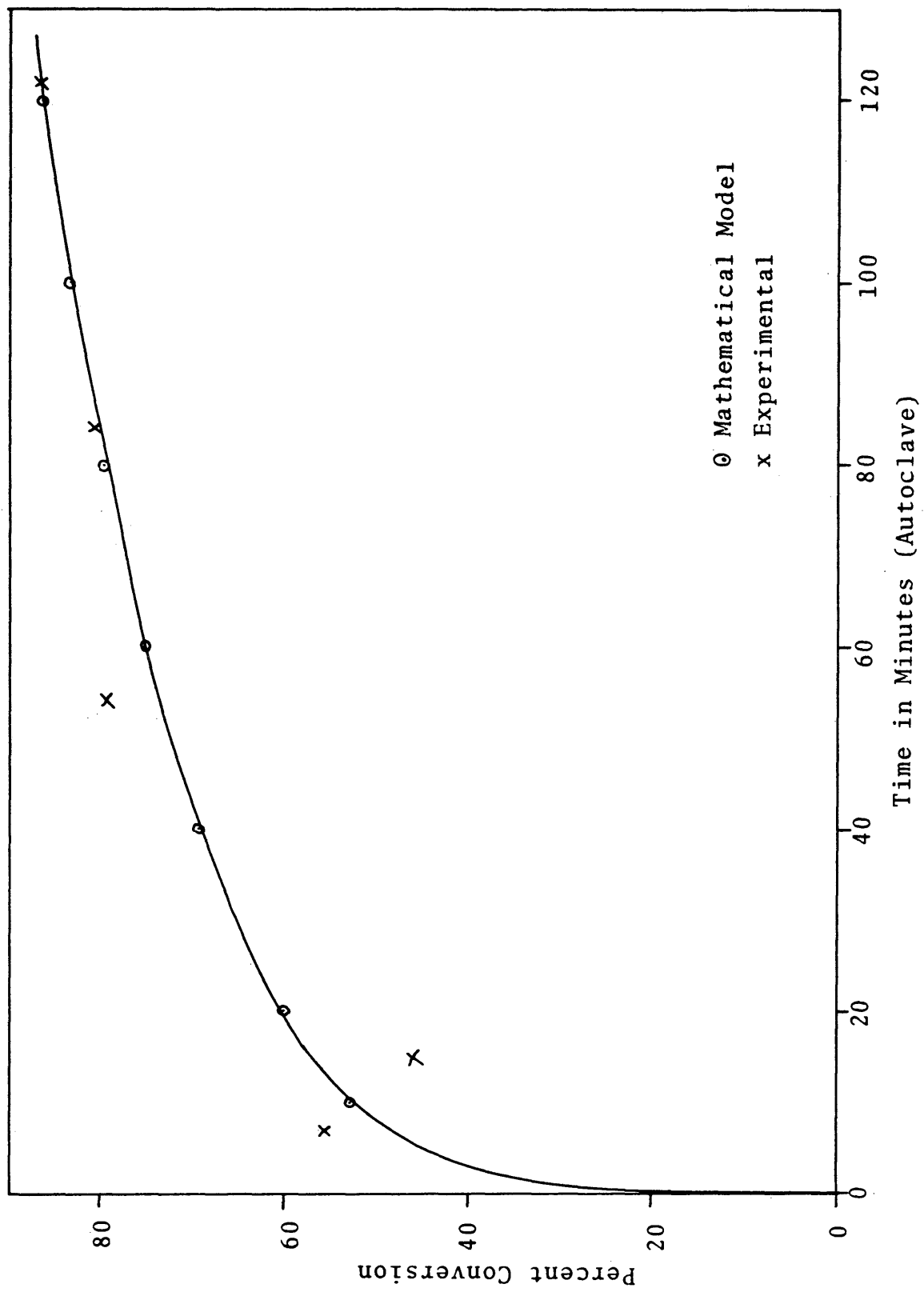


Figure 23. Run 28, Weight Percent Removal of Fixed Carbon from Coal.

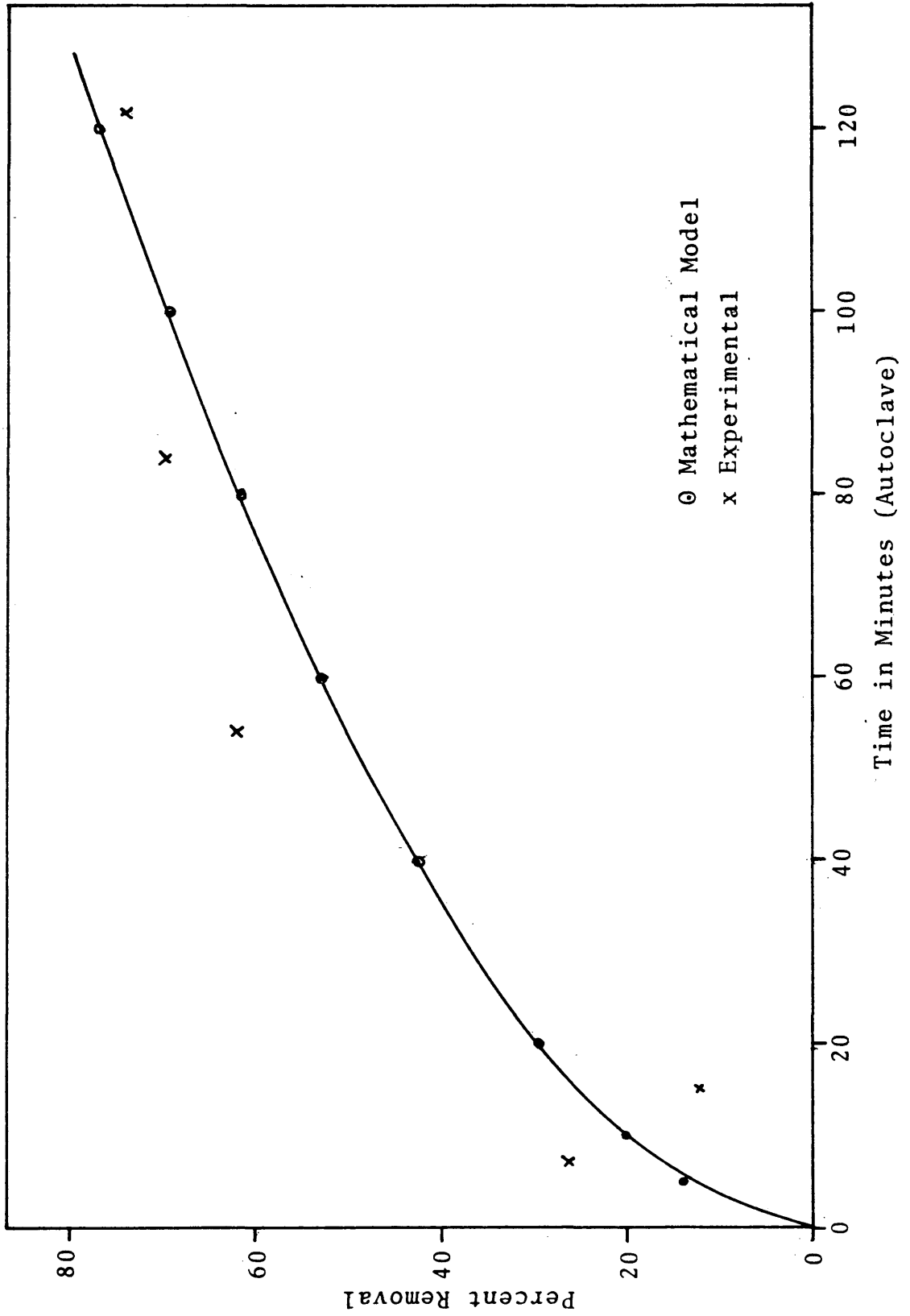


Figure 24. Run 28, Weight Percent Removal of Volatile Matter from Coal.

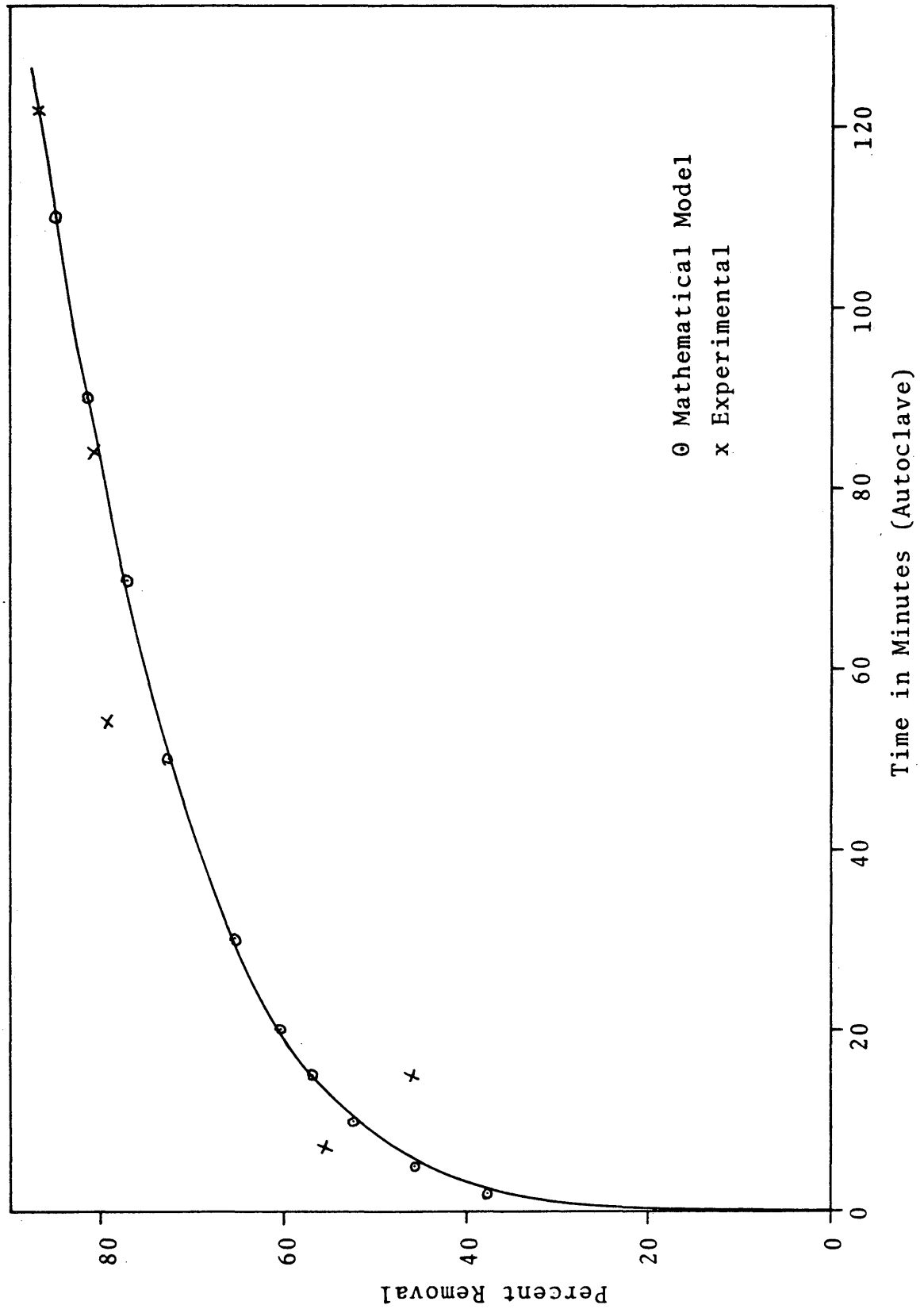


Figure 25. Run 28, Weight Percent Removal of Carbon Monoxide from Coal.

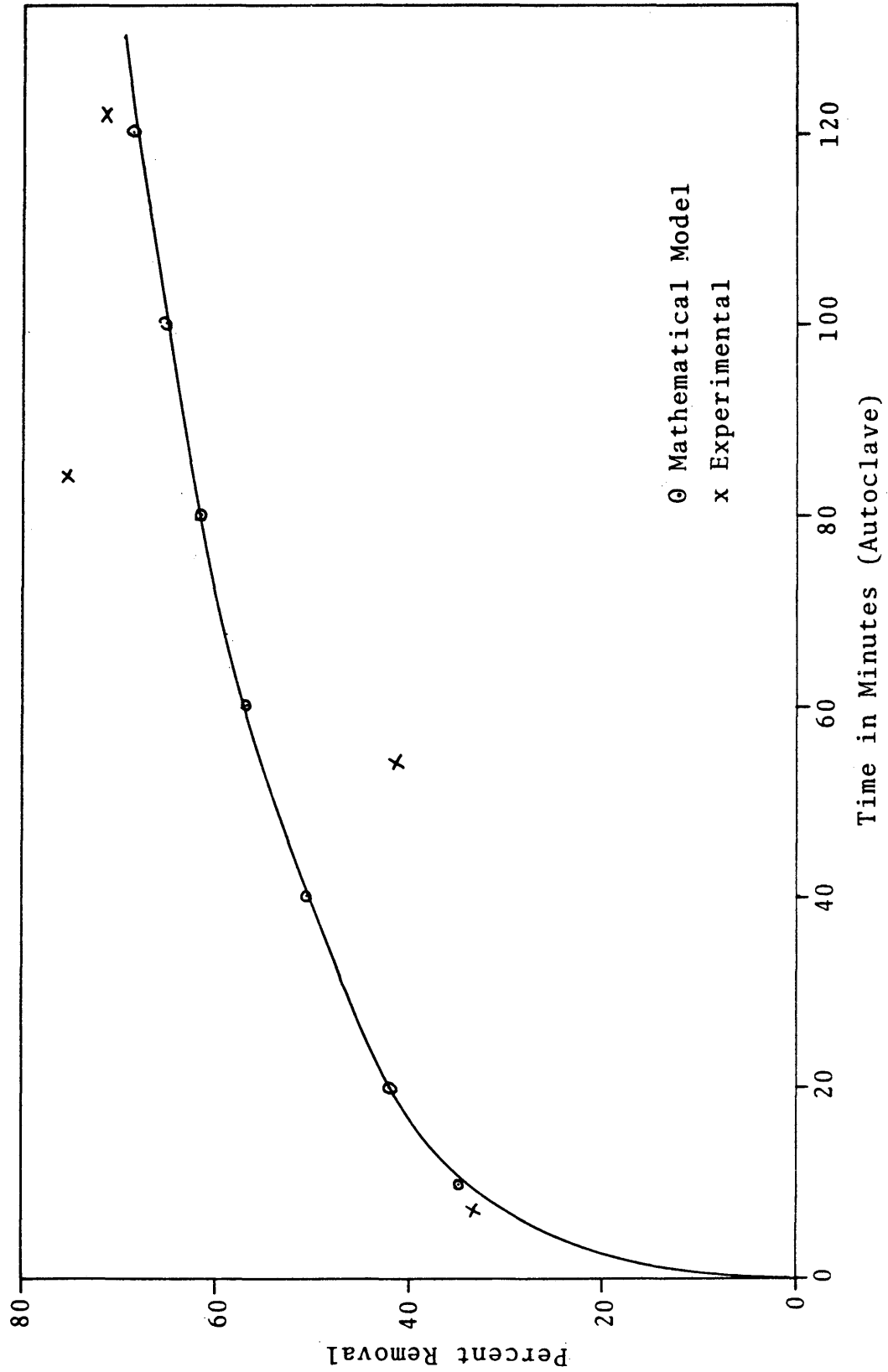


Figure 26. Run 28, Weight Percent Removal of Carbon Dioxide from Coal.

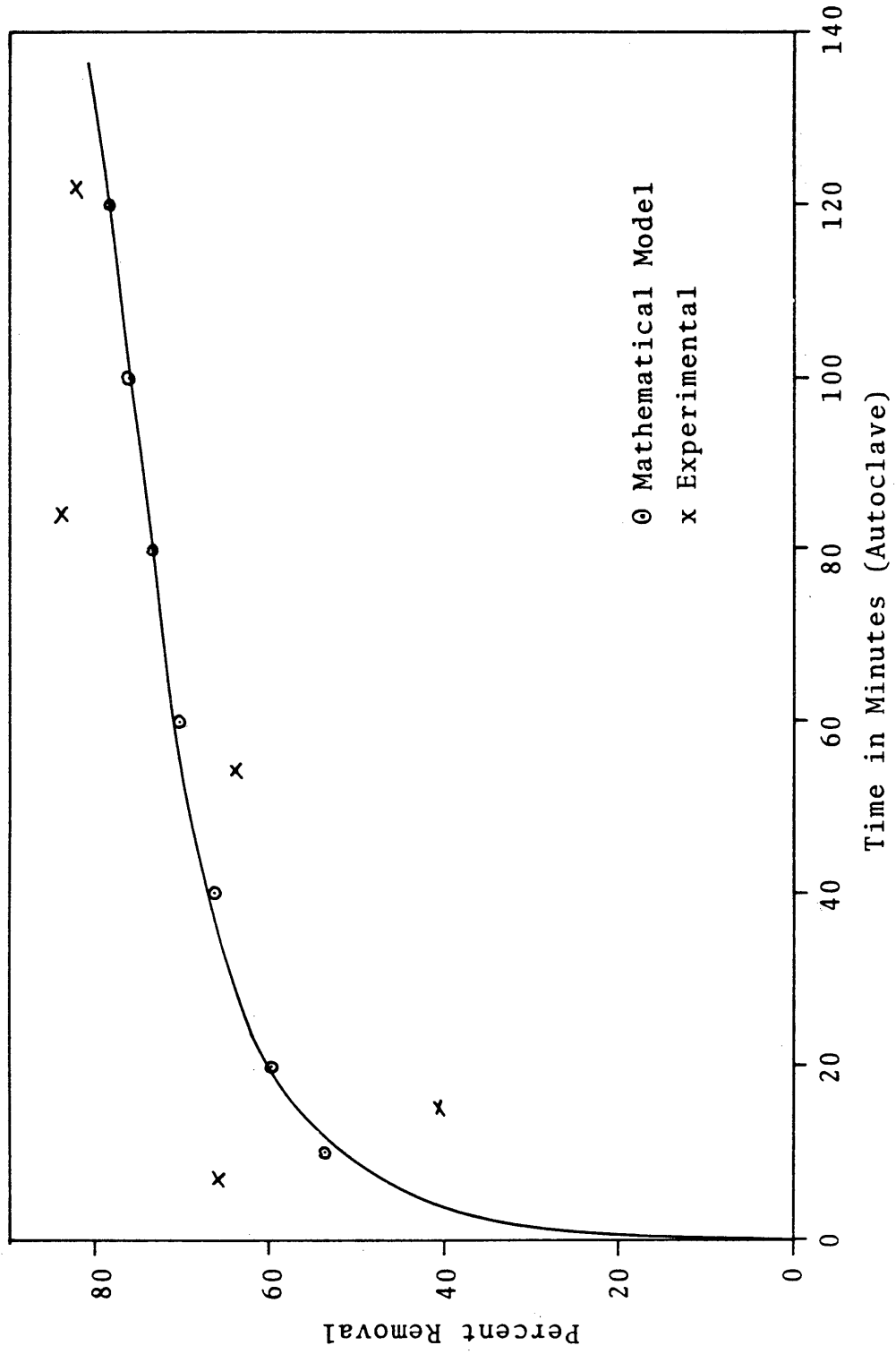


Figure 27. Run 28, Weight Percent Removal of Methane from Coal.

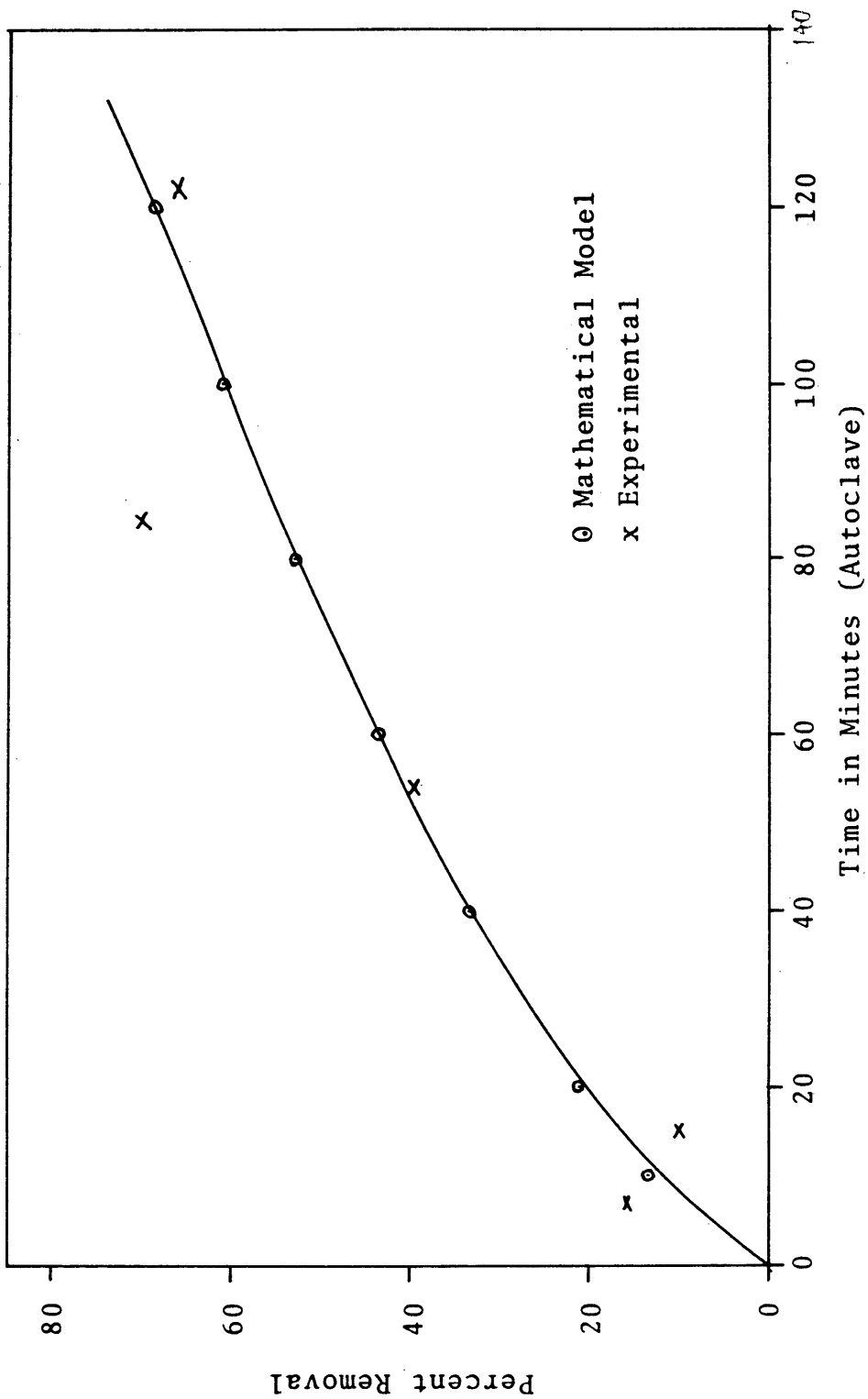
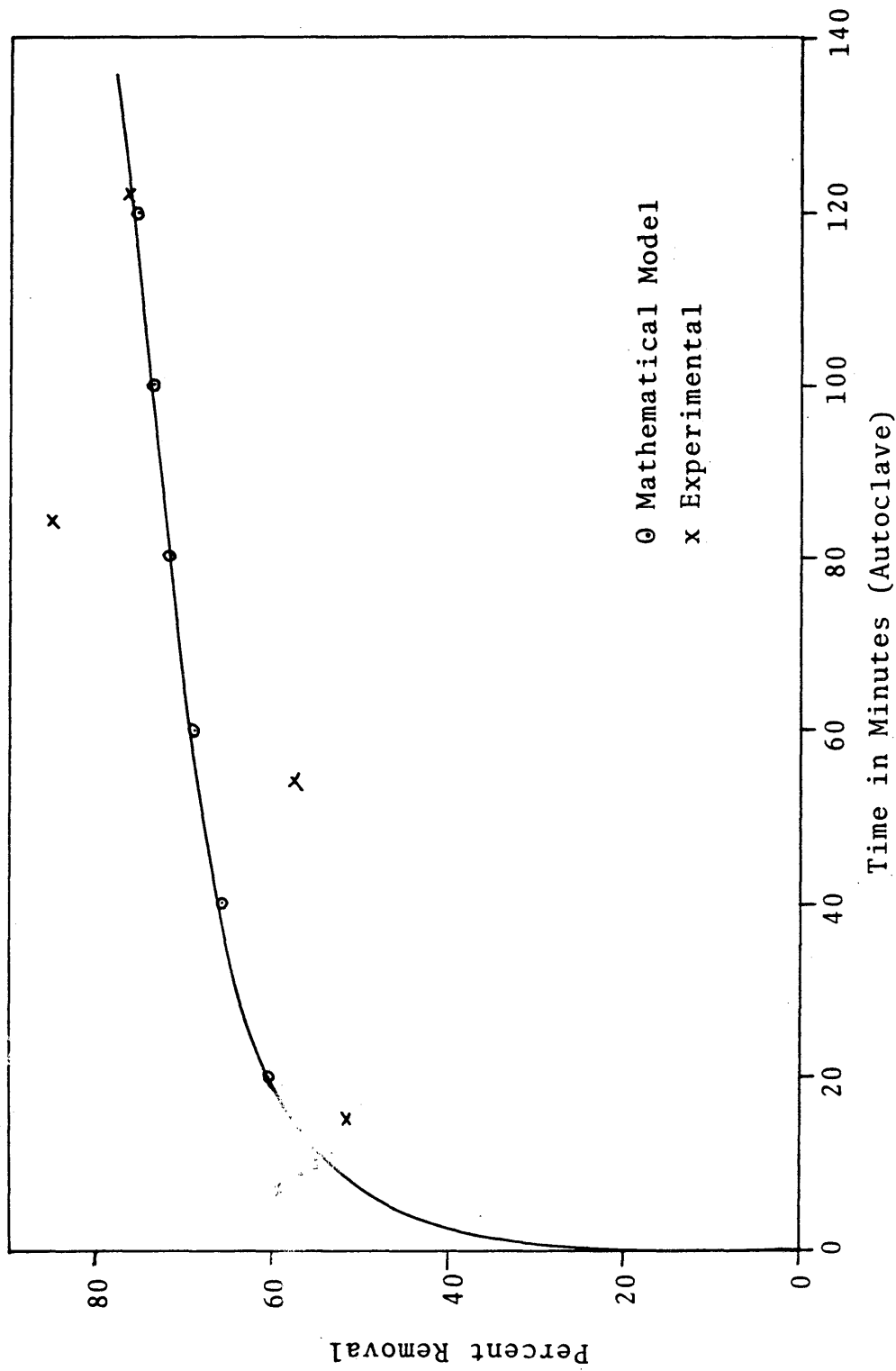


Figure 28. Run 28, Weight Percent Removal of Water from Coal.



The value of 'a' was obtained by changing its value until the square of the sum of residuals between observed and calculated conversions (x's) was a minimum. Figures 29-41 show the conversion obtained by using 1st and 2nd order rate expressions and the experimental data points. Both of the rate expressions seem to fit the data by selecting the proper value of 'a'. In all cases, the result for 'a' was between an upper bound of 1.0 and a lower bound given by the last observation in the data set, thus confirming the validity of the choice for parameter 'a'. Figures 46-53 show the 95% confidence interval plot for residue and volatile matter of Run 27 and Run 28 and indicates once again that 1st and 2nd order rate expressions seem to fit the data equally well. The reasons why both rate expressions fit the data might be due to lack of the reproducible autoclave runs and the selection of the value of 'a'. The values of 'a' and the 1st and 2nd order rate constants k_1 and k_2 are given in Table 15. Figures 42-43 show the plot of $-\ln(1-x/a)$ versus time for residue of Run 27 and Run 28, and figures 44-45 show the plot of $(1/a-x - 1/a)$ versus time for residue of Run 27 and Run 28. The straight line in these plots is drawn by least square method. Examination of these linear plots confirm the above observation that 1st and 2nd order kinetics equally well explain the data. Sample calculations for determining rate constants are given in Appendix B.

Correlation of Results to Run Conditions

The relation between change of autoclave residue vs. time is shown graphically in fig. 54 where results for runs 23, 27, 28, and 30 are recorded. The relation between change

Figure 29. Run 27, Comparison of Experimental Weight Percent Conversion of Coal (Residue) to Liquid Coal with 1st and 2nd Order Kinetic Models.

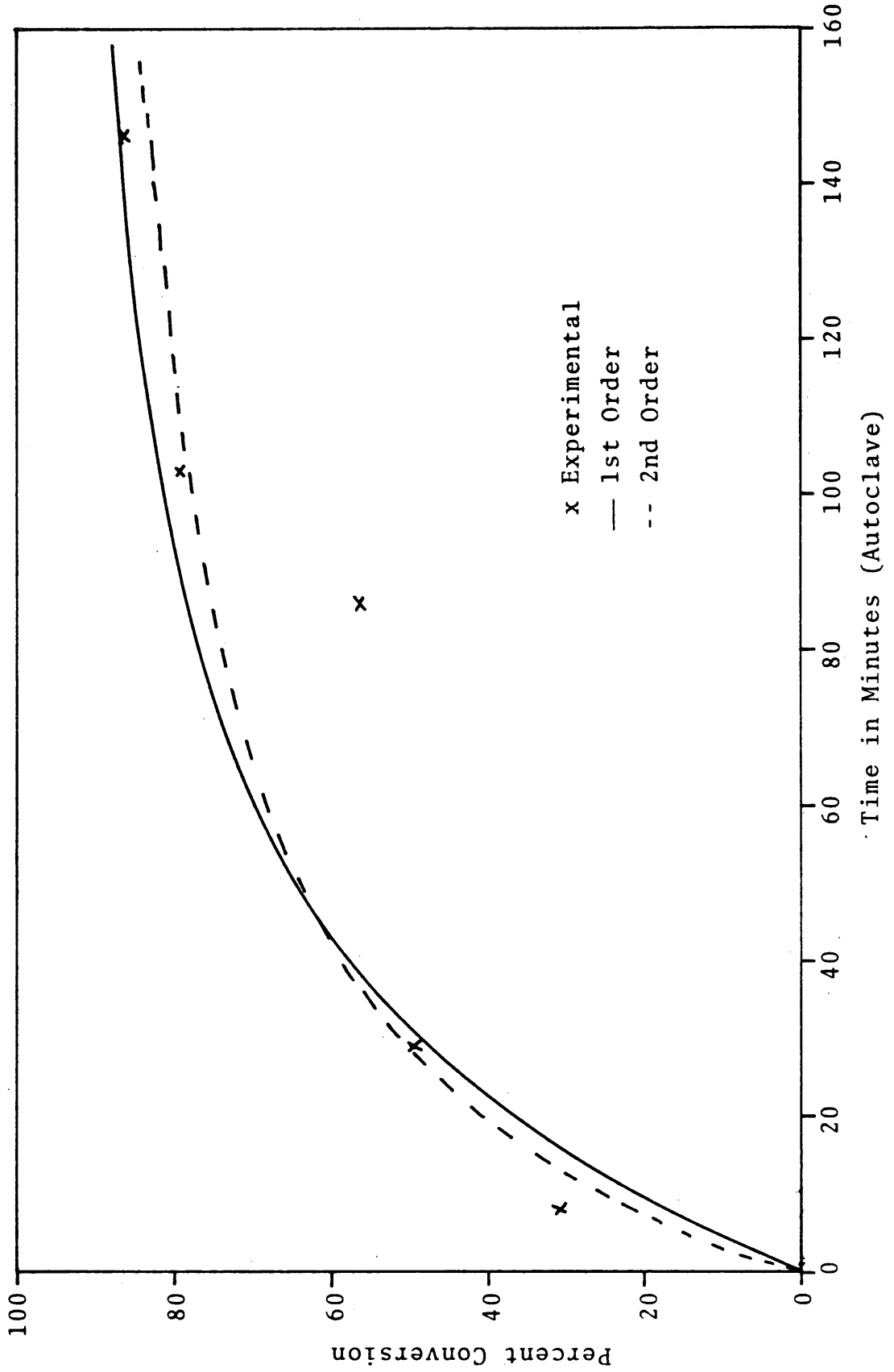


Figure 30. Run 27, Comparison of Experimental Weight Percent Removal of Volatile Matter with 1st and 2nd Order Kinetic Models.

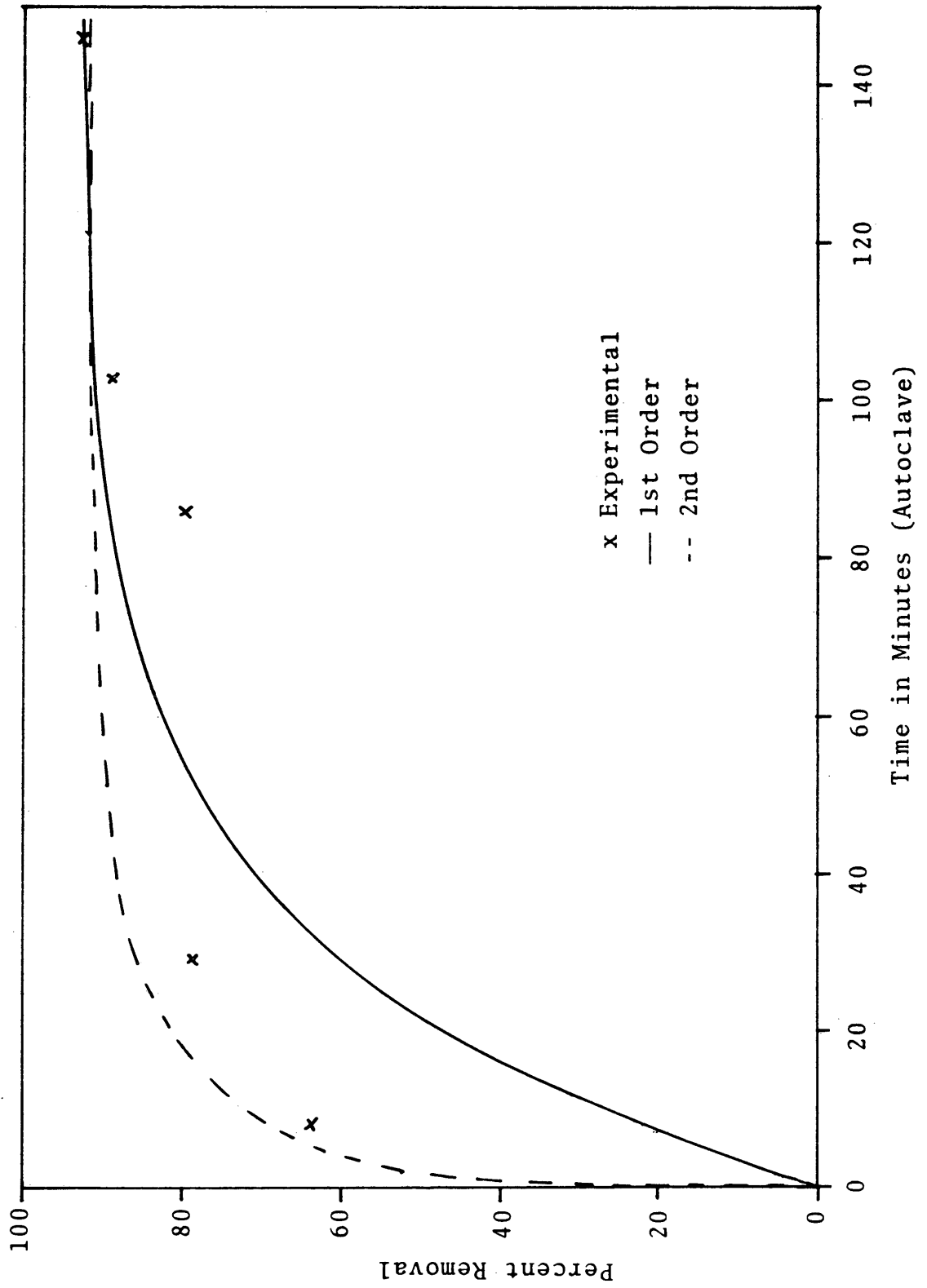


Figure 31. Run 27, Comparison of Experimental Weight Percent Removal of Fixed Carbon from Coal with 1st and 2nd Order Kinetic Models.

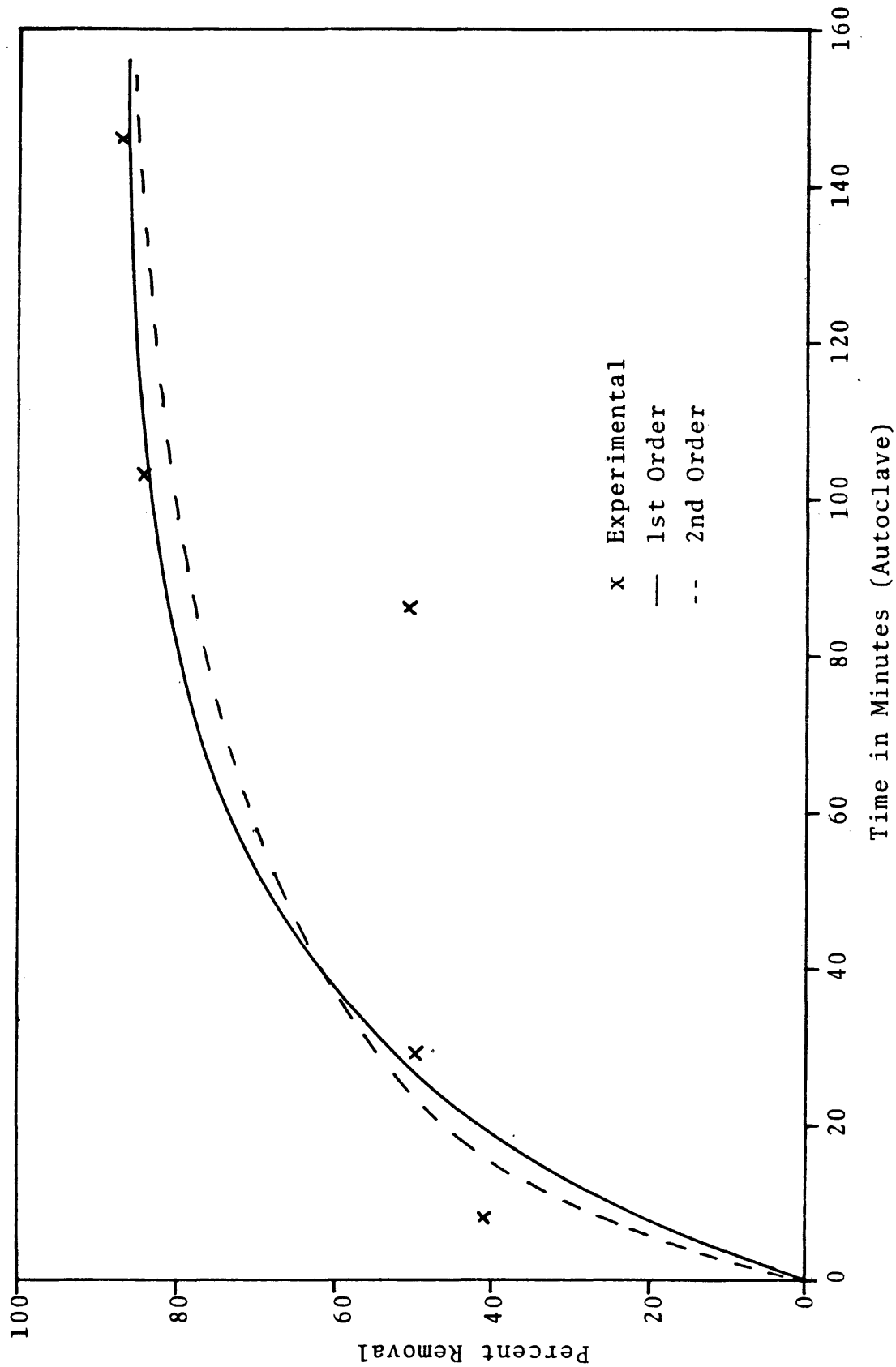


Figure 32. Run 27, Comparison of Experimental Weight Percent Removal of Methane from Coal with 1st and 2nd Order Kinetic Models.

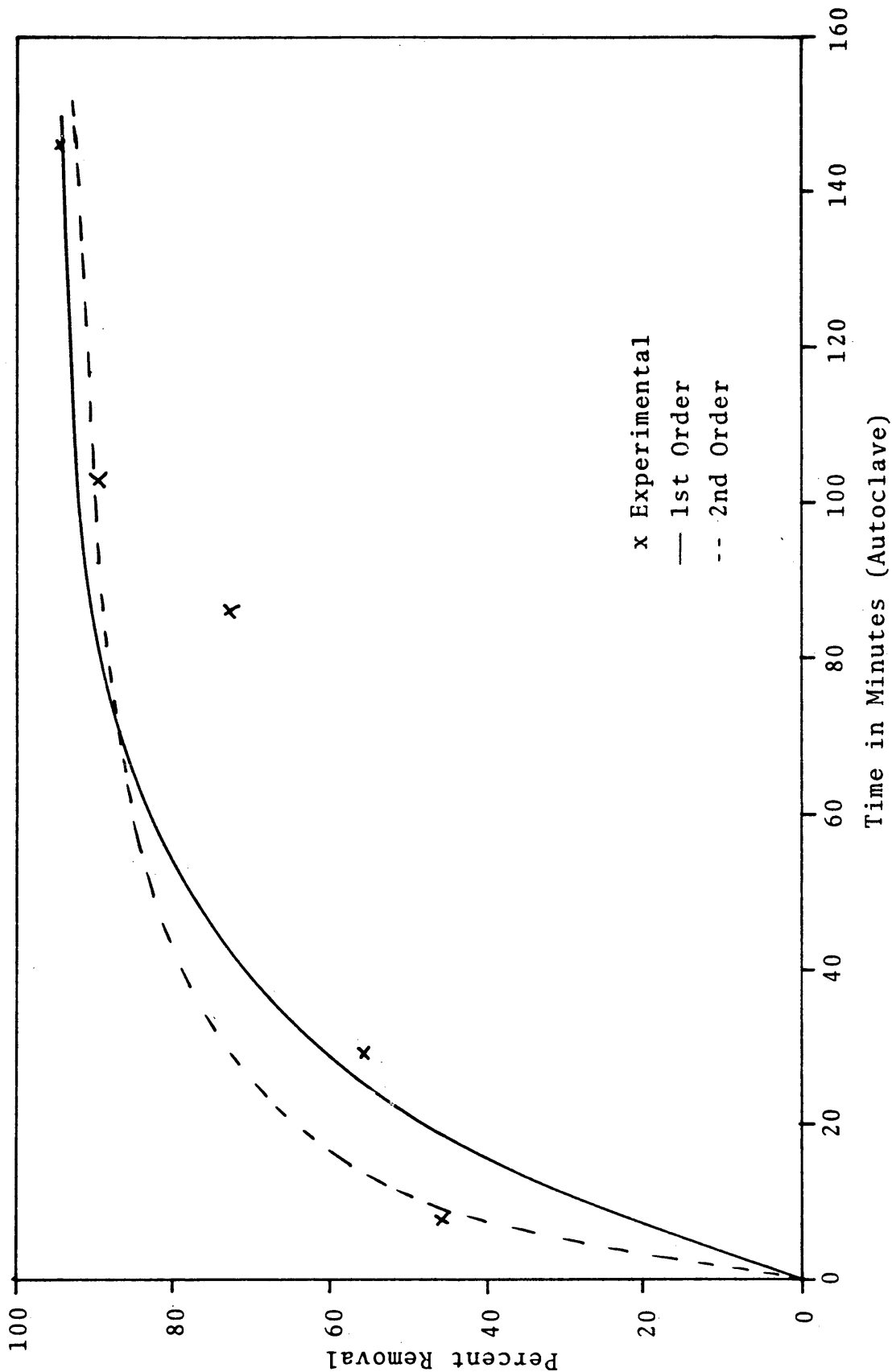


Figure 33. Run 27, Comparison of Experimental Weight Percent Removal of Carbon Dioxide from Coal with 1st and 2nd Order Kinetic Models.

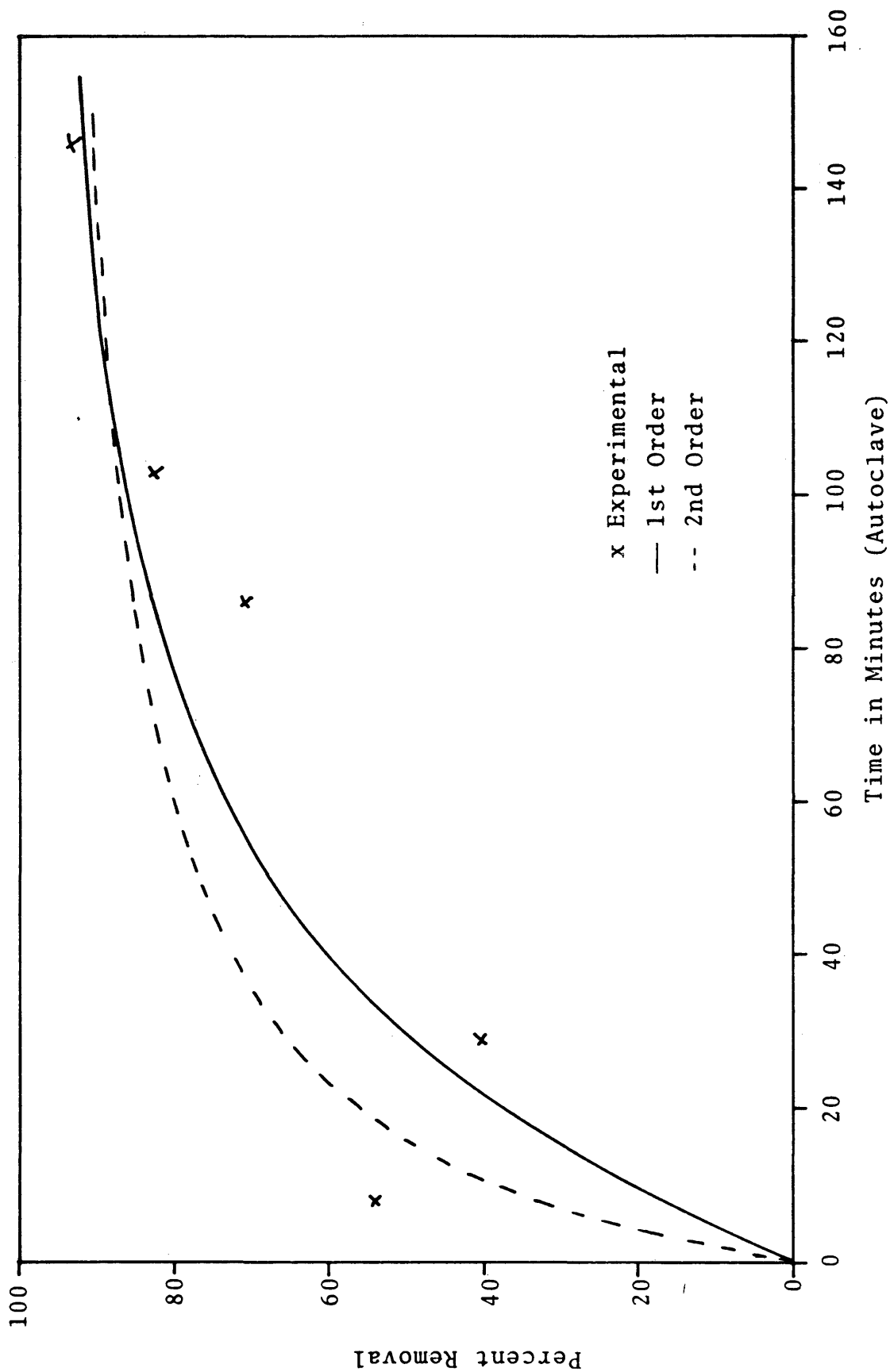


Figure 34. Run 27, Comparison of Experimental Weight Percent Removal of Water from Coal with 1st and 2nd Order Kinetic Models.

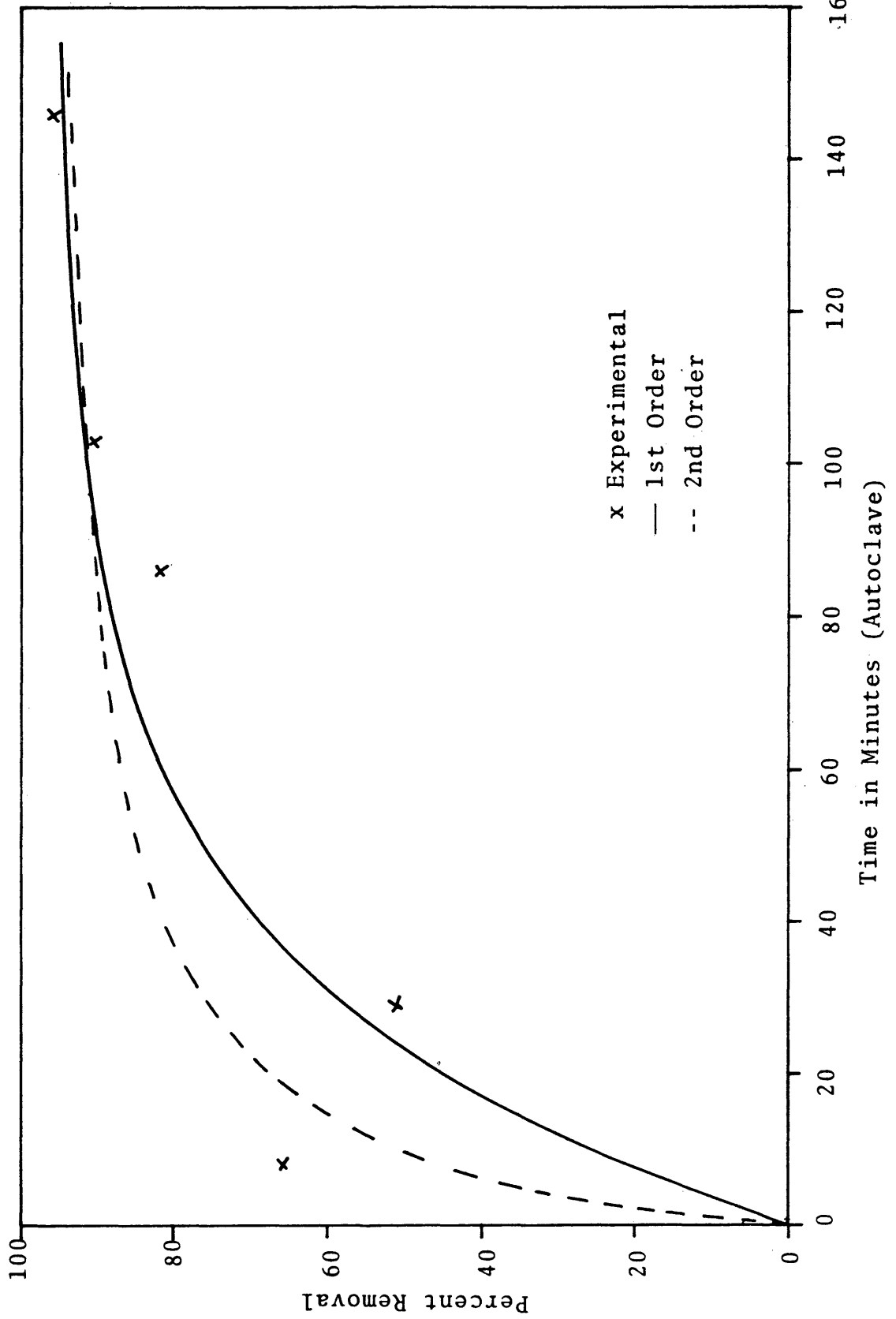


Figure 35. Run 28, Comparison of Experimental Weight Percent Conversion of Coal (Residue) to Liquid Coal with 1st and 2nd Order Kinetic Models.

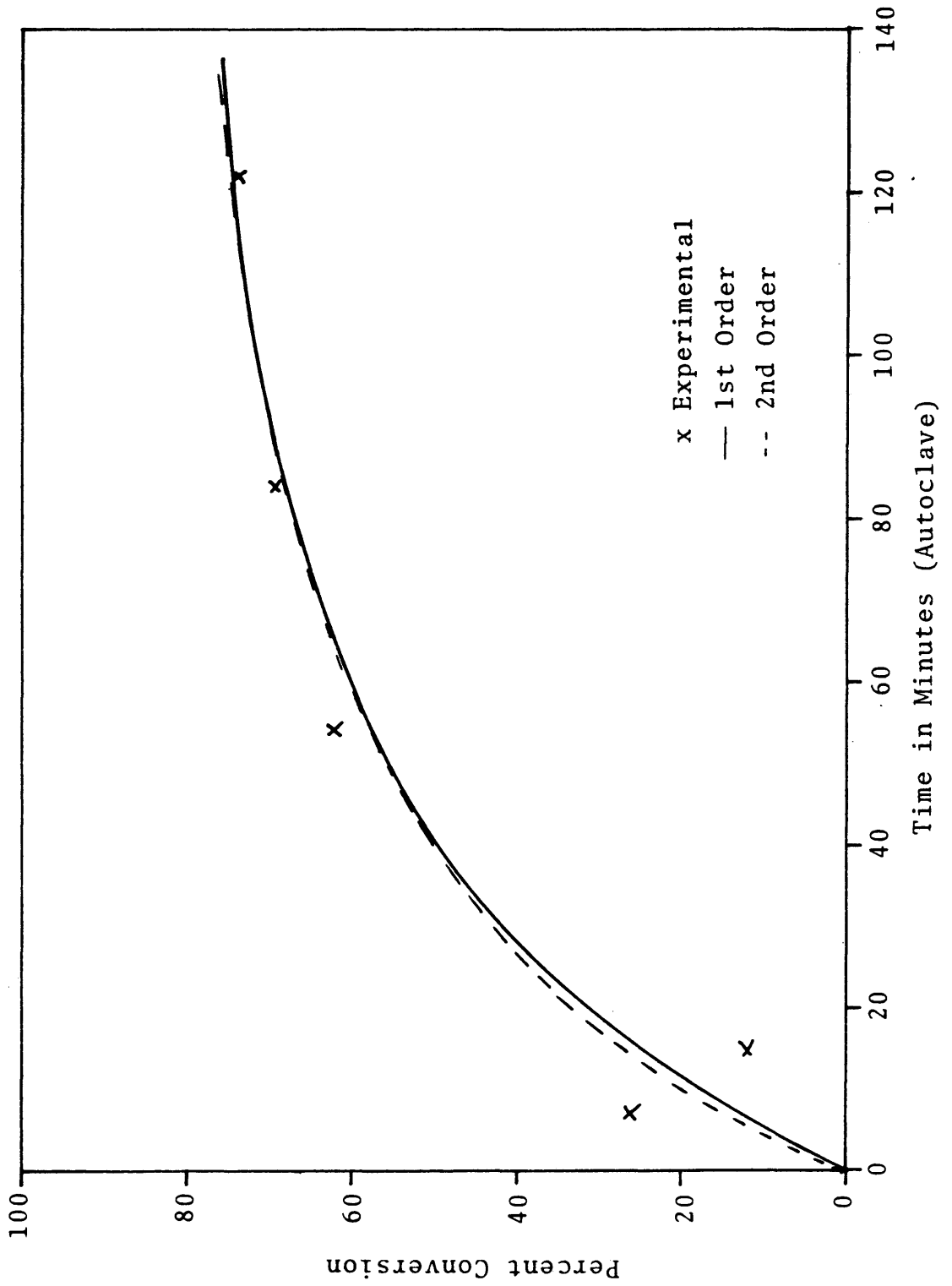


Figure 36. Run 28, Comparison of Experimental Weight Percent Removal of Volatile Matter from Coal with 1st and 2nd Order Kinetic Models.

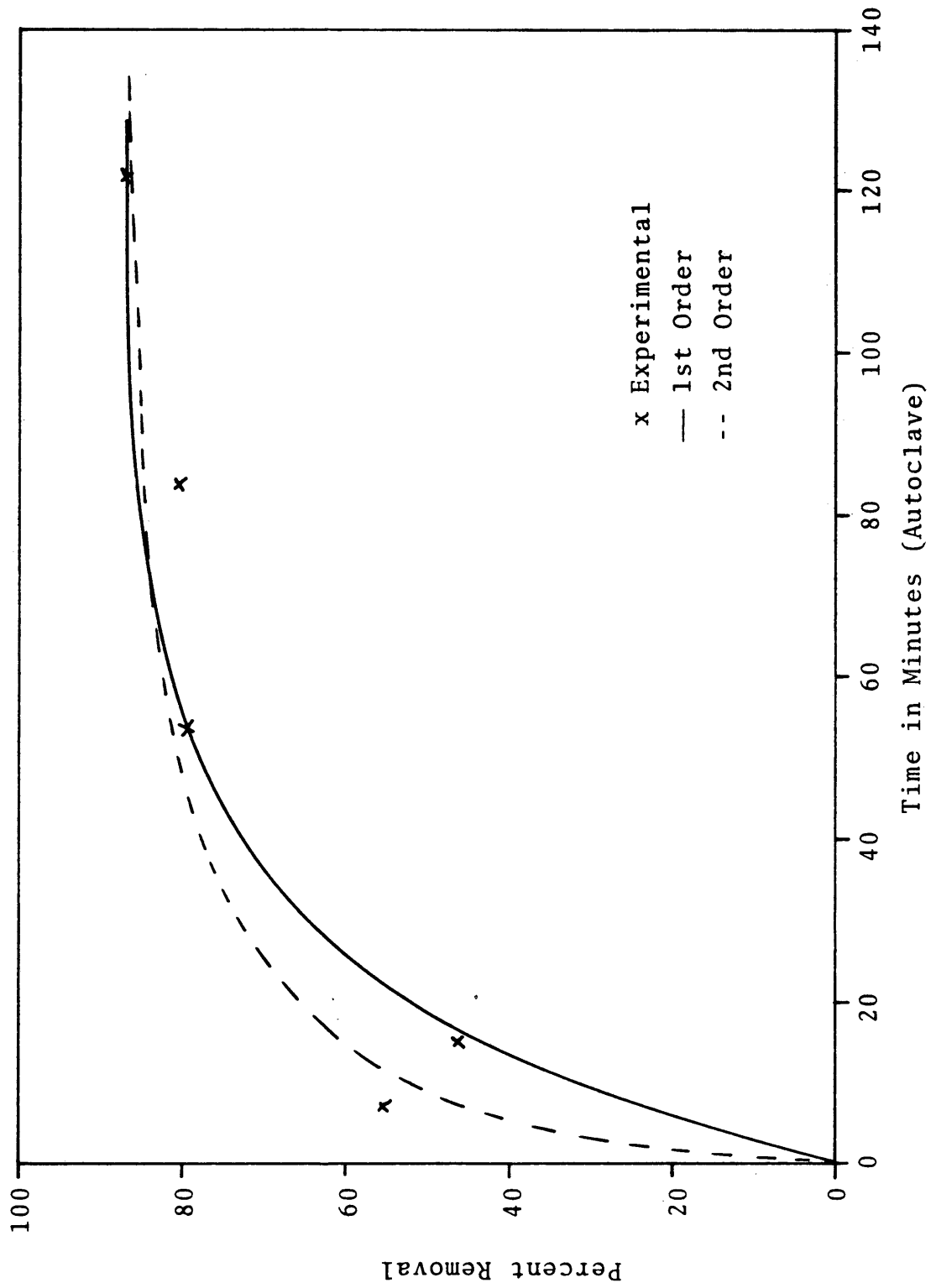


Figure 37. Run 28, Comparison of Experimental Weight Percent Removal of Fixed Carbon from Coal with 1st and 2nd Order Kinetic Models.

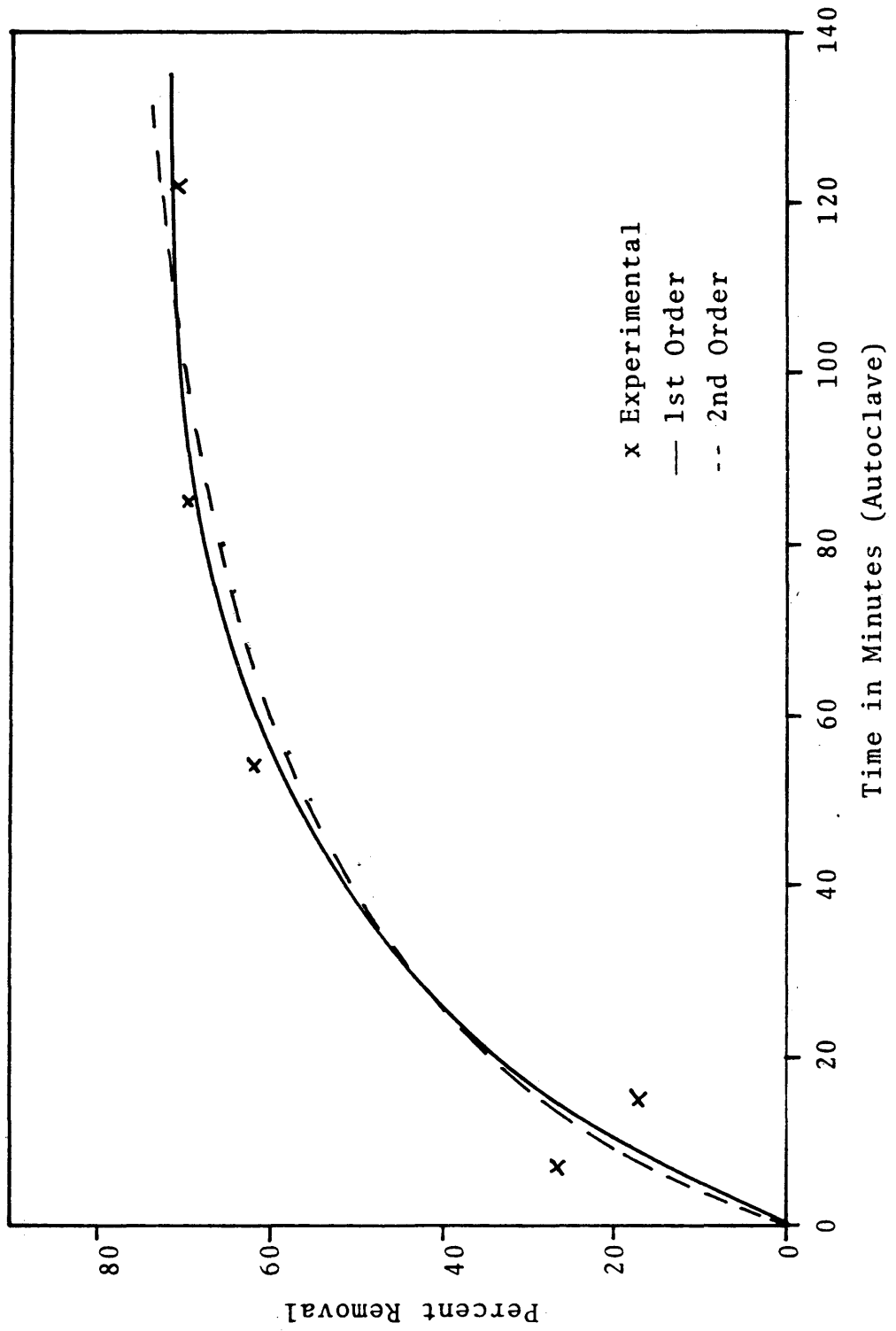


Figure 38. Run 28. Comparison of Experimental Weight Percent Removal of Methane from Coal with 1st and 2nd Order Kinetic Models.

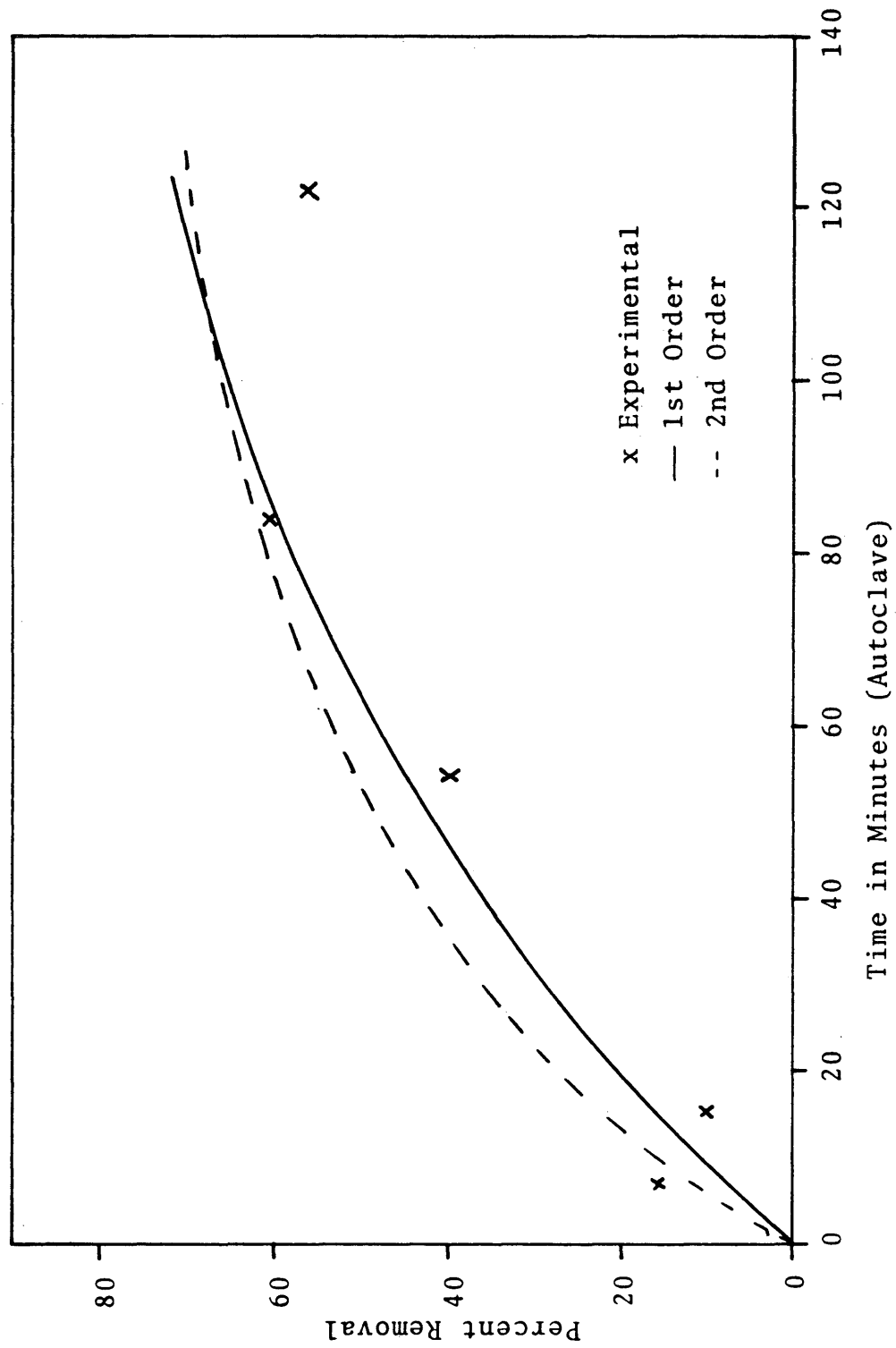


Figure 39. Run 28, Comparison of Experimental Weight Percent Removal of Carbon Monoxide from Coal with 1st and 2nd Order Kinetic Models.

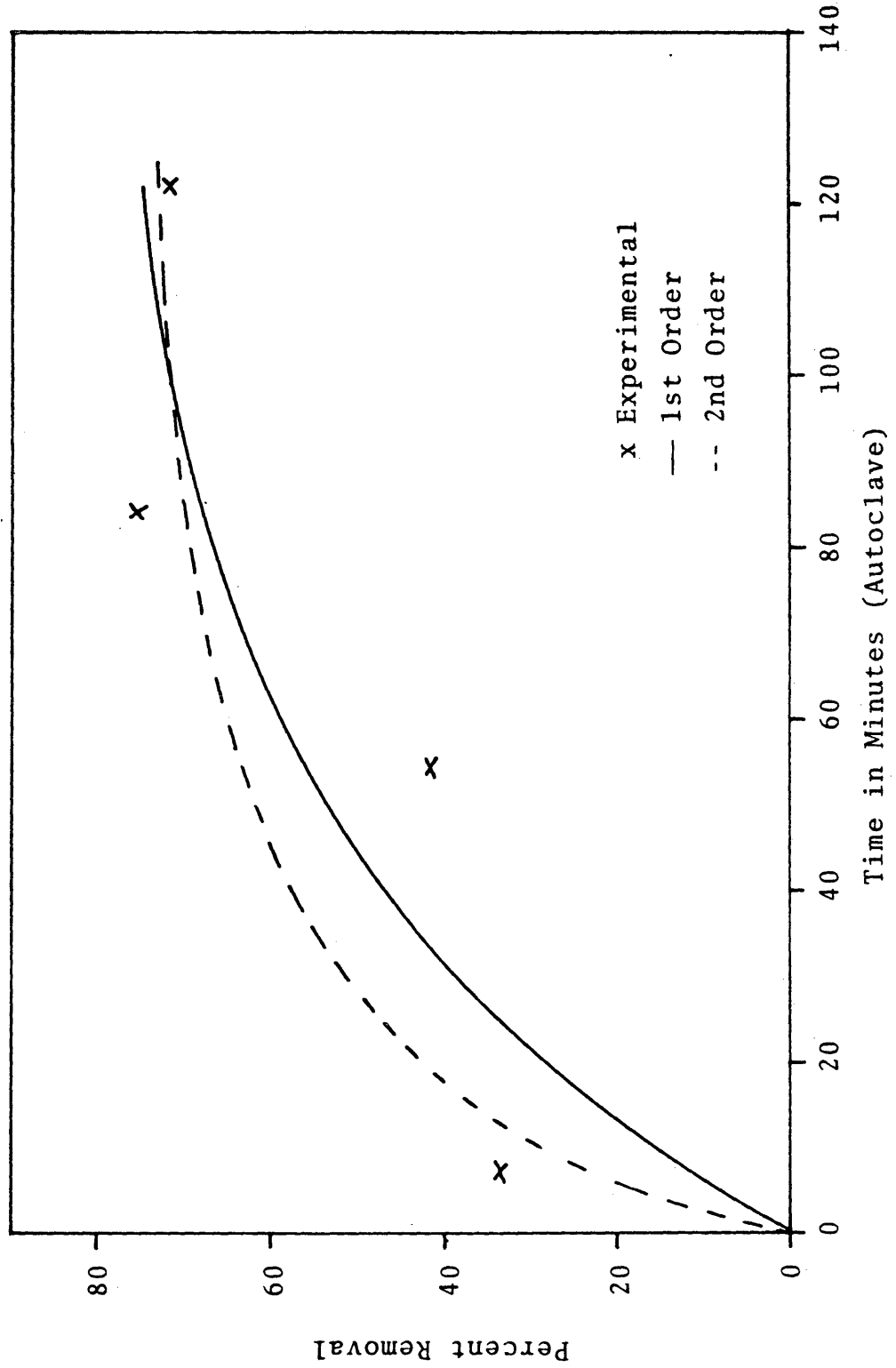


Figure 40. Run 28, Comparison of Experimental Weight Percent Removal of Carbon Dioxide from Coal with 1st and 2nd Order Kinetic Models.

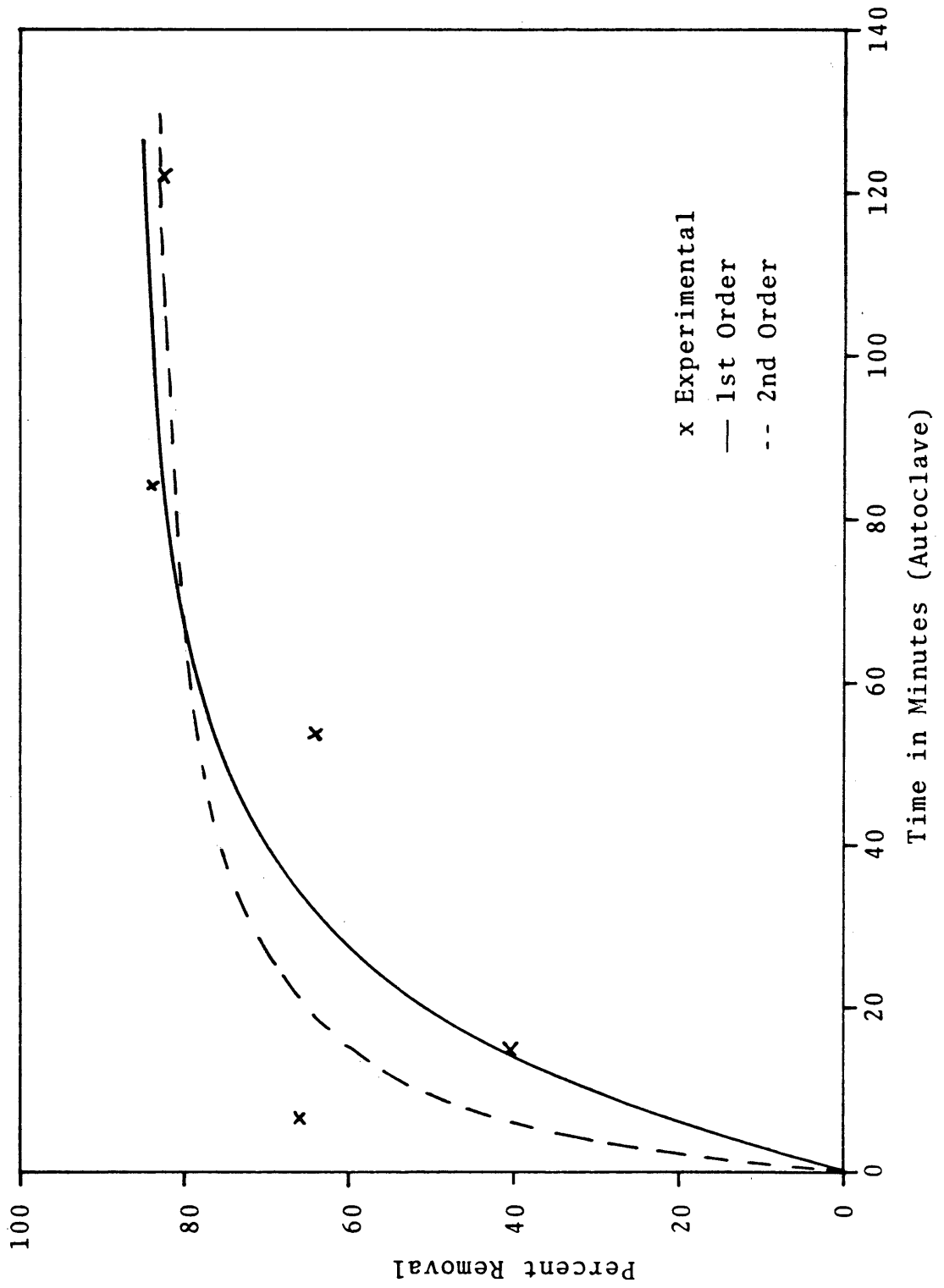


Figure 41. Run 28, Comparison of Experimental Weight Percent Removal of Water from Coal with 1st and 2nd Order Kinetic Models.

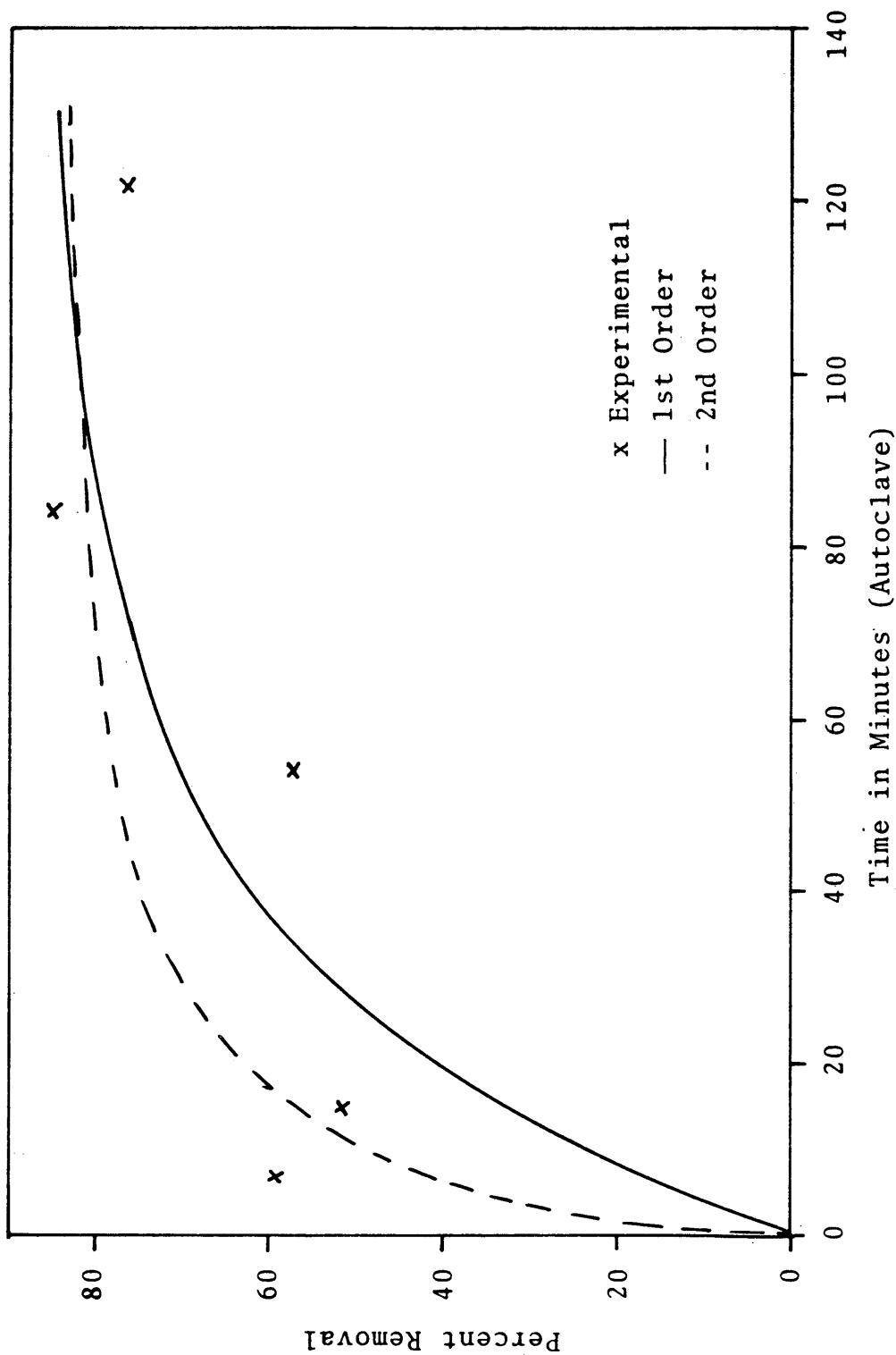


Figure 42. Run 27, Residue, Plot of 1st Order Kinetic Equation.

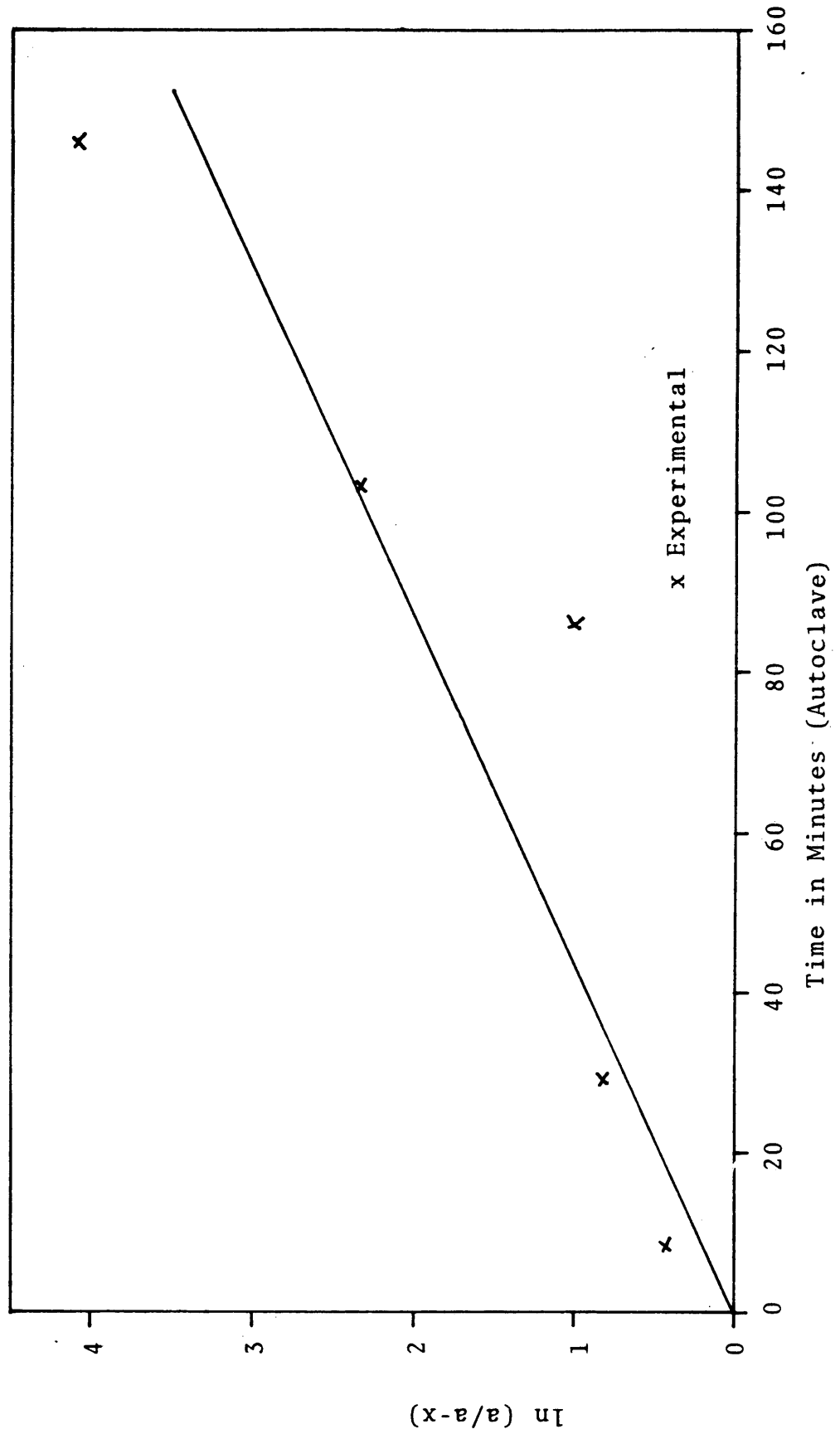


Figure 43. Run 28, Residue, Plot of 1st Order Kinetic Equation.

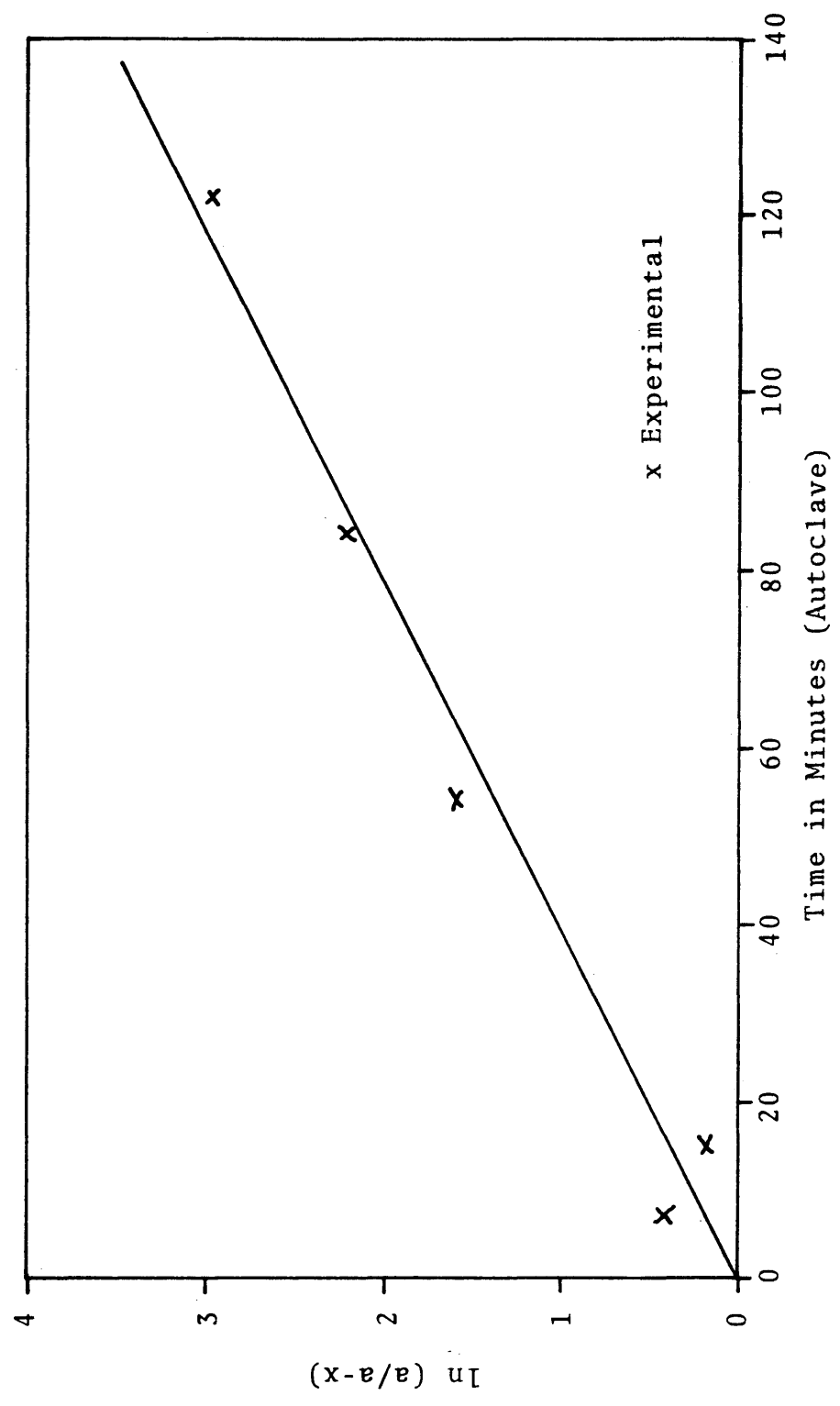


Figure 44. Run 27, Residue, Plot of 2nd Order Kinetic Equation.

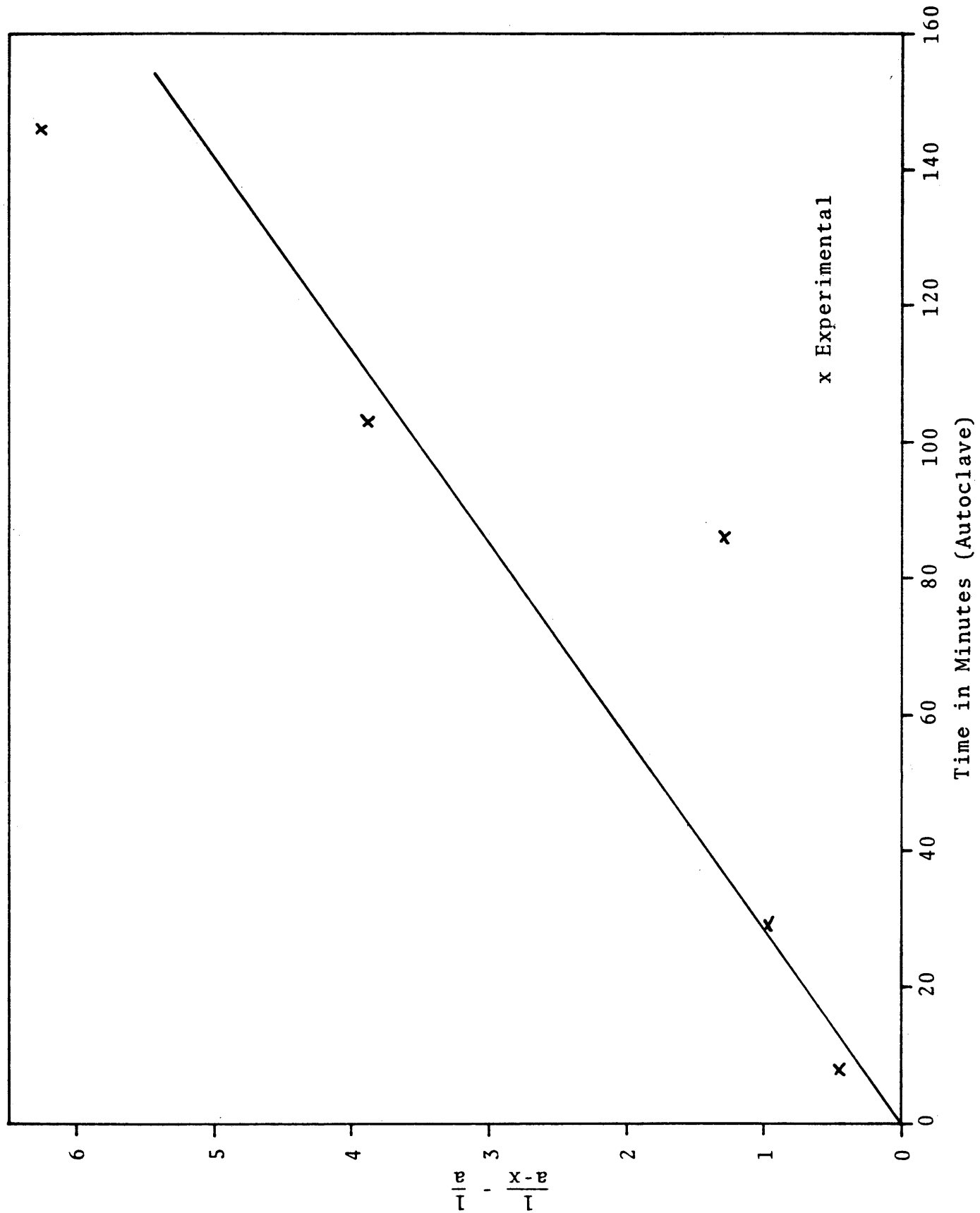


Figure 45. Run 28, Residue, Plot of 2nd Order Kinetic Equation.

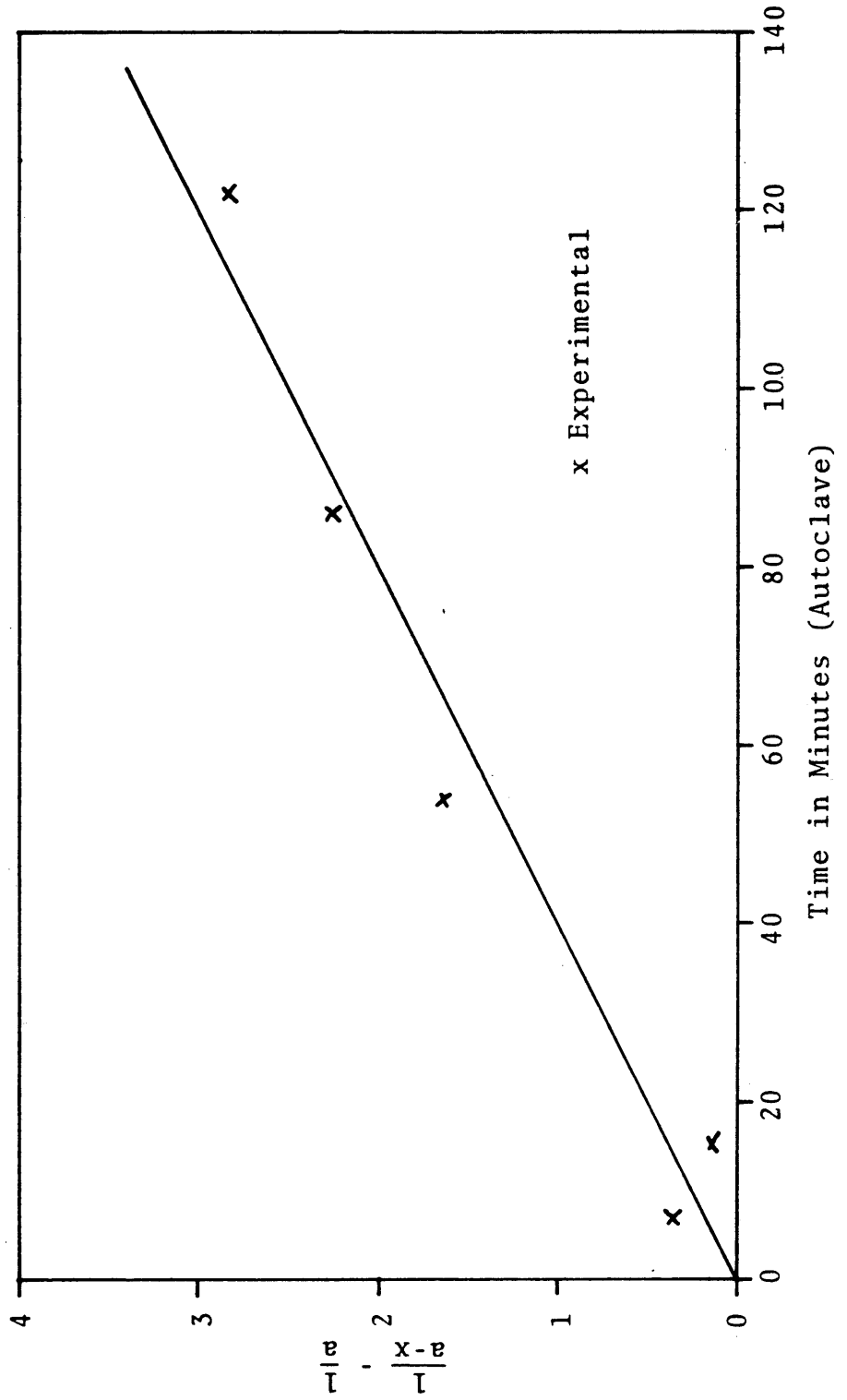


Figure 46. Run 27, 1st Order Plot of Residue with 95% Confidence Interval.

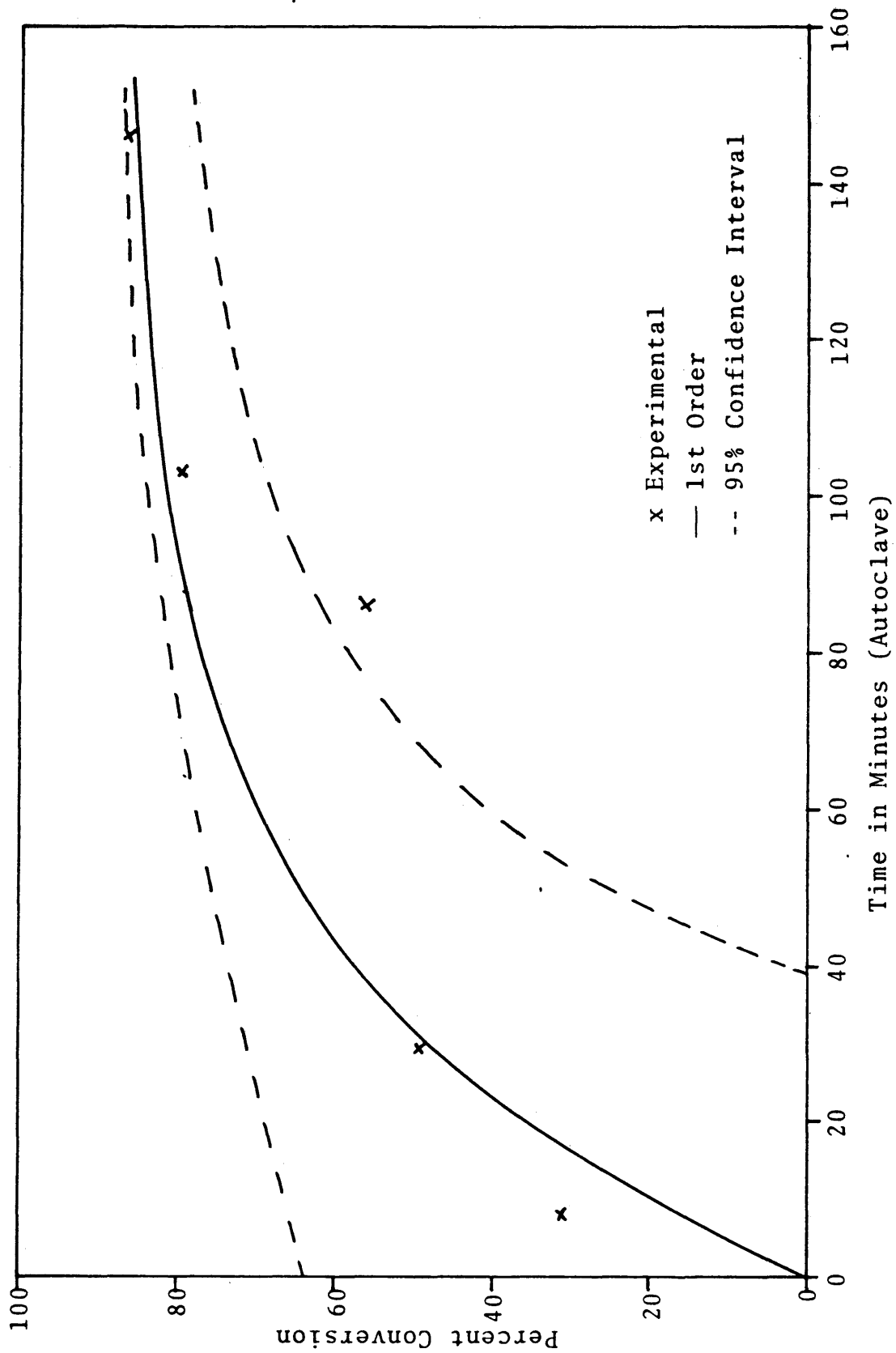


Figure 47. Run 27, 2nd Order Plot of Residue with 95% Confidence Interval.

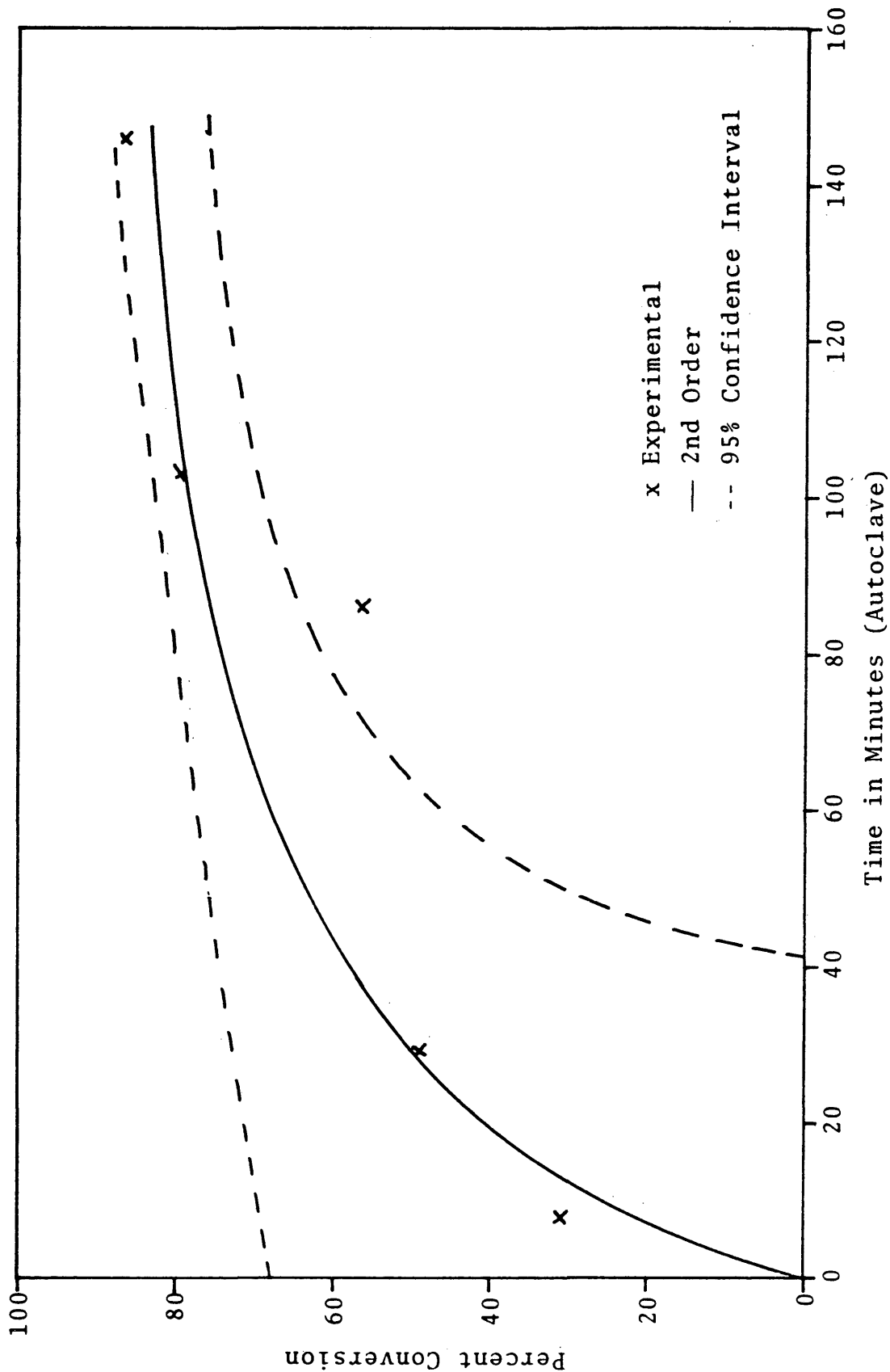


Figure 48. Run 27, 1st Order Plot of Volatile Matter with 95% Confidence Interval.

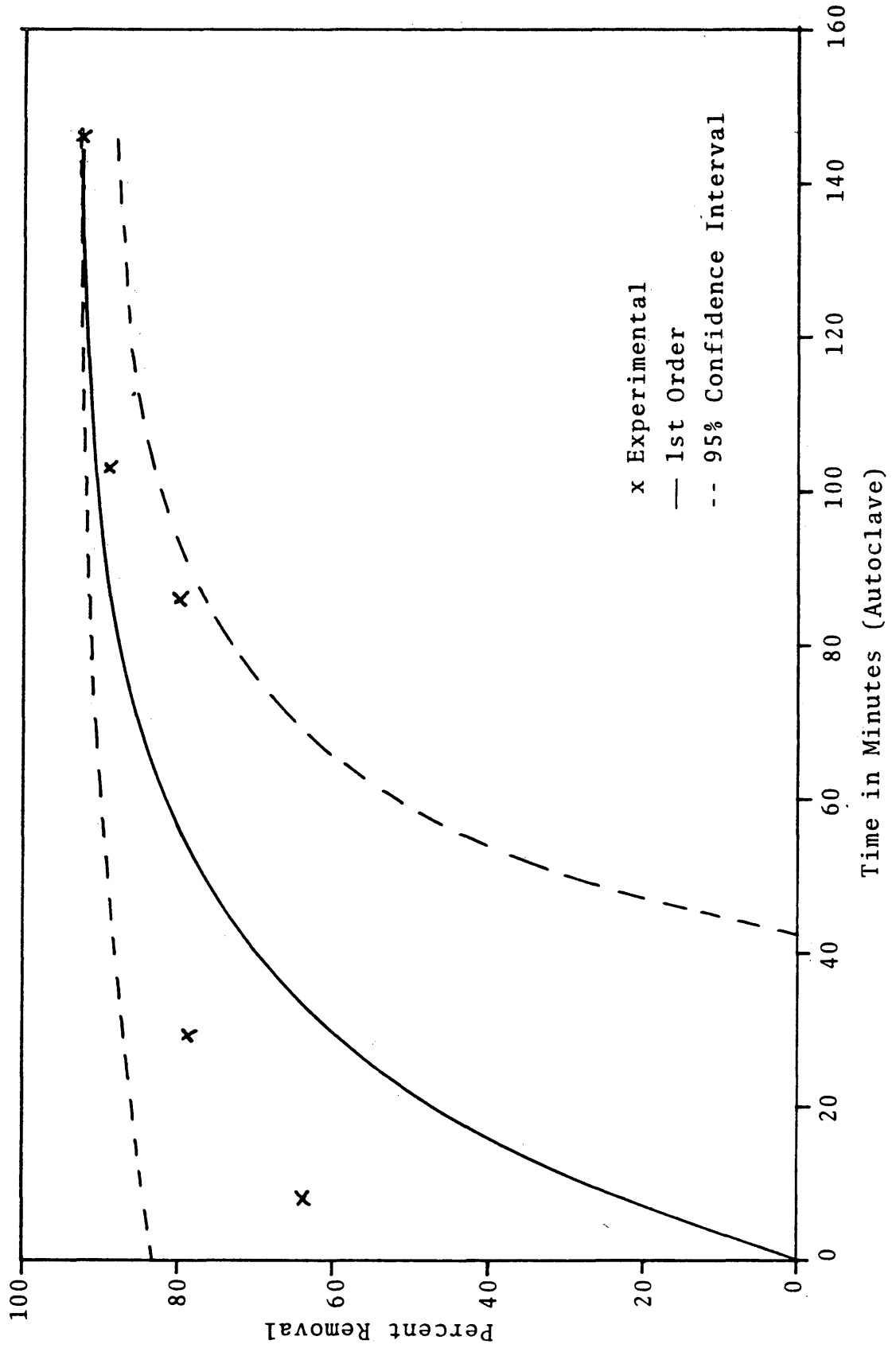


Figure 49. Run 27, 2nd Order Plot of Volatile Matter with 95% Confidence Interval.

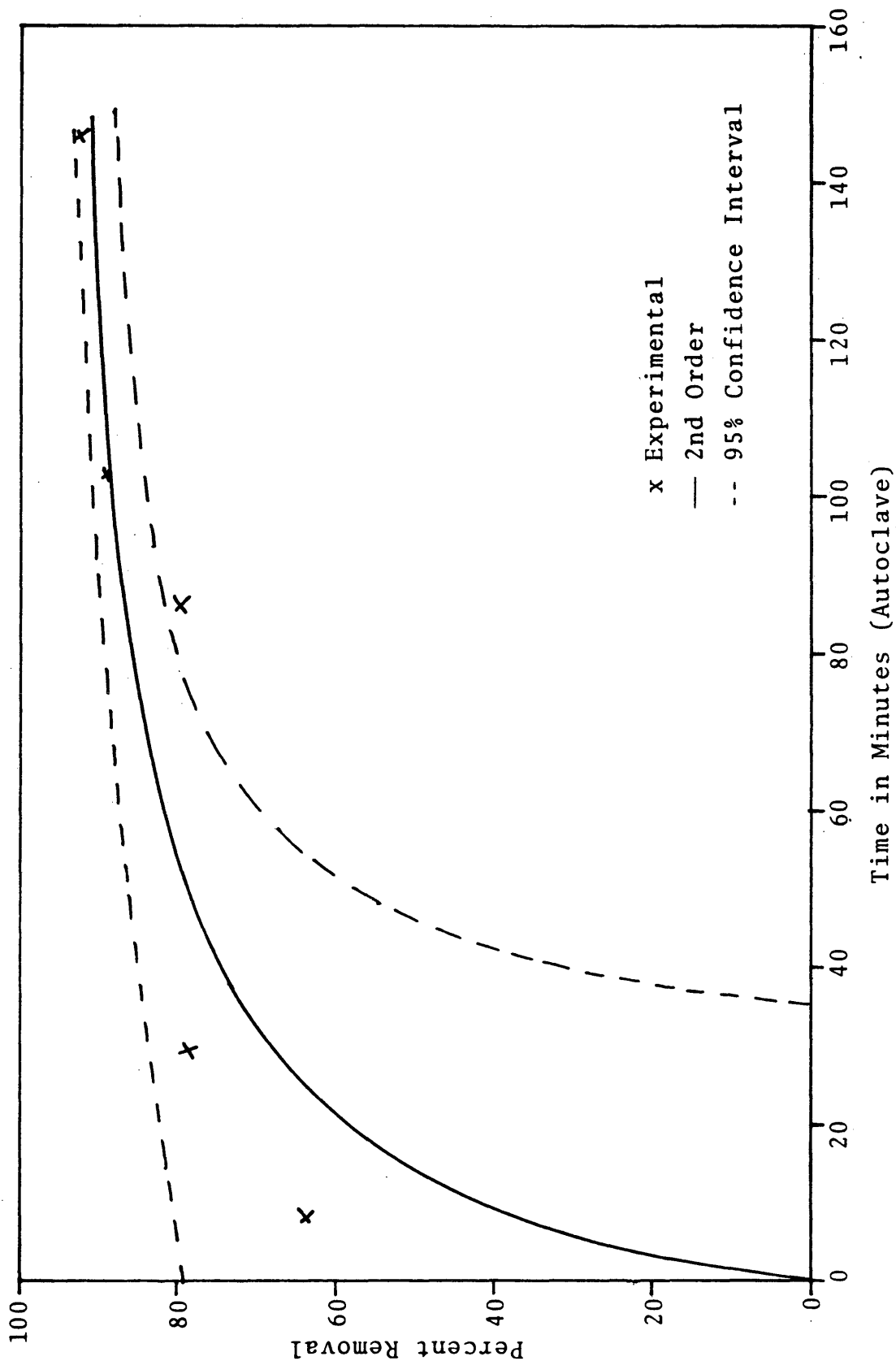


Figure 50. Run 28, 1st Order Plot of Residue with 95% Confidence Interval.

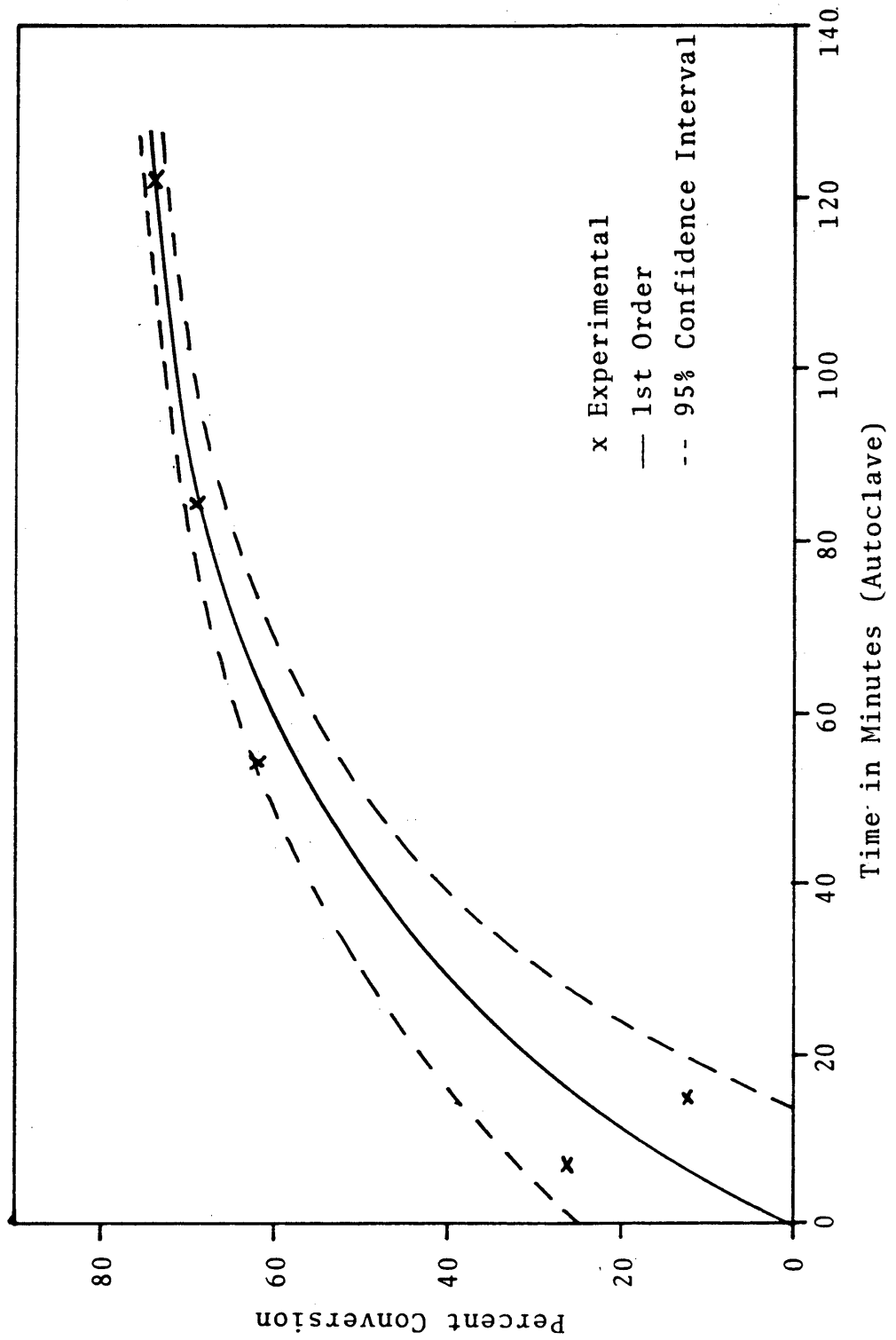


Figure 51. Run 28, 2nd Order Plot of Residue with 95% Confidence Interval.

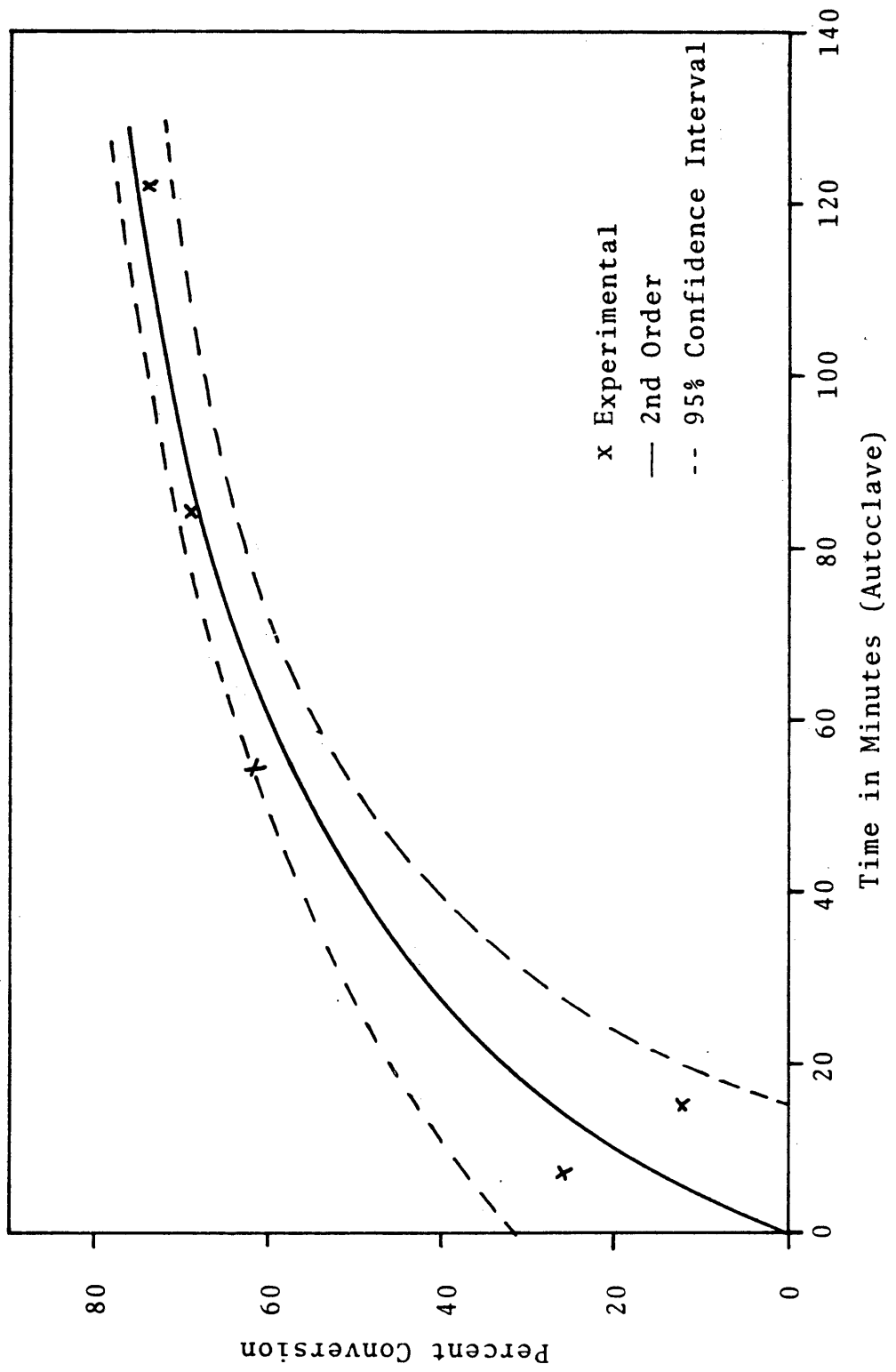


Figure 52. Run 28, 1st Order Plot of Volatile Matter with 95% Confidence Interval.

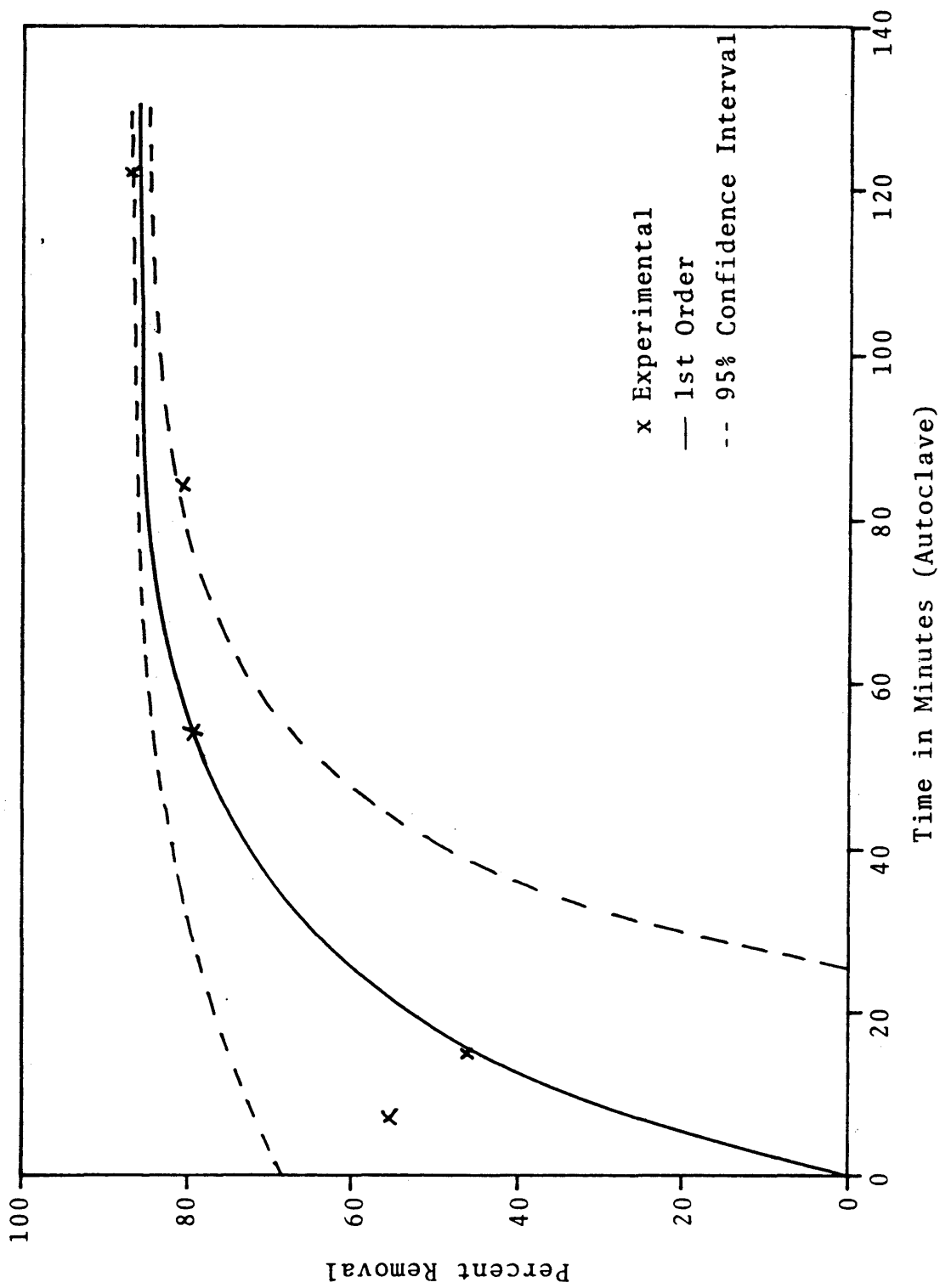


Figure 53. Run 28, 2nd Order Plot of Volatile Matter with 95% Confidence Interval.

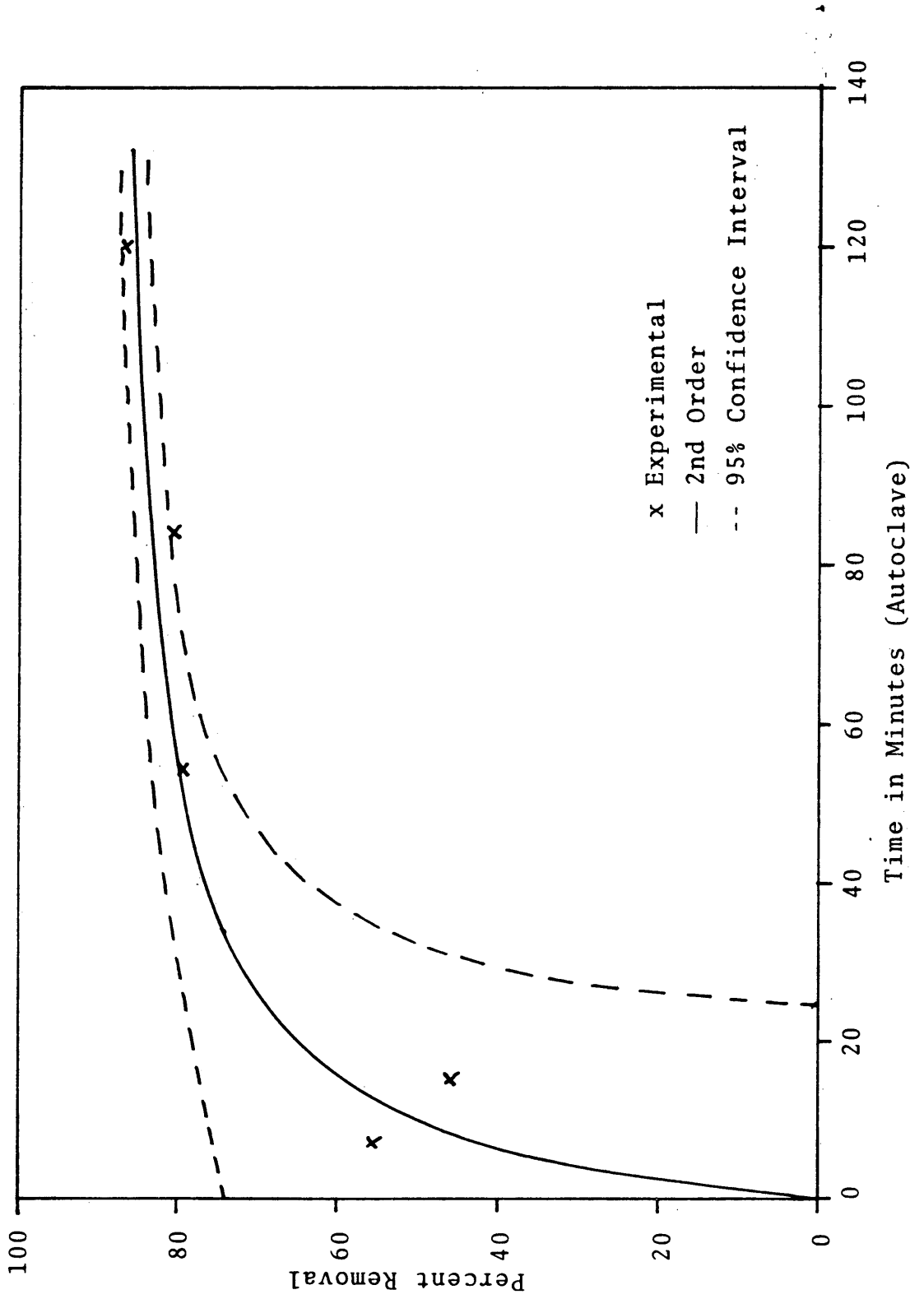
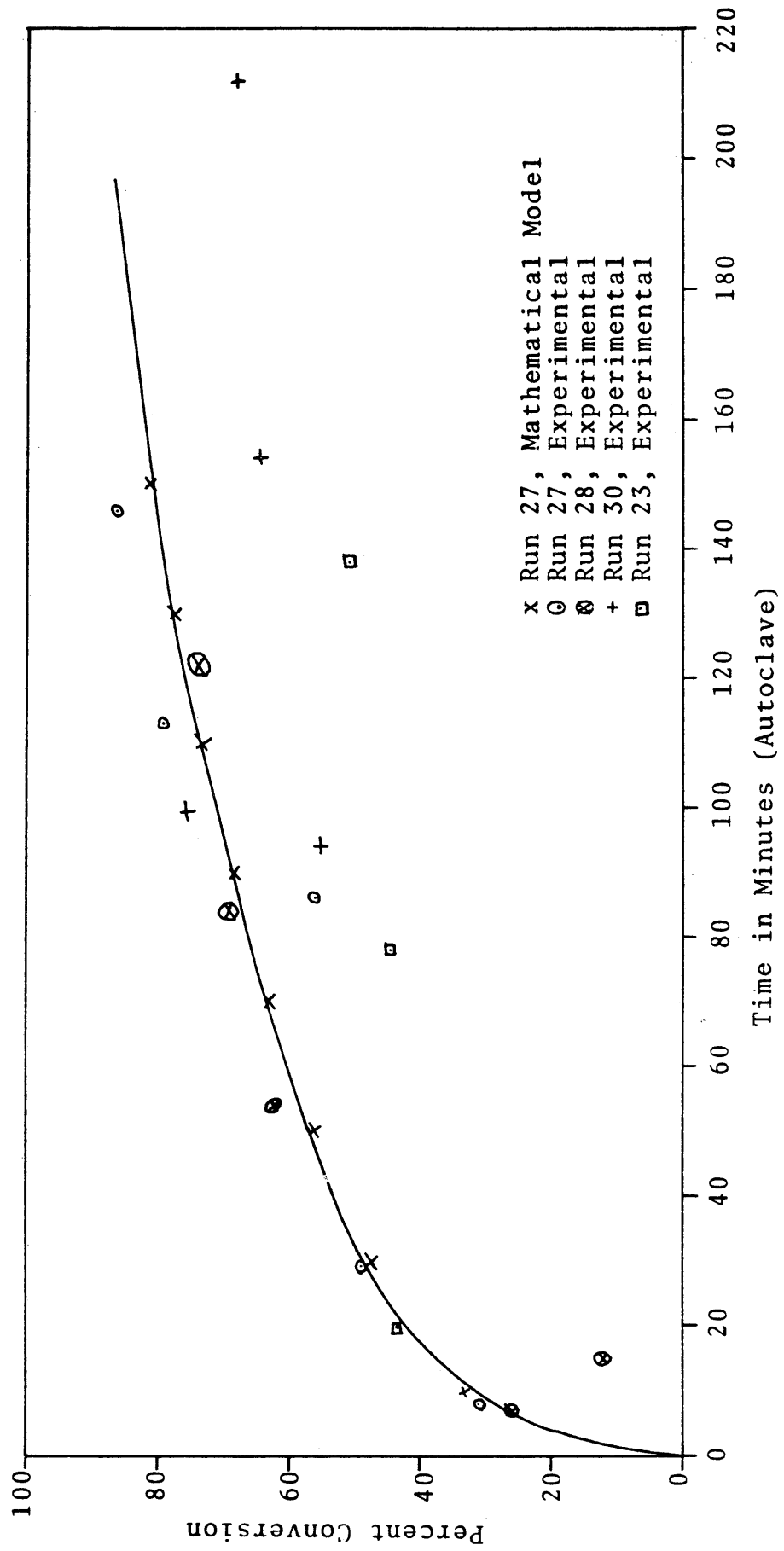


Table 15. - Values of Rate Constants and 'a'.

Run No.	Constituent	1st Order		2nd Order	
		k (min ⁻¹)	a	k (min ⁻¹)	a
R27	Residue	.0272	.87	.0354	1.00
R27	Volatile Matter	.0358	.93	.3613	.94
R27	Fixed Carbon	.0317	.87	.0427	.99
R27	Methane	.0345	.95	.0945	1.00
R27	Carbon Dioxide	.0255	.94	.0656	1.00
R27	Water	.0325	.95	.1078	1.00
R28	Residue	.0254	.78	.0251	1.00
R28	Volatile Matter	.0465	.87	.1444	.91
R28	Fixed Carbon	.0314	.73	.0321	.93
R28	Carbon Monoxide	.0225	.80	.0591	.86
R28	Carbon Dioxide	.0465	.84	.1702	.88
R28	Methane	.0129	.90	.019	1.00
R28	Water	.0326	.85	.157	.88

Figure 54. Comparison of Weight Percent Conversion of Coal (Residue).



of fixed carbon and volatile matter in the autoclave residue as a function of time are shown graphically in figs. 55-56, respectively, where results for runs 23, 27, 28 and 30 are recorded. Runs 23, 27 and 28 were batch runs where reactants were charged into a pre-heated reactor at reaction temperature and pressure. Run 30 was a slow heat up run and in Run 31 fresh gas was charged during the run but initial run procedure was similar to Run 27. The specific conditions (i.e., temperature, pressure, etc.) of the runs were shown previously in Table 5. Residue changed slowly in Runs 23 and 30 as compared to Run 27 (fig. 54). In Run 23 (fig. 54), residue does not change appreciably after the first 20 minutes and coking was also observed after the run was finished. One of the reasons for the formation of coke during this run might be the absence of sufficient hydrogen donor solvent as this run was performed using only anthracene oil (no tetralin) for the solvent. Run 30 was a slow heat up run, therefore slow changes in the residue could be expected. Residue change in Run 28 is comparable to Run 27 indicating that a change in coal does not have a significant effect on residue disappearance during reaction (reaction conditions were identical to Run 27). The volatile matter changed slowly in Runs 23 and 30 as compared with Run 27 (fig. 56). In Run 23, volatile matter does not change appreciably after the first 20 minutes, while the change in volatile matter in Run 30 is slower than in Run 27 as was expected from the residue data. The change in volatile matter of Run 28 is comparable to Run 27 and once again indicates little difference in behavior between coals. Fixed carbon in Run 23 (fig. 55) decreases initially in the run and

Figure 55. Comparison of Weight Percent Removal of Fixed Carbon from Coal.

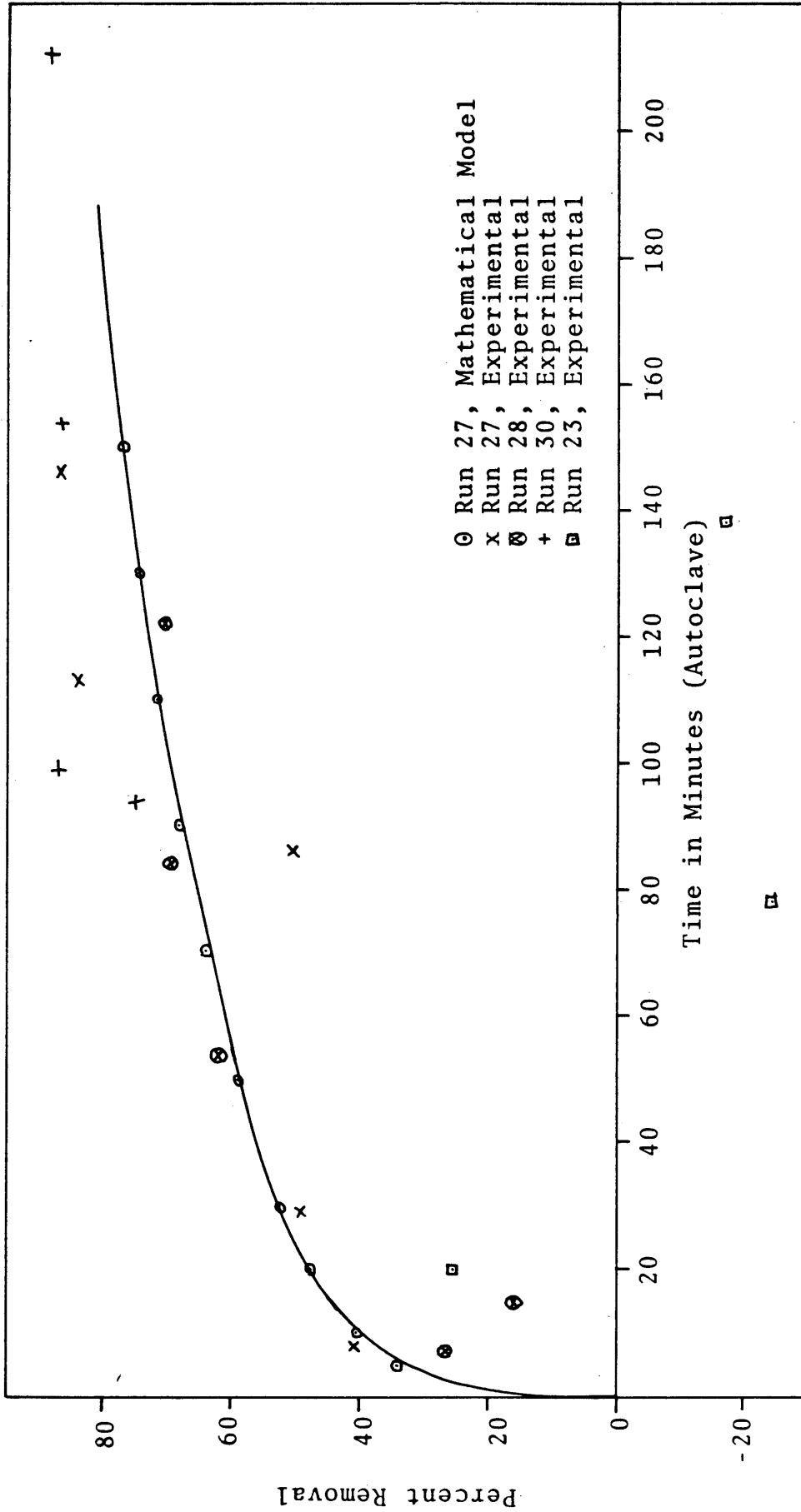
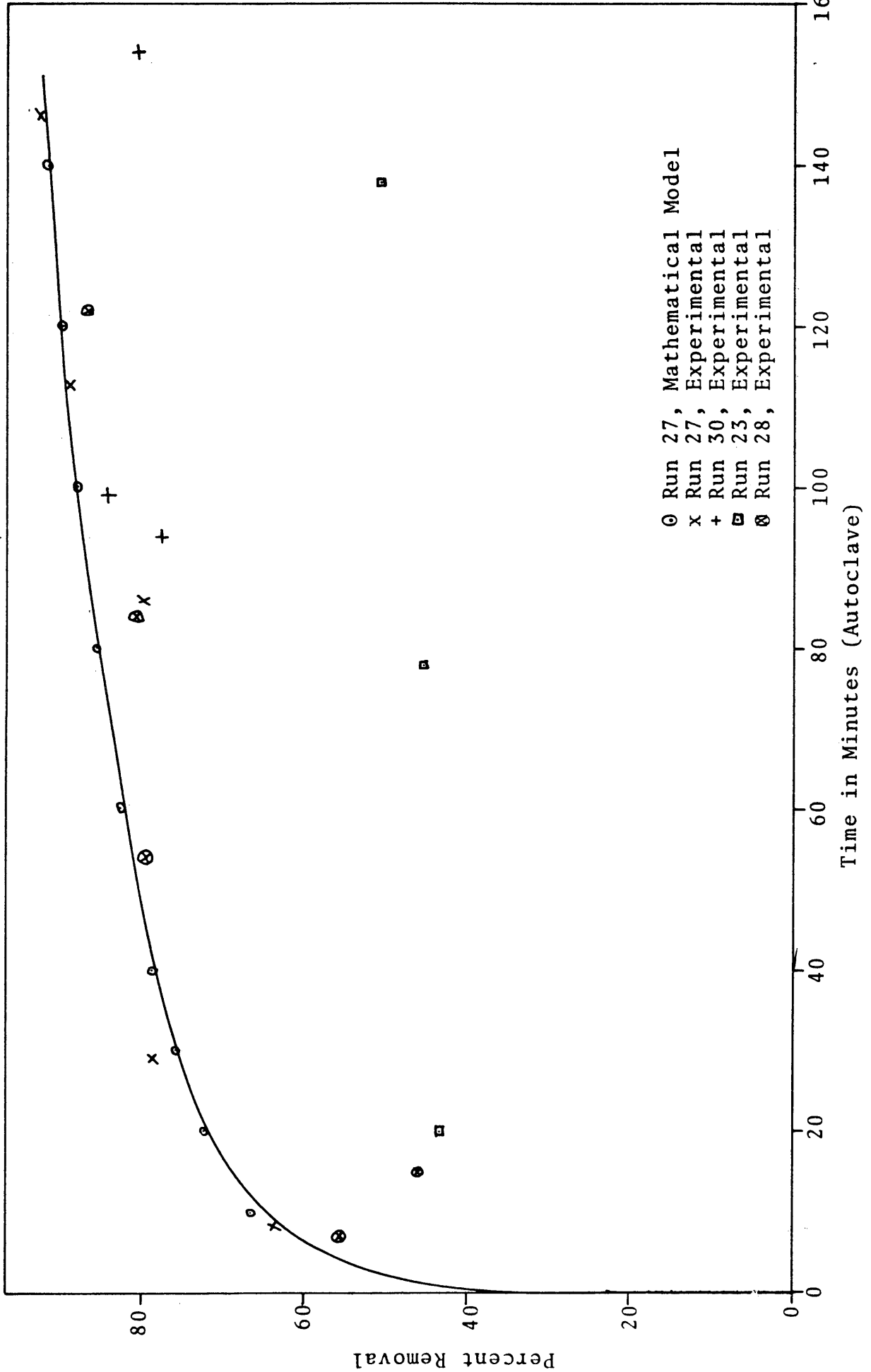


Figure 56. Comparison of Weight Percent Removal of Volatile Matter from Coal.



then starts increasing verifying the coking observed after the run. The change in fixed carbon of Run 30 (fig. 55) is fast compared to Run 27 indicating that slow heating decreases the fixed carbon in the residue. The change in fixed carbon of Run 28 is comparable to Run 27, thereby verifying the inference drawn from residue change. The kinetic rate constants evaluated for different products in the residue, including the residue are quite comparable indicating once again that change in the coal does not affect the rate of change of the products during the run. Behavior exhibited by ash was quite abnormal because instead of staying nearly constant during the autoclave run, it increased 2-2.5 times initially due to solvent volatilization and then started decreasing. Also changes in the color of ash were found during analysis indicating that it is probably acting as a catalyst.

Reproducibility

Every sample was run three times to serve as a check on the reproducibility of data. Sample 1 (at 8 minutes) of Run 27 is presented in Table 16, showing the percent removal of volatile matter and fixed carbon.

Table 16. Reproducibility Results, Run 27, Sample 1.

	<u>Percent Removal of Volatile Matter</u>	<u>Percent Removal of Fixed Carbon</u>
1)	66.46	42.37
2)	63.08	37.59
3)	62.76	43.49
Mean	64.1	43.15

Amounts of Volatile Matter, Heavy Liquids, Light Gases,
Fixed Carbon and Ash Obtained During Pyrolysis

The inferences drawn from these pyrolysis results are for qualitative comparison only since the method used for obtaining concentrations of heavy liquids was not precise. The amount of fixed carbon obtained by analysis might have some volatile matter in it because all volatile matter was not liberated during pyrolysis at a temperature of 800°C. The amounts of volatile matter, heavy liquids, light gases, fixed carbon and ash are given in Tables 17-18 as a percent of the residue and liquid product. The amount of heavy liquids accounted for by the Gas Chromatographic analysis is also given. The heavy liquids calculated by peak analysis of gas chromatograms are not equal to the total amount of heavy liquids liberated during pyrolysis. The reason for the lack of balance is that some of the heavy liquids liberated during pyrolysis have a boiling point higher than 250°C, and are trapped in the transfer lines after they are liberated, since the temperature of transfer lines was maintained only at a maximum temperature of 250°C. The individual concentrations of different heavy liquid components are given in Appendix C.

Correlation of Results to Run Conditions

The results of runs in this section will be compared with Run 27 because the run conditions used in this run gave least amount of residue and maximum amount of heavy liquids (best quality residue by the previously-mentioned standard).

Table 17. Products of Pyrolysis at 800°C Based on Residue.

Run No. & Sample	Time (min.)	% Residue in Ash as % of Residue	% Residue in Liquid Coal of Residue	V.M. as % of Residue	Light Gases as % of Residue	Heavy Liquids as % of Residue	Fixed C as % of Residue	Heavy Liquids Accounted by Peak Analysis as % of Residue
R27 Raw Slurry		23.29	6.19	37.03	19.57	17.46	56.79	3.54
R28 Raw Slurry		23.34	5.47	32.34	14.88	17.46	62.19	2.47
R23 Raw Slurry		20.19	7.58	33.69	27.71	5.98	58.73	1.28
R27 Sample 9 146 mins.		3.14	35.60	12.96	1.43	11.53	51.44	3.19
R28 Sample 6 84 mins.		7.16	11.66	27.54	13.07	14.46	60.80	3.81
R23 Sample 11 138 mins.		21.61	27.84	4.33	3.12	1.21	67.82	.89
R30 Sample 6 180 mins.		8.57	56.19	9.59	2.63	6.96	34.22	3.42
R31 Sample 7 259 mins.		8.42	47.50	10.34	1.96	8.38	42.16	4.81

Table 18. Products of Pyrolysis at 800°C Based on the Liquid Product.

Run No. & Sample	Time (min.)	% Residue in Ash as % of Liquid Coal	% of V.M. as % of Liquid Coal	Light Gases as % of Liquid Coal (V.M.-Light Gases)	Heavy Liquids as % of Liquid Coal	Fixed C as % of Liquid Coal	Heavy Liquids Accounted by Peak Analysis as % of Liquid Coal
R27 Raw Slurry	23.29	1.44	8.62	4.56	4.07	13.22	.83
R28 Raw Slurry	23.34	1.28	7.55	3.47	4.08	14.52	.58
R23 Raw Slurry	20.19	1.53	6.80	5.59	1.21	11.86	.26
R27 Sample 9	146	3.14	1.12	0.44	.36	1.62	.10
R28 Sample 6	84	7.16	.83	.94	1.04	4.35	.27
R23 Sample 11	138	21.61	6.02	.93	.26	14.66	.19
R30 Sample 6	180	8.57	4.82	.23	.60	2.93	.29
R31 Sample 7	259	8.42	4.00	.87	.71	3.55	.41

The samples used for pyrolysis for different runs do not have equivalent times in the autoclave, therefore their composition can only be used for qualitative purposes.

Run 27 was made at a temperature of 437°C and produced no coke during the run, thus accounting for the heavy liquids observed in the residue. There is an 86% decrease in residue of Run 27 after 146 minutes of autoclave run and there was also a substantial (65%) decrease in the volatile matter, but now the volatile matter consisted essentially of heavy liquids with small amounts of light gases.

The volatile matter in the raw feed slurry of Run 23 consists mostly of light gases and small amounts of heavy liquids as compared to Run 27. This difference indicates that tetralin which is used in Run 27 (other reactants are identical to Run 23) has some effect on the coal structure besides enhancing the hydrogen donor capabilities of the anthracene oil solvent used. Residue in Run 23 does not change even after 138 minutes of autoclave run but there is a 86% decrease in the volatile matter and it consists essentially of light gases with small amounts of heavy liquids. Fixed carbon and ash increased substantially during the run. The formation of coke and the constancy of residue can be explained because of the lack of hydrogen donor solvent mentioned previously. The formation of coke during the run explains the evolution of light gases from the residue and the absence of heavy liquids.

Samples from the raw slurries of Runs 30 and 31 were not pyrolyzed because their feeds were identical to Run 27 as indicated by Table 5. Sample used for the pyrolysis from Runs 30 and 31 was collected after 180 min and 259 min of autoclave run respectively. The amount of residue was the same in both samples but was more than that of Run 27, even though a longer run time was used. The volatile matter in both the runs was quite comparable but was less than that of Run 27 which can be expected because of longer run time. The light gases in the samples of Runs 30 and 31 were comparable and were a little higher than that of Run 27. The heavy liquids from the samples of Runs 30 and 31 were also similar but lower (in quantity) than that of Run 27. Lower amounts of heavy liquids indicate that probably the run conditions were not suitable for the production of heavy liquids. The fact that residue obtained is more than that of Run 27 indicates that a longer run time at those run conditions is also not suitable for converting lignite into a liquid product.

Run 28 was with a different coal but at the same run conditions as Run 27. The heavy liquids present in the raw feed slurry of Runs 28 and 27 are almost identical, while the light gases in Run 28 are lower than in Run 27. The sample for Run 28 was collected after 84 mins of autoclave run and has a higher residue as compared to Run 27 and this can be explained by the lower residence time in the reactor for this sample. Volatile matter of the sample of Run 28 is higher

than that of Run 27, but it is not very different from raw slurry of Run 28. Light gases and heavy liquids in the sample are quite similar to the raw slurry of Run 28. Light gases from the sample are higher than that of Run 27 sample but heavy liquids do not show that much difference. The reduction in residue noted between Runs 27 and 28 and the presence of nearly the same amount of heavy liquids as in the original coal indicate that the coal used in Run 28 would be more suitable for further processing (i.e., carbonization).

CONCLUSIONS

The following conclusions can be made from this study.

1. Nearly 75% of the removal in volatile matter and 55% removal in fixed carbon is achieved during the first 60 minutes of the autoclave run. The reason for making a run for longer periods of time would be to convert heavier coal molecules into lighter components (increase oil yield).

2. The heavy liquids obtained from the residue of the autoclave runs resemble the constituents present in the anthracene oil solvent.

3. Run 27 gives the least amount of residue when compared with other runs for the same time period. The residue of Run 27 contains maximum amounts of heavy liquids and least amount of light gases when compared with Runs 23, 30, and 31.

4. Run 23 exhibits coking indicating that sufficient hydrogen donor solvent must be present during the initial stages of dissolution to prevent coke formation.

5. The rate equation proposed by Wiser represents the data of Runs 27 and 28 reasonably well. The general expression proposed by Wiser is given by:.

$$\frac{dx}{dt} = k_n (a-x)^n \quad \text{where } n \text{ is the reaction order.}$$

Both first and second order expressions seem to fit the data reasonably well.

6. Residue of Run 28 would be best suited for further processing by carbonization or gasification.

RECOMMENDATIONS FOR FURTHER STUDY

More runs are needed under the conditions of Runs 30 and 31 to arrive at a definite conclusion about the effect of these conditions. More runs are needed for the coal used for Run 28 to determine the suitability of this coal for liquefaction. Ash requires more detailed analysis in order to explain the abnormal behavior. Since pyrolysis at 800°C is economically feasible, therefore additional work is required to develop some quantitative analysis method so as to arrive at definite conclusions for the further processing of residue.

LITERATURE CITED

1. Wiser, H. Wendell, A kinetic comparison of coal pyrolysis and coal dissolution, *Fuel*, v. 47, 1968, pp. 475-486.
2. Klass, Donald L., Synthetic crude oil from shale and coal, *Chemtech*, August 1975, pp. 499-510.
3. Nelyubin, B. V., Alaev, G. P., Thermal decomposition of coal, *Izv. Nauch. - Issled. Inst. Nefte - Uglekhim, Sin. Irkutsk Univ.*, 1969, 11 (Pt. 1), pp. 76-8 (Russ.).
4. Van Heck, Karl Heinrich, Juentgen, Harold, New research on the thermal decomposition of bituminous coal (Bergbau-Forsch. Gm.bh., Essen-Kray, (Ger.), Chem. Anlagen Verfahren, 1969 (6), pp. 39-42 (Ger.).
5. Girling, G. W., Evolution of volatile hydrocarbons from coal, *J. Applied Chem.*, Feb. 1963, pp. 77-91.
6. Berkowitz, N., The coal-carbon transformation: Basic mechanisms, *Symp. Sci. Technol. Coal*, 1967, pp. 119-55, Mines Br., Dep. Energy, Mines Resour.: Ottawa, Can.
7. Brooks, J. D., and Mather, T. P., *Fuel*, 36, 51, 1957.
8. Fisher, F., Schrader, H., Hydrogenation of coal with carbon monoxide, *Brennstoff-Chem.*, v. 2, 1921, pp. 257-261.
9. Appell, H. R., Fu, Y. C., Friedman, S., Yavorsky, P. M., Wender, Irving, Converting organic wastes to oil. A replenished energy source, *BuMines Rept. of Inv. 7560*, 20 pp., 1971.
10. Appell, H. R., Wender, I., Miller, R. D., Liquefaction of lignite with carbon monoxide and water, *BuMines Inf. Circ. 8543*, 1971, pp. 32.
11. Appell, H. R., Wender, I., The hydrogenation of coal with carbon monoxide and water: *Div. Fuel Chem. Preprints, Am. Chem. Soc.*, v. 12, no. 3, 1968, pp. 220.
12. Appell, H. R., Wender, I., Miller, R. D., Dissimilar behavior of carbon monoxide plus water and of hydrogenation, *Div. Fuel Chem. Preprints, Am. Chem. Soc.*, v. 13, no. 4, 1969, pp. 39.
13. Appell, H. R., Wender, I., Miller, R. D., Solubilization of low rank coal with carbon monoxide and water: *Chem. and Ind. (London)*, no. 47, Nov. 22, 1969, p. 1703.

14. Appell, H. R., Wender, I., Miller, R. D., The mechanism of lignite liquefaction with carbon monoxide: Div. Fuel Chem., Am. Chem. Soc., Presented April 10, 1972.
15. Yavorsky, P. M., Friedman, S., Ginsberg, H. H., Wender, Irving, Continuous processing of urban refuse to oil using carbon monoxide: Paper, 3rd Mineral Waste Utilization Symposium, IIT Research Institute, Mar. 14-16, 1972.
16. Handwerk, J. G., CO-Steam coal liquefaction in batch reactor: Masters Thesis, Colorado School of Mines (1974).
17. Chermin, H. A. G., van Krevelen, D. W., Chemical structure and properties of coal XVII - A mathematical model of coal pyrolysis, Fuel 36, 85-104 (1957).

APPENDIX A

Raw Data for Pyrolysis at 1400°C

Sample No.	Time (min.)	Residue as % of* Liquid Product (gm)	Residue Used mgm	V.M. mgm	Fixed Carbon mgm	Ash mgm
R23, Raw Slurry	0	20.19	5.24	2.36	2.73	.45
"	"	"	4.23	1.78	2.2	.32
"	"	"	3.92	1.7	1.96	.29
R23, Sample 5	20	17.12	8.2	2.34	3.54	2.32
"	"	"	9.0	2.51	3.99	2.50
R23, Sample 9	78	21.86	6.24	1.29	3.55	1.40
"	"	"	5.12	1.15	2.97	1.0
"	"	"	5.64	1.23	3.25	1.16
R23, Sample 11	138	21.61	6.04	1.22	3.27	1.55
"	"	"	7.31	1.41	4.0	1.9
"	"	"	5.59	1.05	3.11	1.43
R26, Raw Slurry	0	21.93	5.65	3.54	1.85	.26
"	"	"	6.78	3.55	2.8	.43
"	"	"	6.47	3.88	2.38	.21
R26, End Product	64	20.44	7.09	1.0	4.67	1.42
"	"	"	7.22	1.43	4.47	1.32
"	"	"	6.76	1.43	4.2	1.13
R27, Raw Slurry	0	23.29	6.64	3.54	2.83	.27
"	"	"	7.27	3.82	3.08	.37
"	"	"	7.0	3.8	2.91	.29
R27, Sample 1	8	16.06	5.06	1.46	1.75	1.85
"	"	"	7.09	1.84	2.5	2.75
"	"	"	3.67	1.05	1.4	1.22
R27, Sample 5	29	11.81	12.06	2.88	4.84	4.34
"	"	"	8.76	1.81	3.82	3.13
R27, Sample 7	86	10.16	6.5	1.7	3.15	1.65
"	"	"	7.29	1.74	3.46	2.09
"	"	"	7.85	1.88	3.76	2.21
R27, Sample 8	113	4.76	4.59	1.32	1.51	1.76
"	"	"	5.24	1.46	1.74	2.04
"	"	"	5.24	1.53	1.72	1.99

*The residue data were supplied by GFERC, Grand Forks, North Dakota, and should not be reproduced without their permission.

<u>Sample No.</u>	<u>Time (min.)</u>	<u>Residue as % of Liquid Product (gm)</u>	<u>Residue Used mgm</u>	<u>V.M. mgm</u>	<u>Fixed Carbon mgm</u>	<u>Ash mgm</u>
R27, Sample 9	146	3.14	6.45	1.78	2.69	1.98
		"	4.09	1.17	1.71	1.21
		"	6.39	1.84	2.61	1.94
R28, Raw Slurry	0	23.34	5.42	2.68	2.48	.26
		"	6.03	2.94	2.68	.41
		"	5.19	2.52	2.31	.36
R28, Sample 1	7	17.24	6.65	1.83	2.94	1.88
		"	7.18	2.11	3.07	2.0
		"	6.11	1.76	2.65	1.7
R28, Sample 3	15	20.50	5.13	1.55	2.21	1.37
		"	4.59	1.37	1.94	1.28
		"	4.75	1.43	1.99	1.33
R28, Sample 5	54	8.85	7.98	2.12	3.60	2.26
		"	9.11	2.41	4.1	2.6
R28, Sample 6	84	7.16	4.34	1.27	1.96	1.11
		"	6.28	1.98	2.82	1.48
		"	6.33	1.93	2.78	1.62
R28, Sample 7	122	6.07	9.24	2.5	4.45	2.29
		"	10.95	2.46	5.75	2.74
R30, Sample 1	94	11.0	6.68	1.5	1.74	3.44
		"	6.99	2.07	1.37	3.55
R30, Sample 2	99	5.72	4.6	1.73	.91	1.96
		"	6.38	2.09	1.67	2.62
R30, Sample 5	154	8.71	6.58	2.14	.84	3.6
		"	6.68	1.8	1.2	3.68
R30, Sample 7	212	7.79	6.15	1.97	.91	3.27
		"	5.98	1.93	.89	3.16
R31, Sample 1	53	15.44	7.76	1.94	2.36	3.46
		"	9.04	2.17	2.85	4.02
		"	8.85	1.83	3.06	3.96
		"	10.68	.86	5.03	4.79
R31, Sample 2	209	12.71	5.63	.79	2.62	2.22
		"	5.09	1.59	1.55	1.95
R31, Sample 4	229	13.75	7.67	1.32	3.21	3.14
		"	8.19	1.27	3.57	3.35

<u>Sample No.</u>	<u>Time (min.)</u>	<u>Residue as % of Liquid Product (gm)</u>	<u>Residue Used mgm</u>	<u>V.M. mgm</u>	<u>Fixed Carbon mgm</u>	<u>Ash mgm</u>
R31, Sample 6	251	10.64	6.71	2.06	1.77	2.88
		"	6.57	1.92	1.83	2.82
R31, Sample 8	269	7.67	3.57	1.24	.46	1.87
		"	5.46	1.89	.64	2.93

Constituents of V.M. (Light Gases)

Sample No.	Time (min.)	Residue*	Residue				
			Used mgm	CO mgm	CH ₄ mgm	CO ₂ mgm	H ₂ O mgm
R23, Raw Slurry	0	20.19	5.24	.544	.118	.338	.182
R23, Sample 5	20	17.12	8.2	1.306	.25	.80	.494
R23, Sample 9	78	21.86	6.24	.409	.133	.301	.204
R23, Sample 11	138	21.61	5.59	.418	.093	.342	.165
R26, Raw Slurry	0	21.93	5.65	.907	.215	1.173	.154
R26, End Product	64	20.44	7.09	.296	.451	.208	.121
R27, Raw Slurry	0	23.29	7.27	.432	.225	.713	.469
R27, Sample 1	8	16.06	7.09	.809	.173	.461	.226
R27, Sample 5	29	11.81	12.06	2.180	.324	1.392	.749
R27, Sample 7	86	10.16	7.29	.692	.141	.476	.194
R27, Sample 8	113	4.76	4.59	.497	.069	.387	.136
R27, Sample 9	146	3.14	6.45	.457	.076	.319	.142
R28, Raw Slurry	0	23.34	5.19	.566	.111	.632	.291
R28, Sample 1	7	17.24	6.65	.654	.162	.373	.206
R28, Sample 3	15	20.50	4.75	.682	.104	.390	.147
R28, Sample 5	54	8.85	7.98	1.344	.271	.921	.503
R28, Sample 6	84	7.16	4.34	.379	.09	.277	.118
R28, Sample 7	122	6.07	9.24	1.096	.258	.754	.465
R30, Sample 1	94	11.0	6.68	.747	.08	.522	.276
R30, Sample 2	99	5.72	4.6	.665	.102	.555	.269
R30, Sample 5	154	8.71	6.58	1.747	.085	1.857	.32
R30, Sample 7	212	7.79	6.15	1.577	.058	1.572	.255
R31, Sample 1	53	15.44	8.85	1.40	.159	1.288	.502
R31, Sample 2	209	12.71	5.63	.197	.023	.16	.056
R31, Sample 4	229	13.75	7.67	.824	.097	.817	.297
R31, Sample 6	251	10.64	6.71	1.137	.107	1.429	.441
R31, Sample 8	269	7.67	3.57	.674	.034	.963	.164

*The residue data were supplied by GFERC, Grand Forks, North Dakota, and should not be reproduced without their permission.

APPENDIX B

Sample Calculation for the Weight Percent Removal of Volatile Matter
for Run 28

Sample No.	Time (min)	Residue as % of Liquid Product (average)	V.M. as % of Residue (average)	V.M. as % of Liquid Product (average)	% Removal
Raw Slurry	0	23.34	$\frac{8.14}{16.64} = 48.92$	(23.34) (.4892) = 11.42	0
S 1	7	17.24	29.35	5.06	$\frac{11.42 - 5.06}{11.42} = 55.69$
S 3	15	20.50	30.06	6.16	46.06
S 5	54	8.85	26.51	2.35	79.51
S 6	84	7.16	30.06	2.18	80.91
S 7	122	6.07	24.77	1.5	86.87

Sample Calculation for Data Fitting of Volatile Matter
of Run 28

Time (t)	ln t (T)	Conversion (x)	ln x (X)
0		0	
7.0	1.946	.5569	-.585
15.0	2.708	.4606	-.775
54.0	3.989	.7951	-.229
84.0	4.431	.8091	-.212
122.0	4.804	.8687	-.141

$$ST_T = n(\Sigma T^2) - (\Sigma T)^2$$

$$= 5(69.744) - (17.878)^2 = 29.097$$

$$ST_X = n(\Sigma XT) - (\Sigma T)(\Sigma X)$$

$$= n(-5.767) - (17.878)(-1.942) = 5.884$$

$$B = \frac{ST_X}{ST_T} = \frac{5.884}{29.097} = .2022$$

$$\bar{X} = \frac{\Sigma X}{n} = \frac{-1.942}{5} = -.3884 \quad \bar{T} = \frac{\Sigma T}{n} = \frac{17.878}{5} = 3.576$$

$$A = \bar{X} - B\bar{T} = -.3884 - .2022(3.576) = -1.111$$

$$X = -1.111 + .2022 T$$

Taking the anti-logarithm

$$x = .3290 t^{.2022}$$

Determination of Kinetic Constants for the
Volatile Matter of Run 28

First Order

The rate equation used for evaluating first order rate constant is of the form:

$$\ln \left(\frac{a}{a-x} \right) = k_1 t$$

where a is the maximum possible reactive fraction obtained by changing its value until the square of the sum of residuals between observed and calculated conversion was a minimum, x is

the conversion at time t , and k_1 is the first order rate constant.

$a = .87$		
x (% removal)	t (time) (min)	$\ln(a/a-x)$
.5569	7.0	1.022
.4606	15.0	.7538
.7951	54.0	2.4523
.8091	84.0	2.6593
.8687	122.0	6.5061

$\ln(a/a-x)$ was plotted against time t and a straight line was drawn through these points using the least square method. The slope of the line so obtained is equal to the rate constant k_1 .

$$\text{slope 'b'} = k_1 = .04648 \text{ min}^{-1}$$

Now,

$$\ln\left(\frac{a}{a-x}\right) = .04648 t$$

The values of x were calculated at different times using the above relation.

x (% removal)	time t (mins.)
.323	10
.527	20
.734	40
.816	60
.849	80
.862	100
.867	122

The calculated percent removal and experimental percent removal are plotted in figure 36. The following equation was used for obtaining 95% confidence interval values for the $\ln(a/a-x)$ versus time plot.

$$\ln\left(\frac{a}{a-x}\right) = \text{R.H.S.} = bt_0 \pm t_{\alpha/2} \cdot S \sqrt{\frac{1}{n} + \frac{n(t_0 - \bar{t})^2}{St_t}}$$

$$\text{where } St_t = n(\Sigma t^2) - (\Sigma t)^2$$

Here t's are the experimental time values

\bar{t} is the average value

n is the number of observations

b is the slope of line

$t_{\alpha}/2$ is t distribution value

t_0 's are the chosen time values

S is the standard deviation.

Now for our case

$$b = .04648$$

$$n = 5$$

$$\Sigma t = 7 + 15 + 54 + 84 + 122 = 282$$

$$\bar{t} = \frac{282}{5} = 56.4$$

$$\Sigma t^2 = 49 + 225 + 2916 + 7056 + 14884 = 25130$$

$$St_t = 5(25130) - (282)^2 = 46126$$

$$S = .8276$$

$$t_{\alpha}/2 = 2.127$$

Now the R.H.S. is evaluated at different t_0 's. The value of percent removal at different t_0 's is then evaluated from R.H.S.

<u>t_0</u>	<u>R.H.S.1(+ sign)</u>	<u>R.H.S.2(- sign)</u>	<u>x1</u>	<u>x2</u>
0	1.57	-1.57	.688	-3.311
10	1.865	-.935	.735	-1.346
20	2.177	-.317	.771	-.325
40	2.878	-.842	.821	.495
60	3.745	1.835	.849	.731
80	4.805	2.634	.863	.808
100	6.005	3.294	.868	.838
120	7.279	3.881	.869	.852

A plot of percent removal (x1 and x2) versus time (t_0) is shown in figure 52.

Second Order

The rate equation used for evaluating second order rate constant is of the form:

$$\frac{1}{a-x} - \frac{1}{a} = k_2 t$$

where the symbols have the same meaning except k_2 is the second order rate constant.

Now $a = .915$

$\frac{1}{a-x} - \frac{1}{a}$	t (mins.)
1.6996	7.0
1.1078	15.0
7.2474	54.0

8.35	84
20.50	122

$[\frac{1}{a-x} - \frac{1}{a}]$ was plotted against time t and a straight line was drawn through these points using the least square method. The slope of the line so obtained is equal to the rate constant k_2 .

$$\therefore \text{Slope 'b'} = k_2 = .1444 \text{ min}^{-1}$$

Now

$$\frac{1}{a-x} - \frac{1}{a} = .1444 t$$

The values of x were calculated at different times using the above relation:

x (% removal)	t (time in mins.)
.521	10
.664	20
.769	40
.813	60
.836	80
.851	100
.861	120

The calculated percent removal and experimental percent removal are plotted in figure 36.

The following equation was used for obtaining 95% confidence interval values for the $[\frac{1}{a-x} - \frac{1}{a}]$ versus time plot.

$$[\frac{1}{a-x} - \frac{1}{a}] = \text{R.H.S.} = bt_0 + t_{\alpha}/2 \cdot S \sqrt{\frac{1}{n} + \frac{n(t_0 - \bar{t})^2}{St_t}}$$

where $St_t = n (\Sigma t^2) - (\Sigma t)^2$

The symbols have the same meaning as before. Now for our case,

$$b = .1444$$

$$n = 5$$

$$t_{\alpha}/2 = 2.127$$

$$S = 2.476$$

$$\Sigma t = 282$$

$$\bar{t} = 56.4$$

$$St_t = 46126$$

Now the R.H.S. is evaluated at different t_0 's. The value of percent removal at different t_0 's is then evaluated from R.H.S.

t_0 (min)	<u>R.H.S.1(+ sign)</u>	<u>R.H.S.2(- sign)</u>	<u>x1</u>	<u>x2</u>
0	4.698	-4.698	.742	1.192
10	5.634	-2.746	.766	1.52
20	6.619	-.843	.785	-3.135
40	8.823	2.729	.814	.653
60	11.521	5.807	.836	.77
80	14.8	8.304	.852	.809
100	18.496	10.384	.864	.828
120	22.414	12.242	.872	.84

A plot of percent removal (x1 and x2) versus time (t_0) is shown in figure 53.

APPENDIX C

Raw Data for Pyrolysis at 800°C

Sample No.	Time (min)	Residue Used mgm	V.M. mgm	Fixed Carbon mgm	Ash mgm
R23, Raw Slurry	0	10.42	3.51	6.12	.79
R23, Sample 11	138	9.23	.40	6.26	2.57
R27, Raw Slurry	0	10.83	4.01	6.15	.67
R27, Sample 9	146	17.36	2.25	8.93	6.18
R28, Raw Slurry	0	10.05	3.25	6.25	.55
R28, Sample 6	84	12.72	3.8	7.52	1.4
R30, Sample 6	180	8.24	.79	2.82	4.63
R31, Sample 7	199	8.8	.91	3.71	4.18

Constituents of V.M.

Sample No.	Time (min.)	V.M. mgm	CO mgm	CH ₄ mgm	CO ₂ mgm	H ₂ O mgm	Total mgm	Actual* mgm	Heavy Liquids mgm
R23, Raw Slurry	0	3.51	.342	.126	1.184	1.032	2.75	2.887	.622
R23, Sample 11	138	.40	.024	.020	.119	.100	.274	.288	.112
R27, Raw Slurry	0	4.01	.215	.087	.826	.828	2.018	2.119	1.89
R27, Sample 9	146	2.25	.045	-	.090	.078	.236	.248	2.00
R28, Raw Slurry	0	3.25	.169	.067	.624	.515	1.424	1.495	1.75
R28, Sample 6	84	3.8	.181	.062	.745	.550	1.583	1.66	2.14
R30, Sample 6	180	.79	.014	.009	.140	.037	.207	.217	.57
R31, Sample 7	199	.91	.019	-	.106	.024	.165	.172	.74

*The weight in this column are the actual weight of light gases because in going from CAPS unit to EA, 1/20 of the light gases are sent to flame ionization detector (FID), therefore the total weight is multiplied by 20/19 factor to get actual weight.

Constituents of the Heavy Liquid

H

R23, Raw Slurry (mgm) R23, S11 (mgm) R27 Raw Slurry (mgm) R27, S9 (mgm) R28 Raw Slurry (mgm) R28, S6 R30, S6 R31, S7

Component (mgm) (mgm) (mgm) (mgm) (mgm) (mgm) (mgm) (mgm)

Naphthalene	.0125	-	.0097	.0104	.013	-	.0057	-
β Me-Napthalene	.146	-	.0108	.0121	.012	-	.0057	.0088
α Me-Napthalene	.0125	.003	.0097	.014	.009	.011	.005	.007
Biphenyl	.0114	-	.0075	.0121	.009	.009	.0057	-
Di-Me-Napthalene	-	.003	.0335	.033	.0181	.010	.0148	.0114
Acenapthene	.0104	.0036	.0476	.0677	.021	.0585	.023	.0202
Dibenzofuran	.0083	.0046	-	-	.014	.057	.0181	-
Fluorene	.0104	.0036	.0444	.0677	.021	.093	-	.0246
Phenanthrene	<u>.054</u>	<u>.0646</u>	<u>.221</u>	<u>.337</u>	<u>.132</u>	<u>.247</u>	<u>.203</u>	<u>.351</u>
Total	.134	.082	.384	.554	.249	.486	.282	.423